

## **COPYRIGHT WARNING**

This paper is protected by copyright. You are advised to print or download **ONE COPY** of this paper for your own private reference, study and research purposes. You are prohibited having acts infringing upon copyright as stipulated in Laws and Regulations of Intellectual Property, including, but not limited to, appropriating, impersonating, publishing, distributing, modifying, altering, mutilating, distorting, reproducing, duplicating, displaying, communicating, disseminating, making derivative work, commercializing and converting to other forms the paper and/or any part of the paper. The acts could be done in actual life and/or via communication networks and by digital means without permission of copyright holders.

The users shall acknowledge and strictly respect to the copyright. The recitation must be reasonable and properly. If the users do not agree to all of these terms, do not use this paper. The users shall be responsible for legal issues if they make any copyright infringements. Failure to comply with this warning may expose you to:

- Disciplinary action by the Vietnamese-German University.
- Legal action for copyright infringement.
- Heavy legal penalties and consequences shall be applied by the competent authorities.

The Vietnamese-German University and the authors reserve all their intellectual property rights.





## DESIGNING AN ADJUSTABLE FRAME STRUCTURE FOR AGRICULTURE UGV

BACHELOR THESIS

BINH DUONG 2022

**Submitted by:** Nguyen Dang Minh

**RUB Student ID:** 19220826

**VGU Student ID:** 14809



**Supervisor:** Dr. Hien Vo

**Co-supervisor:** Mr. Duyen Do

## Contents

<b>List of tables .....</b>	<b>vi</b>
<b>Abstract .....</b>	<b>viii</b>
<b>1 Introduction .....</b>	<b>1</b>
1.1 Overview and motivation .....	1
1.2 Goal and scope of the thesis .....	2
<b>2 Fundamental and state of research .....</b>	<b>4</b>
2.1 UGV overview .....	4
2.2 Calculation dimension of UGV total width length.....	5
2.3 Material properties of the frame beams. ....	16
2.3.1 Definition of some material properties.....	16
2.3.2 Strength of material .....	18
2.3.3 Stress, strain curve diagram of material .....	21
2.4 Bending of Beams .....	22
2.4.1 Type of stress in mechanical engineering design.....	22
2.4.2 Normal, shear stress in angle geometry and maximum normal and shear stress of the mechanical component.....	25
2.4.5 The parallel-axis theorem to determine moment of inertia I in specific cross-section geometry.....	28
2.4.7 Basic Equations of Ordinary Bending Theory .....	30
2.4.8 Finite element method .....	31
<b>3 Requirement determination .....</b>	<b>34</b>
3.1 Problem statement clarifying the most central need.....	34
3.2 Functional requirement .....	34
3.3 Functional requirement evaluation .....	35
3.4 Technical requirements.....	36
<b>4 Development and selection .....</b>	<b>38</b>
4.1 Concept evaluation .....	38
4.2 Concept table .....	38
4.2.1 Concept 1 – level basic .....	39
4.2.2 Concept 2 – level intermediate .....	40
4.2.3 Concept 3 – level advance .....	41
4.3 Concept evaluation .....	41
<b>5 Implement of the chosen concept.....</b>	<b>43</b>

5.1	<i>Design of complex aluminum extrusions</i> .....	43
5.2	<i>Bracket design</i> .....	47
5.2.1	Design study of ADC12 bracket.....	47
5.2.2	Design study of blind bracket.....	49
5.2.3	Design study of Stainless Steel bracket.....	50
5.2.4	Study design of extruded L-Bracket.....	55
5.2.5	Comparison between 4 kind of bracket .....	56
5.2.6	Decision matrix for choosing bracket.....	57
5.3	<i>Design of sensor modular mechanism and option</i> .....	58
5.3.1	Option 1 : Common linear mechanism.....	58
5.3.2	Option 2 : Using ball joining .....	68
5.3.3	Decision matrix for the 2 options .....	70
5.4	<i>Frame joining design calculation of pre load to determine the weakest join of the UGV</i> 71	
5.5	General design .....	77
5.5.1	Statics frame analysis using finite elements .....	77
5.6	<i>Design of the steering and motor frame</i> .....	80
5.7	<i>Width adjustable joining</i> .....	84
5.7.1	Option I: Width adjustable using ball screw linear guide mechanism .....	84
5.7.2	Option II: Width adjustable using bracket.....	85
5.7.3	Decision matrix for both options .....	85
5.8	Overall specification of the design .....	86
<b>6</b>	<b>Manufacturing</b> .....	<b>89</b>
6.1	Mechanical Components.....	89
6.2	Electrical part.....	89
6.3	User manual .....	92
<b>7</b>	<b>Results</b> .....	<b>95</b>
<b>8</b>	<b>Conclusion</b> .....	<b>99</b>
<b>9</b>	<b>Appendix</b> .....	<b>100</b>
<b>10</b>	<b>Reference</b> .....	<b>111</b>

## List of figures

Figure 1-1. Scope of thesis .....	3
-----------------------------------	---

Figure 2-1 Normal distribution on mathematica 2019 .....	10
Figure 2-2 Histroy diagram .....	15
Figure 2-3 Bootstrapped confidence interval of 95% graph.....	16
Figure 2-4 Material properties specification .....	17
Figure 2-5 Stress and strain curve .....	19
Figure 2-6 Hooke's Law.....	19
Figure 2-7 The value of E (i.e., modulus of elasticity) of materials.....	20
Figure 2-8 Stress $\sigma$ illustration .....	20
Figure 2-9 Strain $\varepsilon$ illustration.....	21
Figure 2-10 Stress and strain curve diagram .....	21
Figure 2-11 Single force acting on the specimen .....	22
Figure 2-12 Specimen cut through .....	23
Figure 2-13 Shear and normal stress in 3D specimen .....	24
Figure 2-14 Equilibrium state formulation for shear and normal stress around x-axis.....	25
Figure 2-15 The x, y coordinate system with respected to $\xi, \eta$ ,-system.....	26
Figure 2-16 The value of $\sigma_1$ or $\sigma_2$ with respect to the angle $\phi$ *.....	27
Figure 2-17 the stresses $\sigma_1$ and $\sigma_2$ elements of the x-axis, y-axis .....	27
Figure 2-18 Beam bending .....	28
Figure 2-19 The x-axis is aligned with the beam's axis.....	28
Figure 2-20 Inertia force.....	29
Figure 2-21 Moment of inertia .....	29
Figure 2-22 Moment of inertia of any arbitrary geometry .....	30
Figure 2-23 General beam geometry and support locations.....	31
Figure 3-1 Functional requirement .....	35
Figure 3-2 Ranking definition for functional requirements.....	35
Figure 3-3 Technical requirements solution procedure .....	37
Figure 5-1 Tensile and yield strengths of frequently used aluminum [65] .....	43
Figure 5-2 Categoriess of alumium profile.....	44
Figure 5-3 Cross-section area of the choosen beam .....	45
Figure 5-4 L- Bracket (ADC12 material) .....	47
Figure 5-5 Top side and bottom view of the bracket (respectively).....	48
Figure 5-6 Blind Bracket (S45C material) .....	49
Figure 5-7 Stainless steel bracket .....	51
Figure 5-8 2D dimension secification given by Misumi .....	52
Figure 5-9 Loading condition to determine the allowable load of bracket .....	56

Figure 5-10 Linear guides and roller wheel guide respectively .....	58
Figure 5-11. Exflow view of the V-Wheel roller mechanism .....	59
Figure 5-12. Linear mechanism in 2d and 3d.....	60
Figure 5-13. Constrain visualization of the simulation .....	60
Figure 5-14. Max and Min Von Misses (MPa) and displacement (mm) value.....	61
Figure 5-15. Safety factor of the mechanism .....	61
Figure 5-16. Components layout and assembly method for V-Slots wheel guide mechanism .....	62
Figure 5-17. Mass distribution of the driving components .....	63
Figure 5-18. 3D modelling for the simulation.....	64
Figure 5-19. 24V Ritar batteries .....	65
Figure 5-20. 12V Honda Vision batteries.....	65
Figure 5-21. Constrain study of senerio I.....	66
Figure 5-22. Von mises and safety factor results (I) .....	66
Figure 5-23. Constrain study for senerio II .....	67
Figure 5-24. Von Mises and safety factor results (II) .....	67
Figure 5-25 Ball head illustration.....	68
Figure 5-26. Connection bracket design and dimension .....	69
Figure 5-27 Ball head and housing connecting to the alumium surface .....	70
Figure 5-28 Schematic sketch of the joint in the UGV frame .....	72
Figure 5-29 Load distribution on the bolts .....	73
Figure 5-30 Bolts M6 in solidworks.....	74
Figure 5-31 Overall specification of the bolts according to misumi .....	75
Figure 5-32. Finite element process .....	77
Figure 5-33. Frame structure and nodal coordinates .....	78
Figure 5-34. Applied constrain and force onto the frame.....	79
Figure 5-35. Stiffness K equation using to solve the problem .....	79
Figure 5-36. Maxium stress, and displacement and stafety factor plot of the frame with the correspond applied force of 20kg .....	80
Figure 5-37 Front,side and top view of the steering and motor frame .....	82
Figure 5-38 Static results of the lower frame as exposed to the loading weight include on the upper frame.....	82
Figure 5-39. The actuator that will be used to steer the UGV and its fixtured beam.....	83
Figure 5-40 Beam stress and safety factor results of the actuator fixture beam.....	83
Figure 5-41 The motor frame and the steering frame after installation.....	84

Figure 5-42 Width adjustable using bracket.....	85
Figure 5-43 Virtual design of a UGV .....	86
Figure 6-1 List of mechanical components .....	89
Figure 6-2 PLC S7-1500 .....	89
Figure 6-3 Wiring diagram system for the PLC .....	90
Figure 6-4 PLC programming .....	91
Figure 6-5 Electrical cabinet after installing the PLC and others electrical component .....	91
Figure 6-6 5V relay is on.....	92
Figure 6-7 Reciever Power is on .....	92
Figure 6-8 Actuator control module and control knob.....	93
Figure 6-9 Motor control knob and the control module .....	94
Figure 7-1 Virtual design of a UGV .....	95
Figure 7-2 Testing loading capacities.....	96
Figure 7-3 UGV moving on the grass field .....	98
Figure 7-4 The UGV final phototype after testing .....	98



## List of tables

Table 2.1. Land characteristics .....	6
Table 2.2. Recommended plant plots width .....	7
Table 2.3.Means width vegetable plots dimension for each sample .....	10
Table 2.4. Mean and standard deviation of the original data .....	11
Table 2.5. Resul table in Excel .....	12
Table 2.6. P-value for the hypothesis test.....	14
Table 3.1. Importance ranking of functional requirements .....	35
Table 4.1 Options table.....	38
Table 5.1.Material of the beam.....	43
Table 5.2. Code name of the choosen crossed section with respect to the manufacture .....	45
Table 5.3. Cross Sectional of Moment of Inertia of extruded aluminum profile .....	45
Table 5.4.Allowable deflection limit.....	46
Table 5.5.Result analysis of each type of beam under assumption load [at length of 1200mm] .....	46
Table 5.6. Specification of bracket ADC12 .....	48
Table 5.7. Material of the bracket with ADC12 .....	49
Table 5.8. Material of the bracket with Stainless steel (C45).....	50
Table 5.9. Mechanical Properties of Chrome Stainless Steel.....	53
Table 5.10. Properties of the Bracket corresponding to the each load .....	54
Table 5.11 Material properties of the extruded L-bracket.....	56
Table 5.12. Result table for 4 type of bracket .....	57
Table 5.13. Grading criteria for bracket.....	57
Table 5.14. Result of decision matrix for bracket .....	57
Table 5.15. Componet list of the driving moule.....	63
Table 5.16. Specification of the batteries .....	64
Table 5.17 Grading criteria for the sensor modular mechanism .....	70
Table 5.18 Result table for the sensor modular mechanism.....	70
Table 5.19. Given data for XL1 type joint .....	76
Table 5.20. Results table of the joint of location XL1 .....	76
Table 5.21. Results of simulation .....	80
Table 5.22 Grading criteria for the modular linear mechanism .....	85
Table 5.23 Decision matrix result for the modular linear mechanism .....	86
Table 5.24 Overall design specification .....	87



Table 5.25 Overall component quantities.....	87
Table 7.1 Collected data for loading capacity when the vehical is moving .....	96
Table 7.2 Overall design specification .....	96
Table 7.3 Overall component quantities.....	97

**Abstract**

This project is a part of the large project of making agriculture UGV. This project is focused on researching and developing an appropriate frame with features such as width adjustable and sensor adjusting device for an UGV which is moving on agriculture terrain.

The key parameter of this project is determine the required torque of the motor which is should be not only meet the requirement for driving and steering smoothly, but also saving the money. The key method using is researching the interaction between the wheel and deformable terrain.

# 1 Introduction

## 1.1 Overview and motivation

Agriculture has a history from 12000 years ago and has drastically changed the way humankind developed and lived. They switched from hunting lifestyle to settlements and farming. Since then agriculture has been an essential component in almost all fields regarding the food-consuming industry.

As societies have become significantly developed throughout the years, along with the high demand of food provision, agriculture still plays a highly crucial role in supplying the people's demand. However, with a traditional way of cultivation, it will take up a lot of time to grow and harvest crops and food. To improve the efficiency of cultivation, in the early 17<sup>th</sup> century the British people started to apply new techniques namely Selective Breeding, Enclosure Mechanization, etc. From then, in the 20<sup>th</sup> century intensive agriculture has taken its place. Intensive agriculture replaced draft animals and created more value with smaller takt time. Most notable is the successfully introduced gasoline-powered general-purpose vehicles. This set a new standard for modern agriculture and resulted in the application of many mechanical devices such as self-propelled harvesters, gasoline tractors for cultivation, etc. and further revolutionizing agriculture. Not only has new industrial technology been incorporated into agriculture, but also new biological technology plays a huge role in propelling agriculture towards mechanized style.

Nowadays, due to the declining quality of environment, polluted air, acid rain and contaminated water source, mechanized style of agriculture has been reduced, instead people are shaping the agriculture cultivation into an eco-friendly style. Because, mechanization contributes a huge factor for urbanization and industrial economy. Mechanized style of agriculture encourages large scale productions and sometimes benefits the farming procedures while causing considerable environmental degradation. With that reason, the green and modern revolution has been promoted to prevent and minimize environmental crisis and risk. "Green" is the term for eco-friendly, every creation regarding agriculture must be least harmful to the environment as possible. "Modern" is easy to use and effective. With the contribution of two factors, agriculture is and will be entering another revolution, not only new technology but also new concepts of production.

With the populations of the world being around 7.5 billion, the farming industry must be sufficient, not only being able to cultivate on such a scale, but also be economical and clean. There have been numerous means of improving the whole farming system which can be

known as automatic agriculture. Automated agriculture is a hybrid of robotics, mechanical design and automated control devices. More and more companies are working on robotic innovations to develop drones, automatic tractors, harvesting machines, automatic watering and seeding robots. Although these technologies are fairly new, the agricultural industry has seen more and more traditional companies adopt farm automation into their production processes.

Up to now, agriculture still plays one of the important economic sectors of Vietnam, although over time, the share of the agricultural sector in the economy has decreased due to the economic restructuring, increasing the proportion into new industries. The agricultural sector has made a great contribution, helping to create jobs for many workers, solving the problem of the unemployment rate of our country. Moreover, our country's agriculture has created many key export products such as rice – this is the product that helps Vietnam rank second in the world in exporting this commodity, in addition to coffee, cotton yarn, peanuts, rubber, sugar and tea.

In addition to the above successes, our country's agriculture still faces many difficulties and challenges. In particular, the biggest challenge is still that agriculture is still organized mainly on a small, fragmented, household-type scale. Another difficulty is that although the tropical climate is favorable for agricultural development, it is also greatly affected by climate change. Hence, tracking what is happening to the crops every day is vital, in order to cope with the erratic climate in Vietnam. Tracking crops on farms is one of the fundamental steps to push productivity in agriculture. Since, knowing what happens to the crop will have the farmer to predict and make decisions as fast as possible. Harvesting and growing crops in large volumes is becoming more and more popular, in order to meet the demand for agricultural products and output of the people. Therefore, in order to increase food efficiency and safety, automation agriculture has been on a growing trend in recent years. In the process of researching and testing the seedling stage crop care process, there is a need to collect real-time crop data (height, size, tree color) ... From those data comes the most optimal process for plant care. However, if the problem was continued to be issued manually, it would be very time consuming and cannot be précised.

## ***1.2 Goal and scope of the thesis***

This project will make a device move above the vegetable bed; sensors will be placed in the middle to collect data. However, the project will focus on building the initial base, making it possible for the car to move simply with a handheld controller. Automatic scrolling functions and other advanced function improvements will be added later. The UGV projects consist of

the designing of the frame and moving mechanism. However, the thesis is only focusing on the design of the frame. Which will consist of the mechanical properties such as stress, strain, deflection, bending of each beam under a certain condition of load and method of assembly of the whole frame. Also, to build a prototype and run it. The idea of the thesis was based on the idea of UGV vehicles, it's very flexible and easy to use, especially in the farm environment. Following that, a list of requirements for the system, including drive part, design, and manufacturing conditions, is examined. It is critical for ensuring that the work is precise and unambiguous. To make further progress, it is critical to thoroughly review previous research and existing products. Each design's positivity and negativity are analyzed and observed in order to build a more suitable design later on.

Each idea already visualized at the previous stage is compared by evaluation methods based on technical and economic criteria, as well as the selection of a concept for implementation. It reveals the concepts' strengths and weaknesses. The decision-making process is now transparent, which aids in selecting the best candidate for the next step. Before making a physical prototype, part of the feature system is designed in a virtual environment. Solidworks 2022 is the CAD program used in this project. Without changing the essence of the chosen concept, criticizing and developing it. It is necessary to repeat virtual design in order to improve the final product's attributes.

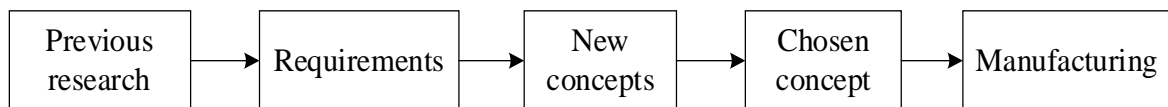


Figure 1-1. Scope of thesis

## 2 Fundamental and state of research

### 2.1 UGV overview

The loss of manual labor from rural areas and the transition from labor-intensive industries to automated facilities, both caused by social, technological, and economic difficulties, can be greatly mitigated by agriculture [16]. A further possibility is the introduction of robots. Small farmers will be able to escape the current agricultural crisis paradigm, which asks for significant expenditures in the search of increased yields [17], by making small-scale operations more realistic. The crucial components have improved. Robots provide effectiveness and efficiency as contrasted to physical labor, with the former accounting for a sizeable amount of the entire cost of a traditional field operation. These components suggest significance. Given that robots can now execute 80% of the activities that people traditionally undertake, reducing the gap between something has potential and is real [18]. The cause is connected to current developments in robotics and artificial intelligence that may be utilized to do unusual jobs, i.e., by mimicking human talents and increasing them to improve the use cases, such as the ability to function in a range of locations. Indeed, as they try to fit navigation skills into compact packaging, agricultural robots are gadgets are getting more and more complex nowadays. Because they are not distinct from one another, detection, action, and mapping are frequently carried out in tandem to meet a number of purposes [19].

According to a recent analysis of the state-of-the-art in the industry, agricultural robots may be divided into three main categories by weed identification, chemical control, and fertilizer delivery sensors and sprays installed on wheeled platforms [21–25]. For mechanical weed eradication, spot spraying, and weed identification, the small farm vehicle AgBot II developed by Queensland University of Technology serves as an example [21]. Similar to this, the University of Osnabrueck, Amazonen-Werke, and the Robert Bosch GmbH firm collaborated to develop the BoniRob for soil monitoring, weed phenotyping, and precision spray application [22] [23].

The attachment of specialized environmental sensors and robotic arms for precision motions or the collection of field samples distinguishes the second class of agricultural robots from the first [26–29]. For instance, the GRAPE ground robot, which the European Union has funded, is employed to protect and keep an eye on the vines' state of health. It is equipped with a robotic arm with six degrees of freedom (DOF), whose main job is to deftly manipulate and deploy a pheromone dispenser [26]. Another example is the Trimbot2020 project, which intends to create an algorithmic notion to control a modified Bosch Indego that has been fitted

with a six-DOF manipulator on a sturdy platform for robotic bush trimming [27]. This project is funded by the EU's H2020 program. Also, Sydney Field Robotics at the University of Australia Sydney designed the Ladybird robot with a 6-DOF arm, solar panels, and a four-wheel drive system for the vegetable industry [28]. Agricultural robots that harvest are now equipped with more accurate vision sensors and algorithms [30,31]. To modify the robot's work area to plant profiles, the robotic arm may occasionally be installed on a movable platform with a single DOF. On occasion, the robotic arm may be mounted on a mobile platform with a single DOF to plant profiles. As an illustration, a project supported by China's National Technology Research and Development Program recommended using specialized machinery and a lifting support for harvesting tomatoes [32].

## *2.2 Calculation dimension of UGV total width length.*

Generally speaking, agricultural land is land that is utilized for agriculture, which is the planned and systematic exploitation of other living forms [1], especially the breeding of livestock and the cultivation of crops, to supply food for people. [2] [3] It is usually used synonymously with farmland or cropland as well as pasture or rangeland. Yet the United Nations' Food and Agricultural Organization (FAO) and those who follow its guidelines also use the phrases "agricultural land" or "agricultural area" as terms of art to refer to the collection of [4] [5]



Vietnamese-German University

The term "arid land," sometimes known as "cropland," refers to land used for crops that require yearly replanting, as well as fallow land or pasture used for such crops over a five-year period.

Permanent cropland: agricultural land that doesn't need to be replanted every year.

Permanent pastures: meadows and bushes that can be used to graze livestock naturally or artificially.

The term "agricultural land" is thus used to refer to a sizable amount of land that is not utilized for farming. Rather, "sown land" or "cropped land" is the term used to describe the real area that is planted with crops each year. Permanent farmland includes forested plantations that are used to produce coffee, rubber, or fruit; it does not include tree farms or actual forests that are used to produce timber or lumber. Cultivable land is land that is appropriate for farming.

For our modulization purpose, the width of the car has to be changed proportionally to the width between each vegetable plots. However, due to the budget reason, the width cannot be changed to suit every dimension of every farm. So, the procedure of limiting the width change

range for the car has to be conducted. The goal is to choose and point out the suitable range to cover the majority amount of farm in the interested market (Lam Dong).

Initially, data collection of the farm's dimension is essential, after having investigated 12 different plants local in Vietnam. Data will be put into a table. The vehicle has to be able to move above the vegetable bed and the sensor will be put above. Hence, the data collector stage of the farm dimension will be carried out by measuring the distance of the vegetable beds and adding the distance from the 2 midpoint sides of the path between the beds. The reason for choosing the midpoint of the road is that the wheel point of the vehicle will roll on, to optimize the center of gravity of the vehicle.

Table 2.1. Land characteristics

Region	Width	Dirt characteristics	Type of plant
Lam Dong	1m  Vietnamese-German University	Fleshy soil	Cabbage
Binh Phuoc	1.5m	Bazan	Cashew
Thanh Da	1.3m	Fleshy soil	Water Spanish
Lam Dong	1.2m	Cultivable land	Tomato
Phan Thiet	1.02m	Cultivable land	Dragon Fruit
Ninh Thuan	1m	Bazan	Pepper



Cu Chi	1m	Fleshy soil	Chives
Lam Dong	1.2m	Alluvial soil	Sweet Potato
Lam Dong	1.33m	Cultivable land	Tea
Lam Dong	1.25m	Fleshy soil	Strawberry
Lam Dong	1.2m	Alluvial soil	Bok Choy
Lam Dong	1.05m	Cultivable land	Lettuce



Vietnamese-German University

As illustrated, some sampling data were collected outside Lam Dong province, which will not be put into consideration at the moment. The data somehow consider to be biased due to the amount of sampling were not sufficient enough. Therefore, a reference has to be found in order whether the real data is biased or not. If no biased was to be found, the procedure to find the range will be conduct. The recommended dimensions of vegetable plots specified by each different type of plant as a guideline and reference point to explain why many farmers in Vietnam choose this dimension to optimize their cultivation products. These numbers were all collected from Vietnamese Agricultural Website on farming technique [6][7]

Table 2.2. Recommended plant plots width

Plants type	Width vegetable plots
Corn	0.45 - 0.5
Carrot	1.4

Cabbage	0.8 - 1.2
Chinese Cabbage	1.2
Bok Choy	1.2 - 1.3
Pea	1.2
Green cauliflower	1.2
Purple Cabbage	1.2
Strawberry	1.2 - 1.3
Tomato	0.8 - 1.2
Lettuce	1.0 - 1.1
Chilies	0.5 - 0.65
Tea	1.2 - 1.5
Chrysanthemum	1
Carnation	1.2
Grace Flower	1.2 - 1.3
Lili Flower	0.7-1
Lilies	0.45

Mulberry	1.2 - 1.5
Sweet Potato	1.2
White turnip	1.2-1.5

Comparison between table 2.1 and table 2.2 were made, the planation that appearing in Lam Dong province suit the recommended plant plot width: Cabbage, Sweet Potato, Tomato, Tea, Strawberry, Bok Choy, Lettuce. In conclusion, the real data was not biased, then the next procedure is made.

In statistics, normality tests are used to determine if a data set is adequately described by a normal distribution and to estimate the probability that a random variable underlying the data set will be normally distributed. In particular, the tests constitute a kind of model selection and may be interpreted in many ways depending on how one sees probability. Descriptive statistics looks at how well a normal model fits the data without making any judgments about the underlying variables. A normal distribution cannot adequately explain the data if the fit is poor. In frequentist statistics **statistical hypothesis testing**, data are compared to the null hypothesis that they are normally distributed. The likelihood that the data in Bayesian statistics Instead of being "tested" for normality per se, the data are estimated to (for all) originate from a normal distribution with the supplied parameters. The relative likelihood of seeing the data given various models is provided by a Bayes factor or a Bayesian model, which is then used to compare this likelihood with the likelihood that the data originate from other distributions under consideration. or, more accurately, by calculating a posterior distribution using the calculated likelihoods and a prior distribution of candidate models and parameters.

A type of continuous probability distribution for a random variable with a real value is the normal distribution. It is also known as the Gaussian, Gauss, or Laplace-Gauss distribution. Its probability density function's general form is [8] for  $-\infty \leq x \leq \infty$ , depending on the two parameters, mean and variance  $E(X) = \mu$  and  $\text{Var}(X) = \sigma^2$  of the distribution. The probability density function is a bell-shaped curve that is symmetric about  $\mu$ . The notation  $X \sim N(\mu, \sigma^2)$ . The graph of the normal distribution was being conducted in Mathematica 2019

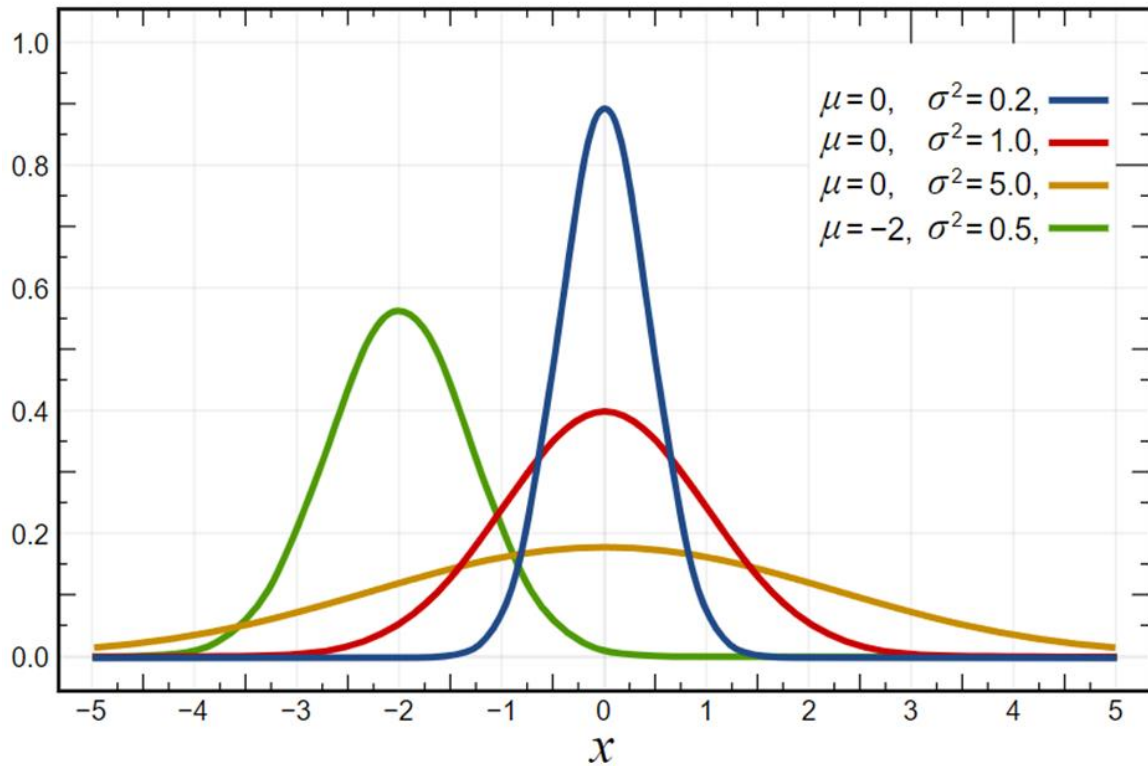


Figure 2-1 Normal distribution on mathematica 2019

At first, we will conduct and try to estimate whether the data can be conducted with means of normal distribution or not. After collecting data from table above, we have a total of 21 different samples, then calculation of means per sample was conducted, by not having the exact distribution of some sample, the means calculation was conducted by simply taking the average of 2 upper and lower bounds of the sample width length. The procedure of determining the appropriate range of the dimension will mostly be conducted via excel.

Table 2.3.Means width vegetable plots dimension for each sample

Plants type	Width vegetable plots	Mean [m]
Corn	0.45 - 0.5	0.475
Carrot	1.4	1.4
Cabbage	0.8 - 1.2	1
Chinese Cabbage	1.2	1.2

Bok Choy	1.2 - 1.3	1.25
Pea	1.2	1.2
Green cauliflower	1.2	1.2
Purple Cabbage	1.2	1.2
Strawberry	1.2 - 1.3	1.25
Tomato	0.8 - 1.2	1
Lettuce	1.0 - 1.1	1.05
Chilies	0.5 - 0.65	0.575
Tea	1.2 - 1.5	1.35
Chrysanthemum	 1 Vietnamese-German University	1
Carnation	1.2	1.2
Grace Flower	1.2 - 1.3	1.25
Lily Flower	0.7-1	0.85
Lilies	0.45	0.45
Mulberry	1.2 - 1.5	1.35
Sweet Potato	1.2	1.2
White turnip	1.2-1.5	1.35

Table 2.4. Mean and standard deviation of the original data

Size	21
Means	1.09
Standard deviation	0.27

Next step is to determine whether the data is a normal distribution or not. The ks test function for the Kolmogorov-Smirnov test on the standardised concentration data (Z Score function)

$$Z = (X - X_T) / s$$

the average of the original data, the original data standard deviation, and each data point (X), where  $X_T$  is the matching standardized data point. 0 is the means value and a 1 is the standard deviation characterize the standardized data. The kstest function tests if the standardized data have a standard normal distribution as the null hypothesis. A statement that specifies potential population mean values is known as a null hypothesis ( $H_0$ ). It is associated with an alternative hypothesis  $H_A$ , which is the “opposite” of the null hypothesis. A two-sided set of hypotheses is  $H_0: \mu = \mu_0$  versus  $H_A: \mu \neq \mu_0$

For a specified value of  $\mu_0$ , and a one-sided set of hypotheses is either

$$H_0: \mu \leq \mu_0 \text{ versus } H_A: \mu > \mu_0 \text{ or } H_0: \mu \geq \mu_0 \text{ versus } H_A: \mu < \mu_0.$$

In this case  $H_0$ : The following sample is normal distributed and  $H_A$ : The following sample is not normal distributed. It is applied that  $H_0: \mu = \mu_0$  versus  $H_A: \mu \neq \mu_0$

Process to find all the leftover factors: expectation, rank, Z-score (standardisation value), normal distribution and the difference.

Table 2.5. Result table in Excel

Plants type	Width vegeta ble plots	Me an [m]	Cumula tive	CDF (expecte d)	Rank (rank- 1/n)	Z-score	F(x)	Differen ce
-------------	---------------------------------	-----------------	----------------	-----------------------	------------------------	---------	------	----------------

Corn	0.45 - 0.5	0.4 75	1	0.04761 9048	0	- 2.22334 3162	0.01309 6335	0.01309 6335
Carrot	1.4	1.4	2	0.09523 8095	0.04761 9048	1.14417 6598	0.87372 4797	0.82610 5749
Cabbage	0.8 - 1.2	1	3	0.14285 7143	0.09523 8095	- 0.31204 8163	0.37750 196	0.28226 3865
Chinese Cabbage	1.2	1.2	4	0.19047 619	0.14285 7143	0.41606 4218	0.66131 8494	0.51846 1351
Bok Choy	1.2 - 1.3	1.2 5	5	0.23809 5238	0.19047 619	0.59809 2313	0.72511 083	0.53463 464
Pea	1.2	1.2	6	0.28571 4286	0.23809 5238	0.41606 4218	0.66131 8494	0.42322 3256
Green cauliflower	1.2	1.2	7	0.33333 3333	0.28571 4286	0.41606 4218	0.66131 8494	0.37560 4208
Purple Cabbage	1.2	1.2	8	0.38095 2381	0.33333 3333	0.41606 4218	0.66131 8494	0.32798 516
Strawberry	1.2 - 1.3	1.2 5	9	0.42857 1429	0.38095 2381	0.59809 2313	0.72511 083	0.34415 8449
Tomato	0.8 - 1.2	1	10	0.47619 0476	0.42857 1429	- 0.31204 8163	0.37750 196	0.05106 9468
Lettuce	1.0 - 1.1	1.0 5	11	0.52380 9524	0.47619 0476	- 0.13002 0068	0.44827 5275	0.02791 5201
Chilies	0.5 - 0.65	0.5 75	12	0.57142 8571	0.52380 9524	- 1.85928 6972	0.03149 3236	0.49231 6287

Tea	1.2 - 1.5	1.3 5	13	0.61904 7619	0.57142 8571	0.96214 8503	0.83201 2494	0.26058 3922
Chrysanthemum	1	1	14	0.66666 6667	0.61904 7619	- 0.31204 8163	0.37750 196	0.24154 5659
Carnation	1.2	1.2	15	0.71428 5714	0.66666 6667	0.41606 4218	0.66131 8494	0.00534 8173
Grace Flower	1.2 - 1.3	1.2 5	16	0.76190 4762	0.71428 5714	0.59809 2313	0.72511 083	0.01082 5116
Lily Flower	0.7-1	0.8 5	17	0.80952 381	0.76190 4762	- 0.85813 2449	0.19540 9666	0.56649 5096
Lilies	0.45	0.4 5	18	0.85714 2857	0.80952 381	- 2.31435 721	0.01032 4068	0.79919 9742
Mulberry	1.2 - 1.5	1.3 5	19	0.90476 1905	0.85714 2857	0.96214 8503	0.83201 2494	0.02513 0364
Sweet Potato	1.2	1.2	20	0.95238 0952	0.90476 1905	0.41606 4218	0.66131 8494	0.24344 3411
White turnip	1.2- 1.5	1.3 5	21	1	0.95238 0952	0.96214 8503	0.83201 2494	0.12036 8459

Result of the hypothesis test has been achieved

Table 2.6. P-value for the hypothesis test

Size	21
Means	1.09
Standard deviation	0.27
Ks test	83%
P-Value	<0.01



As mentioned by Hayes in "Statistics for Engineering" the p-value will determine the result of the test. It is commonly accepted that a p-value of less than 0.01 indicates that the null hypothesis,  $H_0$ , is not a true statement. The null hypothesis  $H_0$  is typically considered to be a credible assertion when the p-value is greater than 0.10. Thus, the null hypothesis  $H_0$  is accepted. In general, it is assumed that a p-value between 1% and 10% indicates that the data analysis is not definitive. Whilst the evidence is not overwhelming, there is some proof that the null hypothesis cannot be true. Which has been proven furthermore in the below diagram.

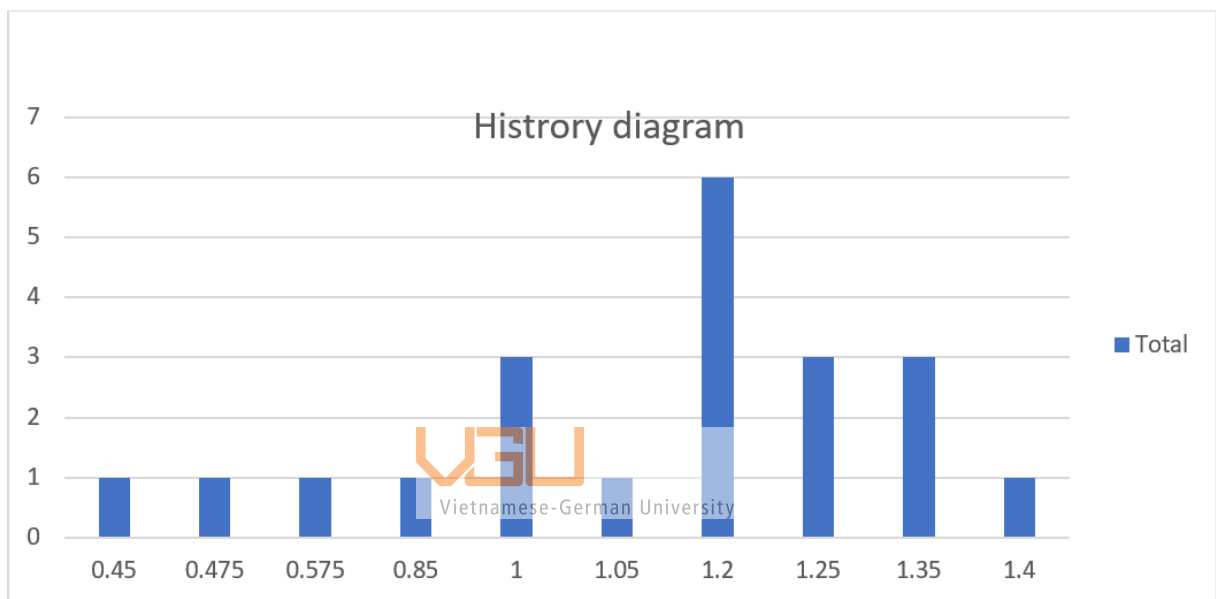


Figure 2-2 History diagram

Hence, the standard z-test and t-test did not apply in this situation. The purpose of the Bootstrap modifications was to identify the ideal width and length range for the vehicles. The bootstrap method assumes that each original data point will have an equal probability of being added at random to the resampled datasets. The approach can choose a data point more than once for a resampled dataset. This attribute is the "with replacement" portion of the procedure. The technique results in resampled datasets that are the same size as the initial dataset. Bootstrapping uses replacement to resample the initial dataset thousands of times in order to create simulated datasets. Random samples are taken as part of this procedure from the original dataset. Here is how it works. The bootstrap method assumes that each original data point will have an equal probability of being added at random to the resampled datasets. The approach can choose a data point more than once for a resampled dataset. This attribute is the "with replacement" portion of the procedure. The technique results in resampled datasets that are the same size as the initial dataset. All the procedures to determine the 99%

probability that the average range that the vehicles will need to fall into will be carried out in MATLAB 2018 and Excel 2018. From Table [2.6], the original means was 1.09 and standard deviation was 0.27, Set the number of Bootstrapped is 100 (nBoot). The afterward results will have.

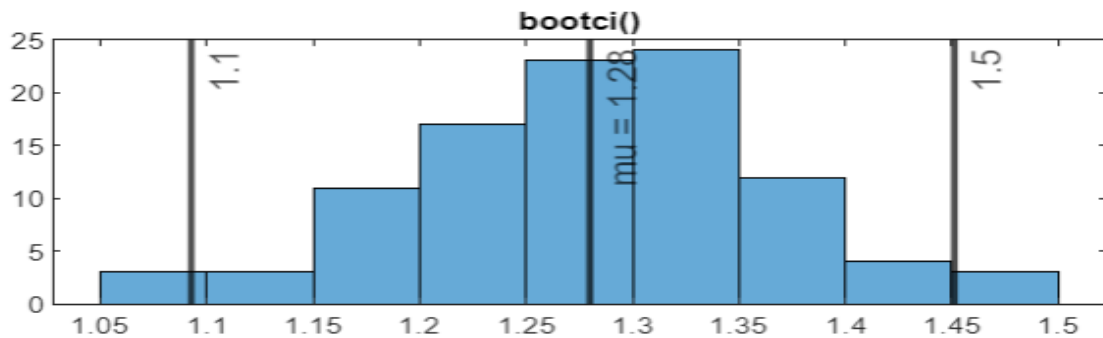


Figure 2-3 Bootstrapped confidence interval of 95% graph

As illustrated, we are having the range for our answers, however due to the original data being not large enough, the confidence interval will be one sided to maximize our range for the dimension width. Following the same procedure for confidence interval formula, this time for after being bootstrapping converted. The procedure was being conducted in excel and the lower bound for the calculation was 0.934183837. It is justified to said that the vehicles limit should be ranging from 0.93m up to 1.5m.

Due to the customers needs for this phase, that the UGV will only need to move on the vegetable plots only so the required dimension width will only be focus on vegetable only. According to [6] the suggested width will fall between 0.8m-1.2m

## 2.3 Material properties of the frame beams.

### 2.3.1 Definition of some material properties.

The essential phrase is "property of the material," which enables us to recognize the qualities of the material and use them in applications to get the most out of them with the least amount of work. Materials differ from one another according to particular qualities, much like the length, width, and height of an object do. The list of definitions for some mechanical properties of materials is provided below.



Figure 2-4 Material properties specification

When a material is deformed by an outside force, elastic behavior refers to the material's attempt to regain its original shape once the force has been removed. This mechanical characteristic of the materials is referred to as "elasticity". A body is said to be fully elastic if it completely regains its prior shape. It has been observed that if a force is applied to a body that causes it to deform over its elastic limit, part of its elasticity is lost. In the event that an external force completely disappears after causing deformation that exceeds the elastic limit, the body won't return to its original size and shape. Some anatomical deformity will be left over and last forever. [12]

**Elastic limit:** This is the distance past which a body cannot return to its original shape even after an external force has been removed. This causes the body's permanent deformity. Within a particular range, copper, aluminum, and steel are regarded as elastic bodies.

Plasticity is the opposite of elasticity is this. When the external force is applied, the material experiences inelastic strain. Plasticity is the reason of this. This helps us find materials that are easily deformed, which is useful in the forging and pressing business.

Brittleness: It is a ductility issue. Unable to be pulled into wire, brittle material fails when subjected to external force without undergoing considerable deformation. Some examples of brittle materials are glass, concrete, and cast iron.

Malleability: A substance is said to be malleable if it can be stretched out in all directions without rupturing. A material that is malleable has a high degree of flexibility but insufficient strength.

Toughness: It is a material's capacity to absorb energy without breaking. Strong material is required for cyclic and shock loads. To determine the material's toughness, a bend test is conducted.

Hardness: The material's resistance to surface abrasion or indentation is referred to as hardness. A Brinell number provides the clue.

Strength: A material's strength is what allows it to withstand fracture under load. This is the most significant characteristic since it enables us to determine the load value at which a material will fail.



Vietnamese-German University

In this thesis, strength of the material is one of the most contributed factors which will affect the design

### **2.3.2 Strength of material**

Material is one of the fundamental aspects to look at when it comes to the statical number detail determination of the structure. Engineering design process is heavily depending on the material selection. The item should be as robust and long-lasting as is practical. There are additional safety issues to take into account. Because of inadequate material selection, dangerous failures are still all too common in many industries. Regarding the requirement of the process, price is also one of the factors that has to be put into consideration. Some of the factor which will affect the design is stress, strain and maximum bending moment and all of this factor has close relationship to the material itself, which is demonstrate via stress, strain curve diagram in Fig [2.9]

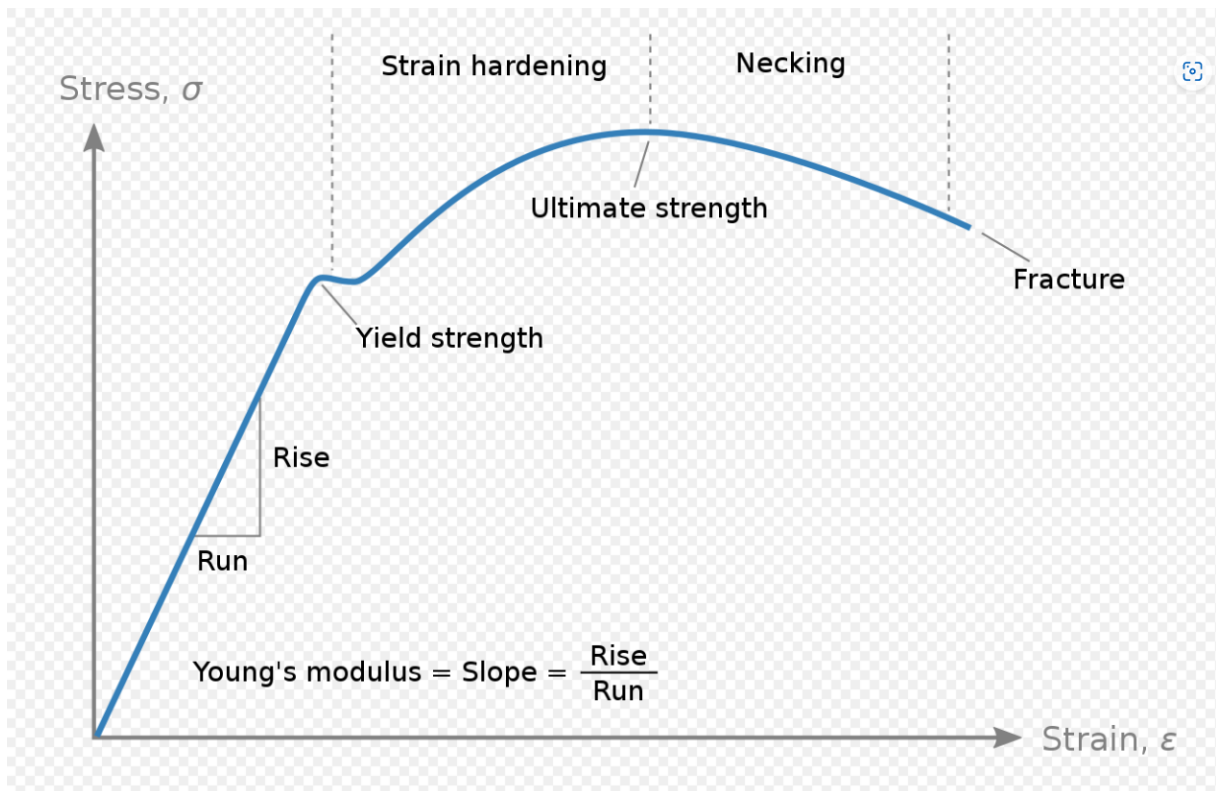


Figure 2-5 Stress , strain curve [9]

As illustrated above, young's modulus = Slope= Rise / Run, so the Young Modulus is equal to Stress / Strain, this is true according to Hooke's Law formular which states that stress is proportional to strain up to the limit of proportionality [9]. When an item quickly returns to its original shape after being distorted by a force, Hooke's law is commonly seen, with the molecules or atoms of its component pieces returning to the initial state of stable equilibrium. [10] . It is consistent with Hooke's law throughout its elastic range (i.e., for stresses below the yield strength). Only a fraction of the elastic range is where Hooke's rule holds true for some other materials, including aluminum. A proportionate limit stress for these materials is defined.

$$\sigma = E\epsilon.$$

Figure 2-6 Hooke's Law

Young modulus is know as the mechanical property E, commonly known as the Young's modulus or the modulus of elasticity in tension or compression, is used to determine a solid material's tensile or compressive stiffness when a force is applied longitudinally  $\sigma$  (i.e., negative tension). It measures the relationship between axial strain  $\epsilon$  (proportional deformation) and tensile/compressive stress sigma (force per unit area) .[11] The limits the use of this derivation to materials with linear elastic properties.

S. No.	Material	Modulus of elasticity (E) in GPa i.e. GN/m <sup>2</sup> or kN/mm <sup>2</sup>		
1.	Steel	200	to	220
2.	Wrought iron	190	to	200
3.	Cast iron	100	to	160
4.	Copper	90	to	110
5.	Brass	80	to	90
6.	Aluminium	60	to	80
7.	Timber	10		

Figure 2-7 The value of modulus of elasticity of some materials

Equation of stress

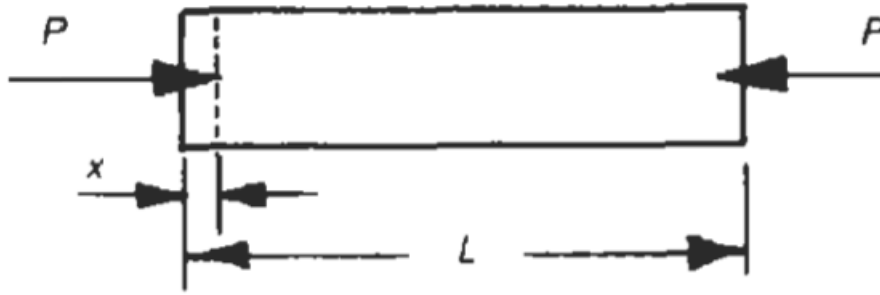


Figure 2-8 Stress  $\sigma$  illustration [9]

$$\sigma = \frac{P}{A} \quad (2.1)$$

In S.I. system, the unit of stress is pascal (Pa) which is equal to 1 N/m<sup>2</sup>. In actual practice, we use bigger units of stress i.e., megapascal (MPa) and gigapascal (GPa), which is equal to N/mm<sup>2</sup> or kN/mm<sup>2</sup> respectively.

Equation of strain

Figure 2-9 Strain  $\varepsilon$  illustration [9]

$$\varepsilon = \frac{\delta l}{L} \quad (2.2)$$

$P$  = Force or load applied on the body,

$l$  = Dimension of length ,

$A$  = Cross-section of the body,

$\sigma$  = Stress occur in the specimen ,

$E$  = Modulus of elasticity of the body,  $\varepsilon$  = Strain,

$\delta l$  = Deformation .

### 2.3.3 Stress, strain curve diagram of material

Vietnamese-German University

For a steel specimen, the graph showing the connection between stress and strain is depicted schematically (not to scale).

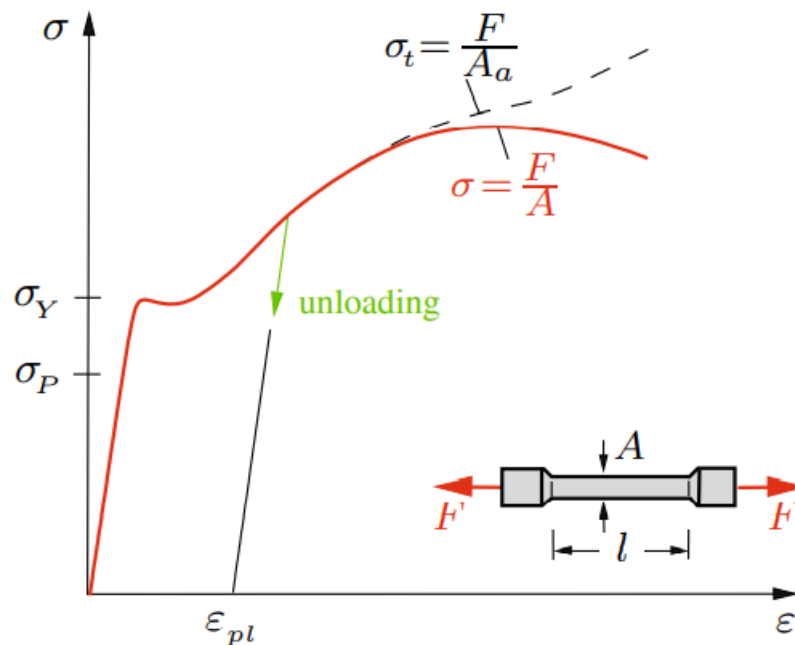


Figure 2-10 Stress and strain curve diagram [12]

This graph is known as a stress-strain diagram. At low levels of the strain, the relationship is linear (straight line), and the stress is proportional to the strain. This behavior is suitable up until the stress approaches the proportional limit  $P$ . If the stress exceeds the proportional limit, the curve's slope drops and the strain begins to rise more quickly. up until the yield stress  $Y$  is reached. At this point on the stress-strain curve, strain increases at virtually constant tension, and the material begins to give. Many materials lack a clear yield point, therefore be careful of this. The slope increases once again at the point of yielding, indicating that the material can support an extra load. Strain hardening is the name of this phenomena. [12]

## 2.4 Bending of Beams

### 2.4.1 Type of stress in mechanical engineering design

To be able to recognize tensions in varied structures, one must generalize the idea of stress. For this reason, imagine a body that has been arbitrarily loaded by a single force  $F_i$  and an area force  $P$ . (Fig. 2.15a). The external load generates internal forces. Internal forces (stresses) are dispersed across the complete area  $A$  in a fictitious segment  $s-s$  through the body [13]. These stresses now typically vary over the cross section, unlike the bar, where they are constant over the cross section.

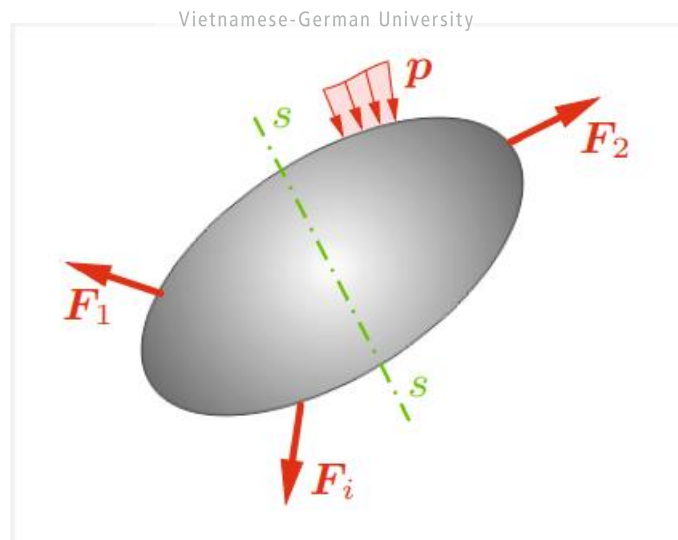


Figure 2-11 Single force acting on the specimen [14]

The stress must be defined at an arbitrary position  $P$  of the cross section because it is no longer constant across the section (Fig. 2.15b).



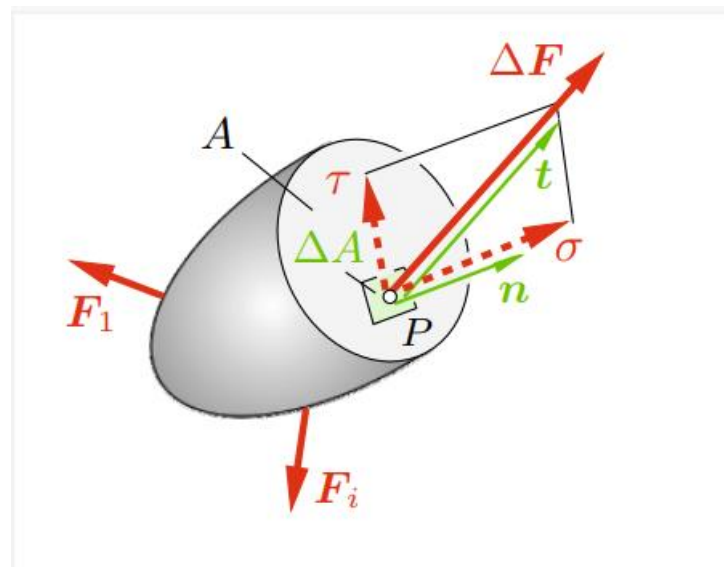


Figure 2-12 Specimen cut through [14]

The resulting internal force,  $F$ , is applied to the area element  $A$  that contains  $P$  (notice that, in accordance with the rule of action and reaction, the same force also operates in the opposite cross section in the opposite direction or 3<sup>rd</sup> Newton's Law). The ratio  $\Delta F / \Delta A$  is used to determine the average stress in an area element (force per area). We presume that the ratio  $\Delta F / \Delta A$  tends to a finite value in the limit  $\Delta A \rightarrow 0$ . This can be illustrated by the equation.

$$t = \lim_{\Delta A \rightarrow 0} \frac{\Delta F}{\Delta A} = \frac{dF}{dA} \quad (2.3)$$



Vietnamese-German University

The stress vector at point  $P$  has two components at the  $t$  value, one tangential to the cross section and the other normal to the cross section. Shear stress is the name given to the tangential component, and normal stress to the normal component. The stress vector  $t$  is impacted by point  $P$ 's location in section area  $A$ . The stress distribution throughout the section may be calculated when the stress vector  $t$  for each location on  $A$  is known. The stress situation at a location  $P$  of the section has not yet been adequately predicted by  $t$  for the reasons listed below. Because of the various ways that the area elements are orientated, if we select portions via  $P$  that have different directions, distinct forces will operate in those parts. As a result, the stresses are also influenced by the section's orientation, which is represented by the normal vector  $n$  [14]. Determining the axis of the Cartesian coordinate system for the respective orientations is useful. We may see the three sections more easily if we think of them as the surfaces of a volume element at point  $P$  with edge lengths  $dx$ ,  $dy$ , and  $dz$ .

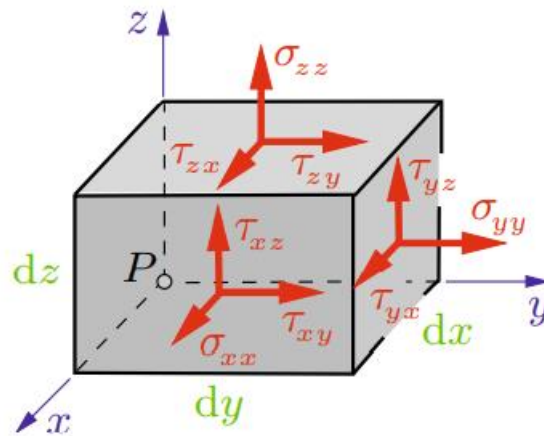


Figure 2-13 Shear and normal stress in 3D specimen [15]

The components are denoted by two subscripts: the first denotes the orientation of the section as indicated by the direction of its normal vector, and the second denotes the direction of the stress component. For instance, the stress  $\tau_{yx}$  operates on a portion whose normal is in the  $y$ -direction even if it points in the  $x$ -direction. (Also seen in Fig. 2.16)

For the typical stresses, the notation can be made simpler. In this instance, the directions of the section's normal and the stress component coincide, as seen in the following illustration.

$$\sigma_x^* = \sigma_x^*, \sigma_y^* = \sigma_y^*, \sigma_z^* = \sigma_z^* \quad (2.4)$$

Vietnamese-German University

Hence it is possible to write the section with the normal vector pointing in the  $y$  direction as follow [15]

$$t = \tau_{yx} e_x + \sigma_y^* e_y + \tau_{yz} e_z \quad (2.5)$$

The acquiree three normal stresses by breaking down the three stress vectors into their component parts ( $\sigma_x^*$ ,  $\sigma_y^*$ ,  $\sigma_z^*$ ) and six shear stresses ( $\tau_{xy}$ ,  $\tau_{xz}$ ,  $\tau_{yx}$ ,  $\tau_{yz}$ ,  $\tau_{zx}$ ,  $\tau_{zy}$ ). Given that equilibrium statements apply to forces, the associated area elements must be multiplied by the stresses which can be illustrated and visualized in Fig 2.17 which establishing the equilibrium condition for the moments along an axis that runs through the volume element's center and is parallel to the  $x$ -axis.

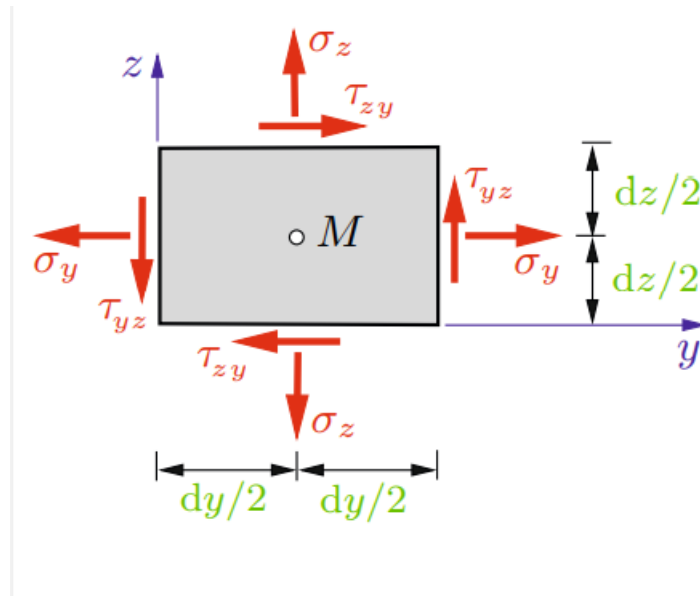


Figure 2-14 Equilibrium state formulation for shear and normal stress around x-axis [15]

Moment around center (C) :

$$2(dy/2) (\tau_{yz} dx dz) - 2(dz/2) (\tau_{zy} dx dy) = 0 \rightarrow \tau_{yz} = \tau_{zy} . (2.6)$$

By applying the formular for all 3 axis we can acquired the shear stresses in two orthogonal sections (like  $\tau_{xy}$ ' and  $\tau_{yx}$ ) with the same subscripts are identical [33]

$$\tau_{xy}' = \tau_{yx} , \tau_{xz}' = \tau_{zx} , \tau_{yz} = \tau_{zy} . (2.7)$$

The components of the three stress vectors can be showed in a matrix

$$\begin{matrix} \sigma_x & \tau_{xy} & \tau_{xz} & \sigma_x & \tau_{xy} & \tau_{xz} \\ \tau_{yx} & \sigma_y & \tau_{yz} & \tau_{xy} & \sigma_y & \tau_{yz} \\ \tau_{zx} & \tau_{zy} & \sigma_z & \tau_{xz} & \tau_{yz} & \sigma_z \end{matrix} = \sigma (2.8)$$

The matrix (2.8) has the symmetry appearance is due to the equation (2.7)

#### 2.4.2 Normal, shear stress in angle geometry and maximum normal and shear stress of the mechanical component

As of yet, the general theory can only explain stresses in sections that are perpendicular to the specified coordinate or parallel to the coordinate axes. But, in the UGV frame design, the task must contend with more, and it is necessary to be able to operate in a variety of coordinated axes. Consider a narrow, wedge-shaped portion that was removed from a disk with thickness  $t$  for this scenario (Fig. 2.18). The angles and the  $x, y$  coordinate system are used to specify the directions of the sections. the creation of an  $x, y$  system that is rotated by an angle with respect to the  $x, y$  system and whose  $z$ -axis is normal to the inclined section. The angle is specified here.. Here, the angle  $\phi$  set to be positive and counterclockwise counted.

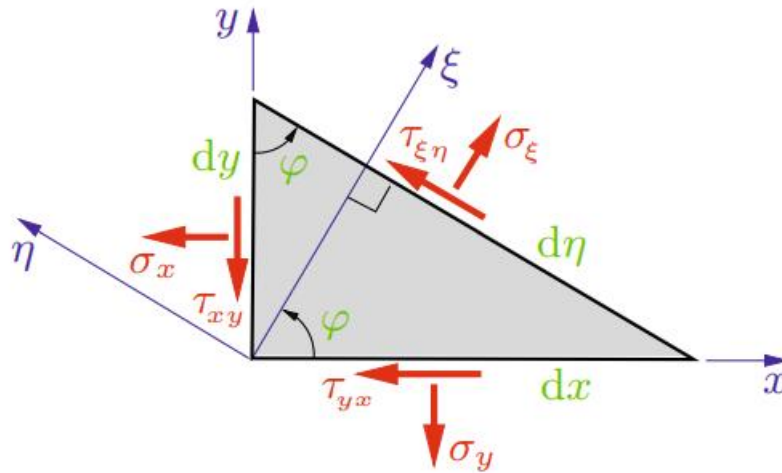


Figure 2-15 The  $x, y$  coordinate system with respected to  $\xi, \eta$ -system [39]

The stresses in the incline are represented by the symbols  $\sigma_{\xi}$  and  $\tau_{\xi\eta}$ .  $dA = d\eta t$  yields the corresponding cross section.  $dA \sin$  and  $dA \cos$  are the other two cross sections that are perpendicular to the  $y$ - and  $x$ -axes, respectively. From the equilibrium definition the corresponding stress and strain accordingly to the axis is presented the (Eqn 2.8a) the proving stage was performed already [39]. In in the thesis, only the finally formulars is used the equation also known as the transformation relation.

$$\begin{aligned} \Sigma \sigma_{\xi} l &= \frac{1}{2} (\sigma_x l + \sigma_y l) + \frac{1}{2} (\sigma_x l - \sigma_y l) \cos(2(\phi)) + \tau_{xy} l' \sin(2(\phi)) \\ \Sigma \eta l &= \frac{1}{2} (\sigma_x l + \sigma_y l) - \frac{1}{2} (\sigma_x l - \sigma_y l) \cos(2(\phi)) - \tau_{xy} l' \sin(2(\phi)) \quad (2.8a) \\ \tau_{\xi\eta} &= -\frac{1}{2} (\sigma_x l - \sigma_y l) \sin(2(\phi)) + \tau_{xy} l' \cos(2(\phi)). \end{aligned}$$

As illustrated in equation (2.8), the components  $\sigma_{\xi}$ ,  $\sigma_{\eta}$  and  $\tau_{\xi\eta}$  is depended on the changing angle ( $\phi$ ). Determination for the extreme value for  $\sigma$  was carried out by derive the relation of  $d\sigma_{\xi}/d\phi = 0$  and  $d\sigma_{\eta}/d\phi = 0$ . Which from (Eqn 2.8a) leading to the following relation

$$-(\sigma_x - \sigma_y) \sin 2\phi + 2\tau_{xy} \cos 2\phi = 0 \quad (2.8b)$$

Called  $\phi^*$  is angle that leads to a maximum or a minimum value of (Eqn 2.8b) which lead to the following relation

$$\begin{aligned} \tan(2\phi^*) &= \frac{2\tau_{xy}}{\sigma_x - \sigma_y} \quad (2.8b) \\ \cos(2\phi^*) &= \frac{1}{\sqrt{1 + \tan^2(2\phi^*)}} = \frac{\sigma_x - \sigma_y}{\sqrt{(\sigma_x - \sigma_y)^2 + 4\tau_{xy}^2}} \\ \sin(2\phi^*) &= \frac{\tan(2\phi^*)}{\sqrt{1 + (\tan(2\phi^*))^2}} = \frac{2\tau_{xy}}{\sqrt{(\sigma_x - \sigma_y)^2 + 4\tau_{xy}^2}} \quad (2.8c) \end{aligned}$$

From (2.8b) use the notations of  $\sigma_1$  and  $\sigma_2$  for the maximum and minimum value of normal stress will be

$$\sigma_{1,2} = \frac{1}{2} (\sigma_x + \sigma_y) \pm \frac{\frac{1}{2} (\sigma_x - \sigma_y)^2}{\sqrt{(\sigma_x - \sigma_y)^2 + 4\tau_{xy}^2}} \pm \frac{2\tau_{xy}^2}{\sqrt{(\sigma_x - \sigma_y)^2 + 4\tau_{xy}^2}} \quad (2.9)$$

$(\phi^*)$  and  $+(\phi^* + \pi/2)$  (principal directions) are given two values in equation (2.8b). For example, these two angles can be used to represent the stresses  $\sigma_1$  and  $\sigma_2$  in equation (2.8a). With that constrain the value for neither  $\sigma_1$  or  $\sigma_2$  would be found.

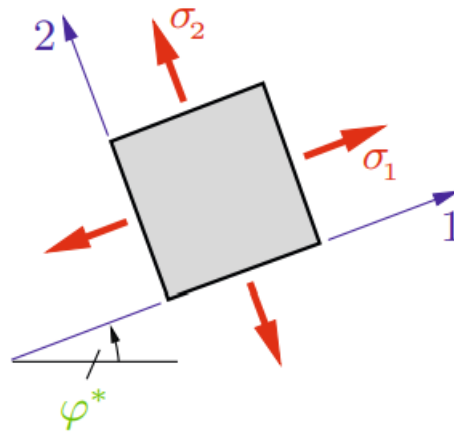


Figure 2-16 The value of  $\sigma_1$  or  $\sigma_2$  with respect to the angle  $\phi^*$  [39]

Applying the same procedure and introduce the new value  $\phi^{**}$  and a new coordinate system with its axes pointing in the principal directions. Let donate  $\sigma_1$  and  $\sigma_2$  as the two axes by 1 and 2.

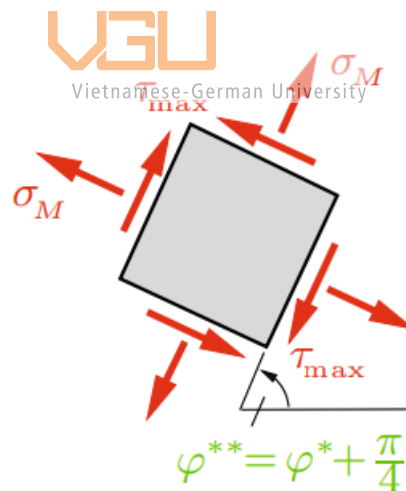


Figure 2-17 the stresses  $\sigma_1$  and  $\sigma_2$  at an element in the x, y-system [39]

The extreme value of shear stress is associated with the angle and direction of the specimen.

From boundaries condition  $\frac{d\tau_{\xi\eta}}{d\phi} = 0$  the angle for which extreme shear is

$$\tan(2\phi^{**}) = -\frac{\sigma_x - \sigma_y}{2\tau_{xy}} \quad (2.10)$$

the direction  $\phi^{**}$  of the extreme shear stress is rotated by  $45^\circ$  with respect to the direction  $\phi^*$  of the extreme normal stress [38] which gives the formular for the maximum shear will be.

$$\tau_{max} = \pm \sqrt{\left(\frac{\sigma_x - \sigma_y}{2}\right)^2 + \tau_{xy}^2} \quad (2.11)$$

### 2.4.5 The parallel-axis theorem to determine moment of inertia $I$ in specific cross-section geometry.

The beam is one of the most important parts in engineering. The geometric shape of a beam is that of a straight bar because its cross-sectional area is significantly less than its length [39]. Nevertheless, unlike the truss Deformation of the originally straight beam, it is loaded by forces that are perpendicular to its axis (Fig. 2.18). In this case, the beam is said to be bent. As a result, the beam experiences internal forces (also known as stresses), which result in the components of the shear force  $V$  and bending moment  $M$ .

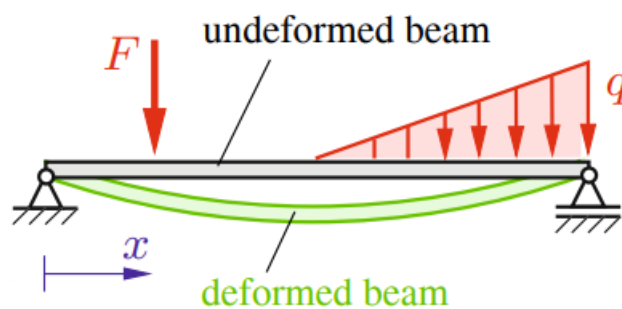


Figure 2-18 Beam bending [40]

Consider the beam shown in Fig. 2.19, where the  $z$ -axis forms a symmetry. According to Volume 1, the  $x$ -axis is parallel to the axis of the beam and passes through the centroid  $C$ 's cross-sectional area  $A$ .

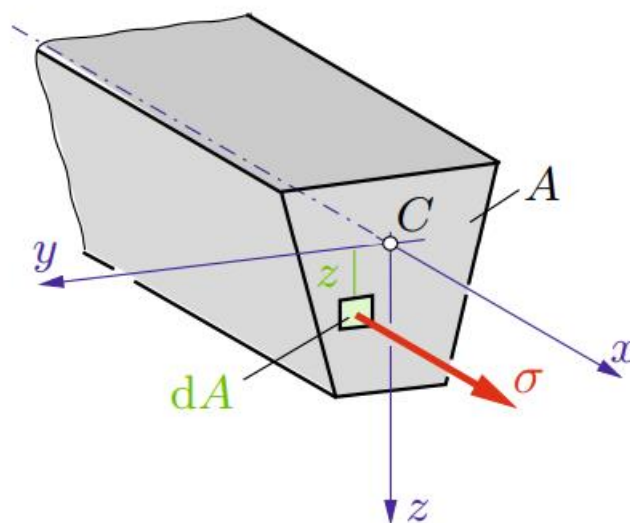


Figure 2-19 The  $x$ -axis is aligned with the beam's axis [40]

When there is neither shear force or normal force present, the load is thought to just produce a bending moment  $M$ . (no shear force and no normal force). Hence, the beam is thought to be in a pure bending condition. For instance, in the region where two forces  $F$  are operating at the beam in Fig. 2.20, this is the case.

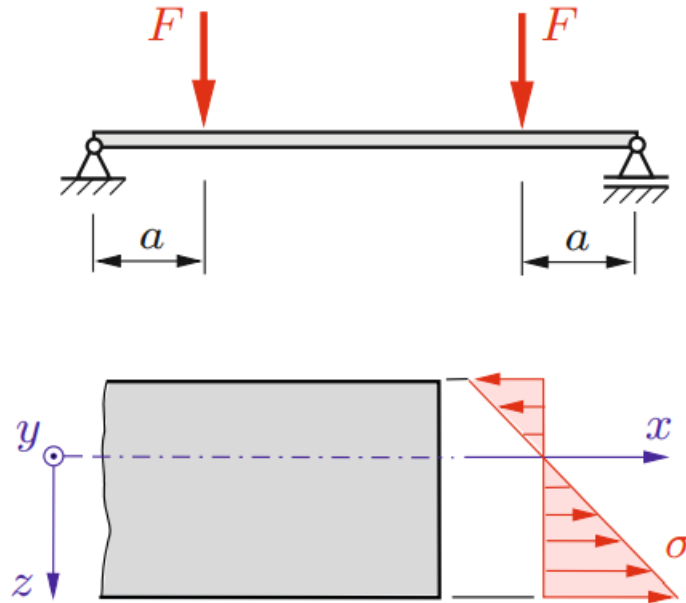


Figure 2-20 Inertia force [41]

About the clear bending, the only stresses are normal stresses, which act in the cross-sectional areas in the direction of the  $x$ -axis (Figs. 2.19, 2.21). They are independent of the  $y$ -coordinate and have a linear distribution in the  $z$ -direction. Dietmar Gross and Khurmi conducted this investigation [40, 41].



Figure 2-21 Moment of inertia [41]

Hence, the normal stresses may be written as with  $c$  being a force acting in the portion  $z$  area

$$\sigma(z) = cz \quad (2.12)$$

With the introduction the infinitesimal force  $dF = \sigma dA$  causes the infinitesimal moment  $dM = zdF = z\sigma dA$  which can be illustrated in Fig 2.19b, d. Integration the yield this gives

$M = \int z \sigma dA$  combined with 2.12 that leading to the moment of inertia formular.

$I = \int z^2 dA$  (2.13) with the addition notation as  $c = M/I$  and relation in (2.12) this give the relation between stress and bending moment as follow:

$$\sigma(z) = \frac{M}{I} z \quad (2.14)$$

According to Christiaan Huygens and Jakob Steiner studies and theorem , calculation for moment of inertia can be done via the axis across the center of gravity of the item and the perpendicular distance between the axes [42] [43]. The moment of inertia is heavily affected by the geometry and cross-section of the specimen with can be seen in Eqn (2.13) and though the studies of Jiankun Peng, Dawei Pi, Yue Wang and Fengyan Yi [44]. As illustrated in Figure below.

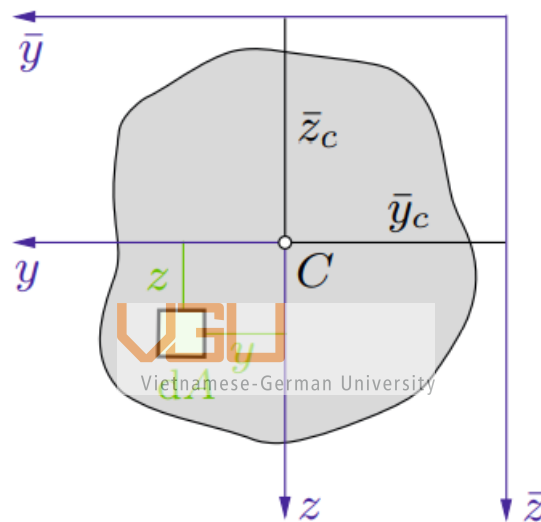


Figure 2-22 Moment of inertia of any arbitrary geometry [40]

From the Fig (2.22), based on the geometry condition the relation for  $\bar{y}$ ,  $\bar{z}$  and  $y$ ,  $z$  can be obtained and with relation in eqn (2.13) the final equation for the moment of inertia in arbitrary geometry is present as follow

$$I_{\bar{y}} = I_y + \bar{z}c^2 A,$$

$$I_{\bar{z}} = I_z + \bar{y}c^2 A,$$

$$I_{\bar{y}\bar{z}} = I_{yz} + \bar{y}c \bar{z}c A, \quad (2.14)$$

#### 2.4.7 Equations of Bending

In conventional beam theories, the beam is viewed as a 1D line that runs along the beam's centroid axis. Thus,  $x$  determines transverse deflection, slope, and other parameters. For the centroid of the beam cross-section, governing equations are established, and supports are



considered to be on the beam's centroid. The equations were developed using the uniformly loaded single span, simply supported beam depicted in Fig. 34 and the derivation of the general formular has been conducted via Hakan T. Türker [56] studies.

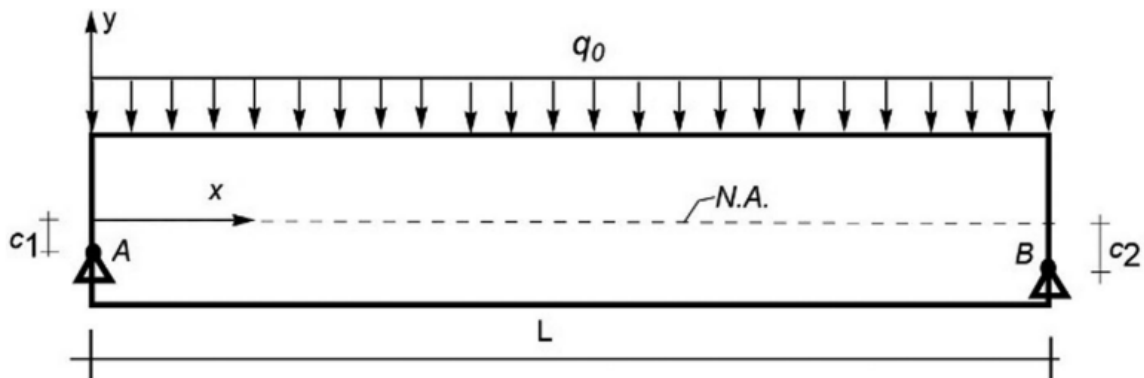


Figure 2-23 General beam geometry and support locations.

Using MacLaurin series the transverse deflection ( $w(x)$ ) curve of a beam in the  $x$ -direction is as follows:

$$w(x) = w(0) + w'(0)x + \frac{x^2}{2!} w''(0) + \frac{x^3}{3!} w'''(0) + \frac{x^4}{4!} w^{(4)}(0) + \frac{x^n}{n!} w^{(n)}(0) + \dots$$

$w^{(n)}$  denotes the value of  $w(x)$  and its  $n$ th derivatives at the origin,  $x = 0$ .

$$q(x) = EI \frac{d^4 w}{dx^4}$$

$$\theta(x) = \frac{dw}{dx}$$

$$M(x) = -EI \frac{d^2 w}{dx^2}$$

$$V(x) = -EI \frac{d^3 w}{dx^3}$$

where  $q(x)$ ,  $w(x)$ ,  $\beta(x)$ ,  $M(x)$ ,  $V(x)$  are distributed load, the transverse displacements, rotation, bending moment and shear forces of the beam, respectively

Thus, the axial normal stress increases linearly from zero at the neutral axis to a maximum at the beam's outer surfaces, much like the strain does [34].

#### 2.4.8 Finite element method

Beam equations are historically significant because they drew the attention of prominent scientists such as Leonardo da Vinci (14th century) and Daniel Bernoulli (18th Century).

Beam uses in practice used equations can be found in mechanical constructions designed on the basis of beam theory. The significance of beam over the years, theory has been detailed in the literature [45] [46] [47]. The Finite Element Method (FEM) is one of the most powerful structural analysis techniques. Finite Element Analysis is founded on the idea that by subdividing a larger complicated structure into smaller non-overlapping components of basic geometry known as finite elements, an approximate solution to any complex engineering issue may be found. The complex partial differential equations that describe these structures may be reduced to a set of linear equations that can be solved quickly using this approach. It is straightforward and gives appropriate engineering approximations for a wide range of situations. In the thesis, the Galerkin Finite Element Method [48] is used to solve the beam problem using Matlab.

There have been many scientific proofs about the accuracy of FEM corresponding to the experiment method. All of which made a conclusion that FEM bring to the table a pretty precise results and now has been widely used in many engineering applications [49] [50] [51] In Galerkin Finite Element Method the problem at hand is the domain or the intervals (the length of the beam) is partitioned into a finite collection of line elements, each with at least two end nodes. The element is geometrically identical to that used for bars.

$$\begin{aligned} \frac{d^2}{dx^2} \left[ EI \frac{d^2 u}{dx^2} \right] &= p(x), \quad 0 \leq x \leq L, \\ u(0) &= a_0, \quad \frac{d^2 u(0)}{dx^2} = b_0, \\ u(L) &= a_L, \quad \frac{d^2 u(L)}{dx^2} = b_L. \end{aligned} \quad (2.15)$$

For the linear case  $f(x, u) = q(x)u + p(x)$ , where  $u(x)$  is the deflection of the beam,  $q(x)$  is the coefficient of ground elasticity, and  $p(x)$  is the uniform load applied normal to the beam. The main ideal of using FEM is to determine the boundaries condition and using integral computation based on backward, forward and central integration [51] [52]

$$\text{Central difference} = \frac{df(x)}{dx} = \frac{f(x+h) - f(x-h)}{2h}$$

$$\text{Forward difference} = \frac{df(x)}{dx} = \frac{f(x+h) - f(x)}{h}$$

$$\text{Backward difference} = \frac{df(x)}{dx} = \frac{f(x) - f(x-h)}{h}$$

It is suggested in [53] investigations that the central delivers the most accurate solutions for the issues under the best assumption. The element is equivalent to the one used for bars geometrically. The objective is to identify the weak form of the differential equation. To spread the order of differentiation on  $u$  and  $w$  evenly, we achieve this by multiplying the

residual of differential equation (2.15) by a weight function  $w(x)$  and then integrating it in sections. The result is the equation.

$$\int_0^L \left[ EI \frac{d^4 u}{dx^4} - p(x) \right] w \, dx = EI \frac{d^3 u}{dx^3} w \Big|_0^L - EI \frac{d^2 u}{dx^2} \frac{dw}{dx} \Big|_0^L + \int_0^L \left[ EI \frac{d^2 w}{dx^2} \frac{d^2 u}{dx^2} - pw \, dx \right] = 0.$$

(2.16)



Vietnamese-German University

### 3 Requirement determination

Problems must first be thoroughly understood in order to go forward appropriately toward a desired objective. The present issue has already been taken into consideration using facts and research, as can be seen in the abstract, introduction, and review sections. However, the lack of a scientifically rigorous framework in the study makes it difficult to communicate this significant issue in a comprehensible manner. The goal of this requirement phase is to make the design objective (problem/issue) clear in order to guarantee that all design tasks, from the fundamental to the intricate, are well understood.

#### 3.1 *Problem statement clarifying the most central need*

In order to develop a more succinct understanding of the problem, the most fundamental components from all descriptions related to it are first removed and compiled into one unit. Three topics, namely the target, its need, and the justifications for that need, may be used to build this unit. By responding to each of these questions in turn, then integrating them into a single phrase, the problem statement for this process can be clarified as follow: “a frame needs to be able to withstand the load of external component also fulfills the modulation feature and the combination of each component needs to be fit with each other without cause any deformation”.

#### 3.2 *Functional requirement*

The issue description provided above is not sufficient for the subsequent design processes since it just serves to remind us of the primary objective that must be fulfilled first while ignoring any other less crucial factors. Additionally, the need lacks information and just provides an overview of this first description. Therefore, using an objective tree diagram helps one gain a deeper knowledge of the core of these demands. The first step in creating an objective tree diagram is to outline every criterion. Because a function only adds value when it meets the expectations of the customer, it is vital to complete this duty by speaking with the supervisor, who assumes the position of the client. By taking this move, time and money wasted on developing unneeded qualities may be avoided. The objective tree below is for the whole robot, however in the thesis the emphasis is on the statics and loading capacities of the frame, thus analysis of each beam component will be put into consideration.

The available criteria are categorized into several groups after the list has been created. Then they are organized from the broadest to the most specific. By identifying ways to fulfill the

need and its function for each group, more elements are added. In order to provide a better illustration, group "practical" is looked into detail to show the processes required to create its branches in figure 3-1A, where the red words stand in for the additional components

Visual Paradigm Online Free Edition

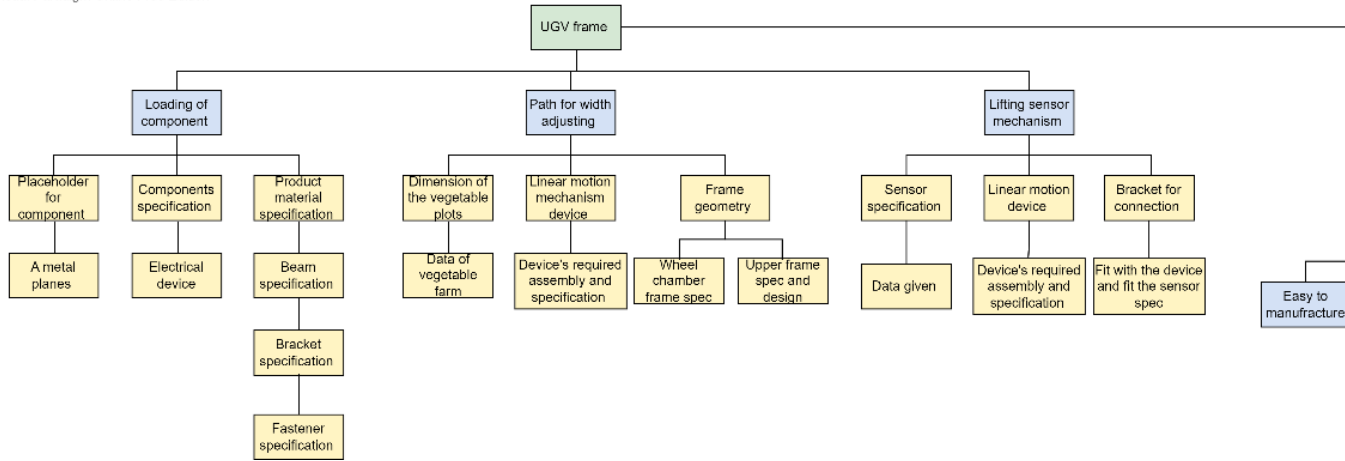


Figure 3-1 Functional requirement

### 3.3 Functional requirement evaluation

Figure 3-1 displays a range of significance scores, from lowest to greatest, before considering the priority of each need described in the tree diagram above.

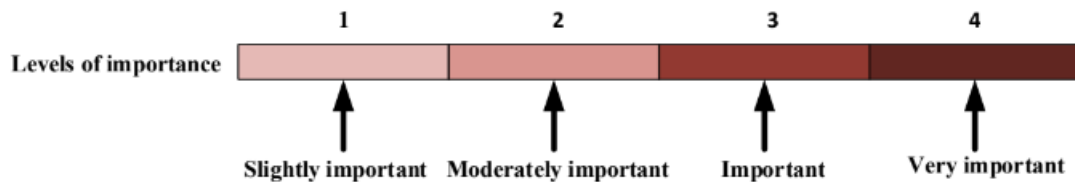


Figure 3-2 Ranking definition for functional requirements

The relevance levels of these functional demands derived from the base of the tree diagram are graded in table 3-1 after understanding the meanings of these scores.

Table 3.1. Importance ranking of functional requirements

No.	Functional requirements	Rank
1	Withstand loading components	4
2	Adjust to fit the required vegetable plots	4
3	Adjustable sensor height	4

4	Sensor stability	3
5	Money saving	3
6	Manufacture easily	3
7	Popular component	2
8	Assemble-disassemble easily	3
9	Safety	2
10	Durable	2
11	Optimize the arrangement of components	2
12	Joining performance	4

Because customer feedback is always at the heart of design, getting the supervisor's permission is crucial for these rankings (Womack, Jones, & Roos, 1991). Additionally, this table plays a key role in the step of selecting the most promising concept to create.

### 3.4 Technical requirements

Vietnamese-German University

The technical requirements relate to the frame analysis, these technological characteristics might allude to issues such as performance difficulties, system dependability and accessibility. Technological requirements, in essence, serve as solutions to technical problems. The system (UGV) in order to head into the design phase needs to have a clear path on what to do in order to fit the functional requirement as stated in index 3.1. Afterward will lead to the procedure of determine the right solution to design the frame.

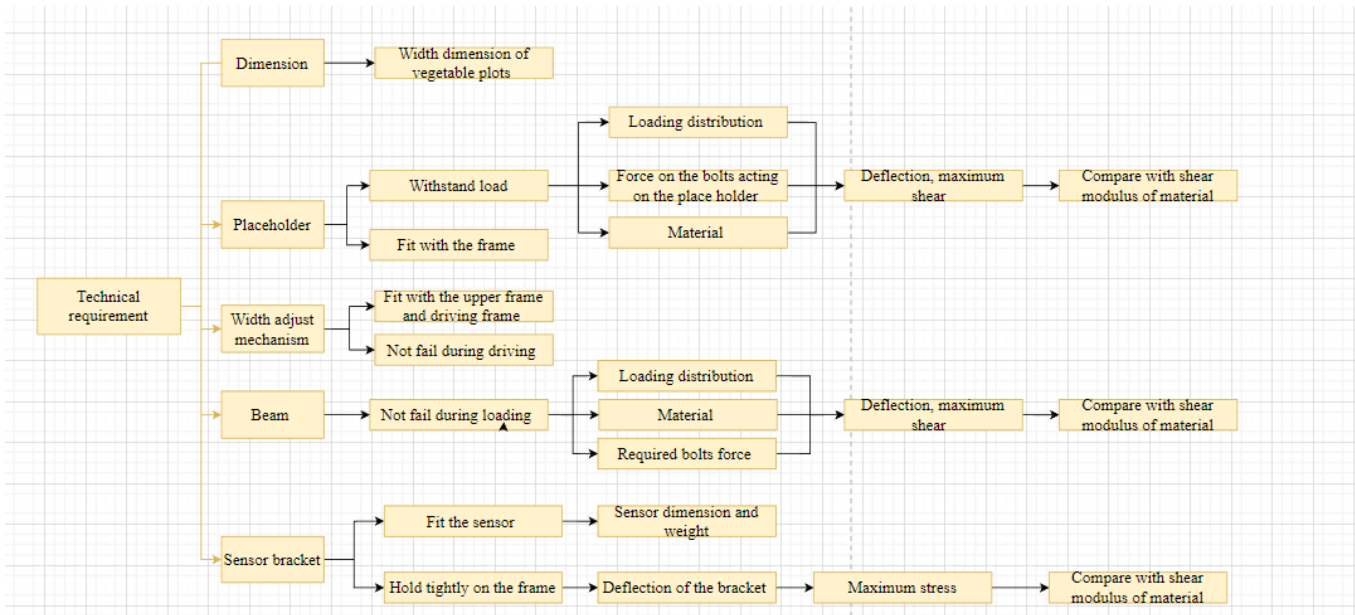


Figure 3-3 Technical requirements solution procedure

## 4 Development and selection

It is not a good idea to start developing an arbitrary solution straight after defining the criteria since better ones can go unnoticed. As a result, this chapter offers workable options for consideration in order to select the best concept for further development.

### 4.1 Concept evaluation

The concepts of decision are widely used in determine and sort out any kind of product means relating to the design. The index corresponding to the functional requirements in table 3.1 is called Criteria. The weighting factor indicates how much of a percentage a requirement's important value takes in comparison to the others.

$$\text{WeightingFactor(\%)} = \text{Important Rank (ImportantRank)} \quad (4-1)$$

Formula 4-2 is then used to compute the weighted score. Finally, consider the total weighted score of all individual solutions that serve as the foundation for selecting the best one. Each criterion's performance level is ranked on a scale of 0 (worst) to 7 points (the best).

$$\text{Weighted Score} = \text{Weighting Factor} * \text{Score} \quad (4-2)$$



### 4.2 Concept table

Table 4.1 Options table

Category		Choice			
Base frame	Material	Profile aluminum	Steel	—	—
	Placeholder material	Aluminum	Sheet metal	—	—
	Joining method	Bracket, screwing	Welding, screwing	Bracket, bolts fastener	—
Sensor lifting	Method	Ball screw	Actuator	Pulley system	Profile aluminum and



					roller
	<b>Motor</b>	Servo	DC motor	Step	Manually
	<b>Method</b>	Manually	Automatics		Manually
<b>Sensor data taken method</b>	<b>Method</b>	Stop and go	—	—	Moving and taken picture
<b>Main frame width adjustment</b>	<b>Feature</b>	Actuator	roller	Vit me	Sliding with stopper
	<b>Control</b>	Manually	Semi-automatics	—	—

Based on the required determination table 4.1 illustrated the options that are available and commonly used based on specific feature

#### 4.2.1 Concept 1 – level basic

Building a product that is simple to manufacture, uses the least number of resources, and satisfies the most basic needs is the goal of level Basic. However, neither the stability nor the user interface have been enhanced, if anything.

Category		Choice			
<b>Base frame</b>	<b>Material</b>	Profile aluminum	Steel	—	—
	<b>Placeholder material</b>	Aluminum	Sheet metal	—	—
	<b>Joining method</b>	Bracket, screwing	Welding, screwing	Bracket, bolts fastener	—
<b>Sensor lifting</b>	<b>Method</b>	Ball screw	Actuator	Pulley system	Profile aluminum and roller
	<b>Motor</b>	Servo	DC motor	Step	Manually
<b>Sensor data taken method</b>	<b>Method</b>	Stop and go	—	—	Moving and taken picture

<b>Main frame width adjustment</b>	<b>Feature</b>	Actuator	Chain and motor	Vit me	Sliding with stopper
	<b>Control</b>	Manually	Semi-automatics	—	—

#### 4.2.2 Concept 2 – level intermediate

Because the structure is no longer really mechanical, level intermediate is harder. In addition, the complexity of the features and the electronics connection drive up the cost of manufacturing this design. However, the product is easier to use and manipulate. Additionally, stability and precision also improve.

<b>Category</b>		<b>Choice</b>			
<b>Base frame</b>	<b>Material</b>	Profile aluminum	Steel	—	—
	<b>Placeholder material</b>	Aluminum	Sheet metal	—	—
	<b>Joining method</b>	Bracket, screwing	Welding, screwing	Bracket, bolts fastener	—
<b>Sensor lifting</b>	<b>Method</b>	Ball screw	Actuator	Pulley system	Profile aluminum and roller
	<b>Motor</b>	Servo	DC motor	Step	Manually
	<b>Method</b>	Manually	Automatics	—	Manually
<b>Sensor data taken method</b>	<b>Method</b>	Stop and go	—	—	Moving and taken picture
<b>Main frame width adjustment</b>	<b>Method</b>	Actuator	Chain and motor	Vit me	Sliding with stopper
	<b>Control</b>	Manually	Semi-automatics	—	—

### 4.2.3 Concept 3 – level advance

In advance level concept, the overall performance is increased, with the addition improvements in material, joining method and more feature will be mostly carried out by semi-automatics devices. Which lead to overall precision and usage increased. As a consequence, it's more time consuming, more budget to fulfill and the manufacturing will be more complex.

Category		Choice			
Base frame	Material	Profile aluminum	Steel	—	—
	Placeholder material	Aluminum	Sheet metal	—	—
	Joining method	Bracket, screwing	Welding, screwing	Bracket, bolts fastener	—
Sensor lifting	Method	Ball screw	Actuator	Pulley system	Profile aluminum and roller
	Motor	Servo	DC motor	Step	Manually
	Method	Manually	Automatics	—	Manually
Sensor data taken method	Method	Stop and go	—	—	Moving and taken picture
Main frame width adjustment	Method	Actuator	Chain and motor	Vit me	Sliding with stopper
	Control	Manually	Semi-automatics	—	—

### 4.3 Concept evaluation

Criteria	1	2	3	4	5	6	7	8	9	10	11	12	Sum
Weighting factor	4	4	4	3	3	3	2	3	2	2	2	4	36

Concept 1	Core	4	3	3	2	3	3	2	3	1	2	1	3	30
	Weighted score	16	12	12	6	9	9	4	9	2	4	2	12	97
Concept 2	Core	4	3	4	3	2	2	1	2	2	2	1	3	29
	Weighted score	16	12	16	9	6	6	2	6	4	4	2	12	95
Concept 3	Core	4	4	4	3	1	1	1	1	2	2	2	4	29
	Weighted score	16	16	16	9	3	3	2	3	4	4	4	16	96



## 5 Implement of the chosen concept

### 5.1 Design of complex aluminum extrusions

Over the past few years, the use of aluminum alloys as structural materials has increased due to their beneficial properties, such as their high strength-to-weight ratio, ease of fabrication, high degree of workability, significant ductility, excellent thermal conductivity, high corrosion resistance, and attractive appearance at their natural finish [64]. Aluminum extrusion profile can be comprised of many material alloys (Fig 5.1) each differ from each other in term of stress yield and tensile strength.

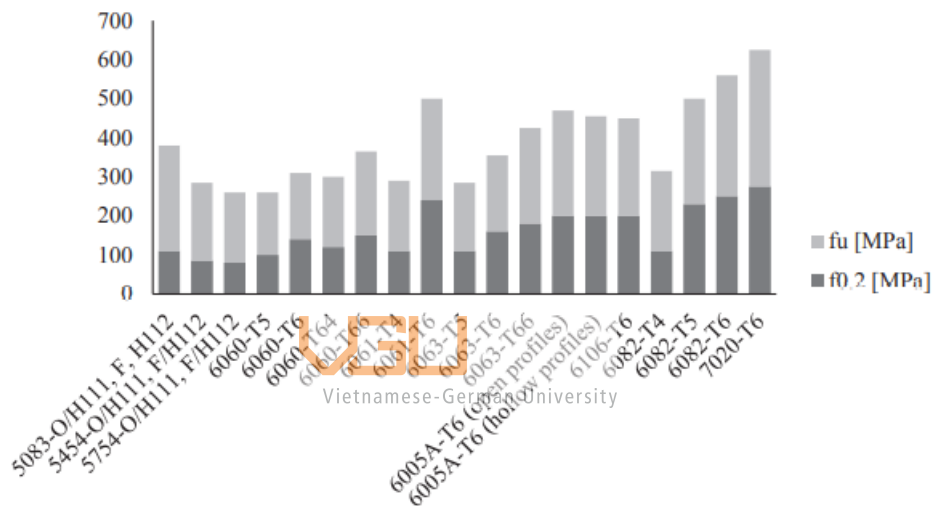


Figure 5-1 Tensile and yield strengths of frequently used aluminum [65]

Due of its mechanical characteristics, the 6xxx series is the most appealing for structural engineering applications [65,66]. However, material of the extruded profile aluminum that being used in VietNam is mostly (6063-T5). The analysis will be based on the mentioned aluminum properties. The considering parameter will be the length of the beam, the cross-section area and the load that distributed on to the beam. From which can determine the right parameter and size of the aluminum beam. The analysis will focus on the stress and maximum loading capacity of the beam. The problem will focus a lot on the uniformly distributed of load onto the beam, since the assumption of the loading problem is an aluminum sheet will be put on the beam and the electrical part of the UGV will also be put on the sheet.

The beam (AL1) will have the mechanical properties as follow:

Table 5.1. Material of the beam

Material	6063-T5
Tensile strength (N/mm <sup>2</sup> )	245
Shear Modulus (N/mm <sup>2</sup> )	25800
Elastics Modulus (N/mm <sup>2</sup> )	69972
Yield strength (N/mm <sup>2</sup> )	145

According to FEM as mention 2.4.8, in order to determine the displacement of the beam, the moment of inertia. The method is to conduct analysis of the stress and deflection the beam in order to find out the right dimension of the beam the calculation will be done by FEM method and the statistics of the stress and deflection will be compare with the properties of the material. As suggested by Misumi VietNam [71], the crossed section of each material being choose is divided into category. As illustrated in Fig 5.2:







	HFS Series	HFSL Series	EFS Series	NFS (NEFS, NFSL) Series	GFS Series	SLF Series
Photo						
Material	A6N01SS-T5	A6N01SS-T5	A6N01SS-T5	A6063S-T5	A6061SS-T6 Equivalent	A6063SS-T5
Features	Standard cross section shape.	Lightweight and economical extrusions. Suitable for use when light weight and economical price are given priority over strength.	Have rigidity equivalent to HFS Series yet lighter and more economical.	Material change to A6063S-T5 led to significant price reduction. The Cross Section Shape and Cross Sectional Moment of inertia are the same as those of HFS, HFSL and EFS Series. Stress and tensile strength decrease due to material change. The color may vary slightly.*	These thick extrusions offer high rigidity and are suitable for use in high load.	Has 4 slotless flat enclosures. Excels in sanitary control since dust is not collected in slots. Various accessories for aluminum extrusions can be utilized by combining with Slot Type (SLF6-4040, etc.)
Surface Treatment	Clear Anodize (HFS) Black Anodize (HFSB) Clear Coating (CAF) Baked Paint (Yellow) (HFSY)	Clear Anodize Black Anodize	Clear Anodize (EFS) Black Anodize (EFSB)	Clear Anodize Black Anodize	Clear Anodize	Clear Anodize
Representative Product	HFS8-4040	HFSL8-4040	EFS8-4040	NFS5-2020 (Different Material of HFS5-2020) NFS8-4040 (Different Material of EFS8-4040) NFSL6-3030 (Different Material of HFSL6-3030)	GFS8-100100	SLF6-4040 (No Slot Type) SLF6-4040 (1 Slot Type)

Figure 5-2 Categories of aluminum profile

The chosen cross section is then being looked up in Fig 5.2 for determination of moment of inertia.

HFS (Standard Type)

HFS (Standard Type)

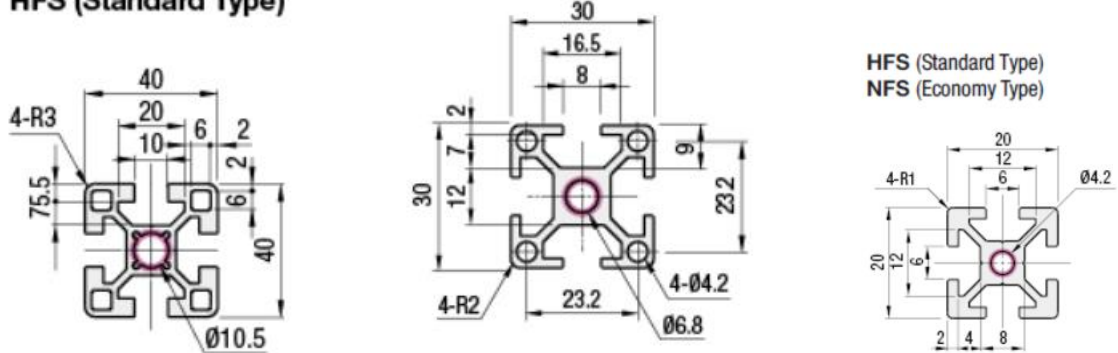


Figure 5-3 Cross-section area of the chosen beam

The chosen crossed section results match the Figure 5.2 is then illustrated in the Table 5.2

Table 5.2. Code name of the chosen crossed section with respect to the manufacture

Type	Code name
30*30	HFS
40*40	HFS
20*20	HFS



Using the The parallel-axis theorem as briefly illustrated in section 2.4.5, the overall formular to calculate the cross-section area will be

$$I_{parallel\ axis} = I_c + A d^2$$

If having a complex or composition cross section area (Fig 5.3) introduction to Eqn

$$I_{cx.IBeam} = I_{cx.W} + (I_{cx.F1} + A_{F1} d_1^2) + (I_{cx.F2} + A_{F2} d_2^2)$$

Then the overall moment of inertia of the component will be as follow,

Table 5.3. Cross Sectional of Moment of Inertia of extruded aluminum profile

Type	Cross Sectional Moment of Inertia x (10 <sup>4</sup> ) (mm <sup>4</sup> )	Height x Width (mm)
20*20	0,742	20*20
30*30	2,83	30*30

40*40	10,4	40*40
-------	------	-------

Knowing the moment of inertia is crucial to determine the maximum stress and deflection of the beam. Thus in chapter 2, the reasonable width of the UGV has been determined 1.2m. So the overall length for the study simulation is 1.2m. Applying Finite Element method as mentioned in section 2.4.7 and 2.4.8 to create the simulation for loading capacity of the frame was done with matlab to construct the problem (A.6) and conducted via solid work to determine the maximum stress and deflection have the results as follows. It is best to mention that in each analysis the distribution of load due to the change of dimension of the aluminum plane sheet will vary respectively to the corresponding size of the aluminum beam. The principle of load is illustrated in Fig 5.2. The overall results are illustrated in (table 5.2). Each beam will receive a force proportionally to the number of beams. For example, there are 4 beams that the aluminum sheet is in contact with. Since the frame will be symmetric so that to calculate the force exerted on one beam element, take the Aluminum sheet weight and divided by 4. This was proved to be the case according to Ashutosh Bijalwan, Anadi Misra study [67]. However the, load is heavily dependent on the component that will be put on the sheet. So to calculate the actual situation is impossible. Instead, try to predict the maximum weight the beam can hold and then set the standard for the component later. The method to determine in the problem condition whether the beam is sufficient to withstand to load is that if the Maximum Stress is lower than the yield stress of the material then the element is proven to be acceptable [68]. Another factor that needs to be kept in mind is the allowable beam deflection. The method to calculate is suggested by the manufacturer themselves (Misumi). MISUMI defines the Load Capacity (Max Allowable Load) to be a deflection  $L/1000$  of the extrusion length [71]. The result of allowable deflection and the load limit is illustrated in table 5.4 and 5.5 respectively. The calculation was done via Solid Work and matlab and the table was carried out by excel.

Table 5.4. Allowable deflection limit

Classification	HFS type
40*40	1.2mm
30*30	1.2mm
20*20	1.2mm

Table 5.5. Result analysis of each type of beam under assumption load [at length of 1200mm]



Type	Max. Deflection (mm)	Max.Stress (Mpa)	Yield stress (Mpa)	Maximum weight each beam can handle (N)	Aluminum sheet weight	Type of nuts bolts
40*40	1.2	30.3	145	1900	4.187kg	M8
30*30	1.2	23.5	145	530	3.7672kg	M6
20*20	1.2	17	145	215	3.3474kg	M4

## 5.2 Bracket design

### 5.2.1 Design study of ADC12 bracket

European standard aluminum alloy casting stand, which is widely used in the right angle connection of European standard aluminum alloy forming rods; made of common domestic ADC12 or Stainless steel material, sandblasted surface, light design lower than standard molded frame load, higher cost performance, suitable for connecting aluminum alloy rods with low load requirements.

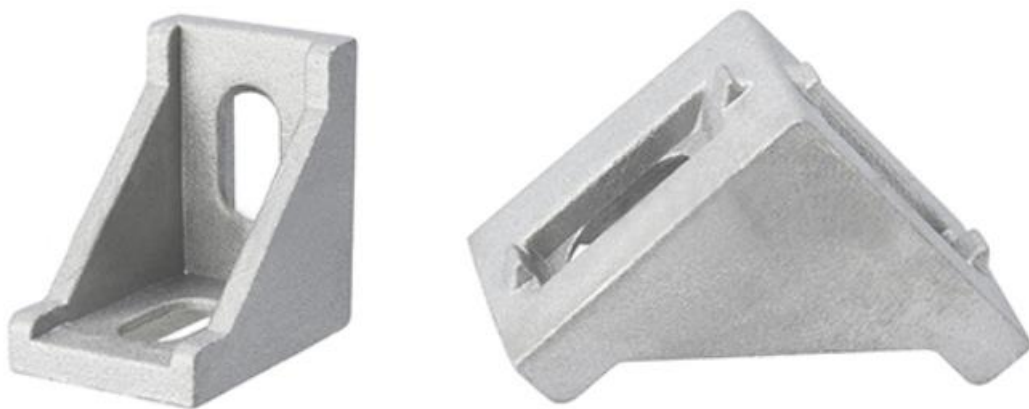


Figure 5-4 L- Bracket (ADC12 material)

Also with the specification, its best to describe all the front, right, top and bottom view of the bracket for further illustration. The specification here only apply for the 30\*30 bracket

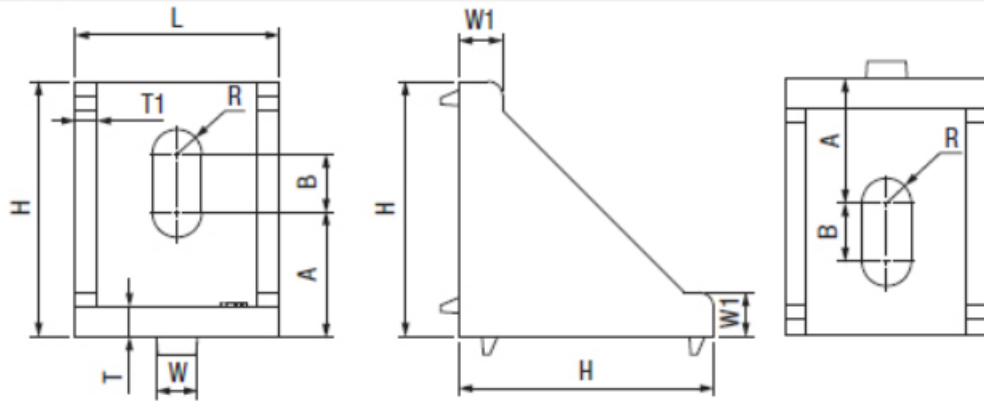


Figure 5-5 Top side and bottom view of the bracket (respectively)

Table 5.6. Specification of bracket ADC12

Code Name	Profile	L	W	W1	H	A	B	R	T	T1
<b>LBSBL</b>	30	28m m	5,8m m	7m m	35m m	12,8m m	11.4m m	3,3m m	4,5m m	3m m



Vietnamese-German University

The 30×30 L-Bracket is designed to fix the profile guide at an angle of 90 °.The product is usually sealed by a high-quality aluminum layer on 2 sides of the aluminum corner with 1 round or oval hole used so that when connecting two aluminum rods together, screws or bolts can be used to attach them together to create certainty. Depending on the size of aluminum profile, there will be each type of aluminum angle ke suitable for that type of aluminum profile. The pros of using this kind of bracket is:

1. Mainly adopt grooved hole design, which is convenient to change the fixed position and easy to assemble.
2. The overhang adopts a trapezoidal oblique angle design, which increases sturdiness and non-brittleness, thanks to which the assembly of alloy aluminum rods is stronger.
3. The method of surface treatment by sandblasting is adopted. The superficial color resembles alloy aluminum, and after assembly there will be no difference in the appearance color.

Table 5.7. Material of the bracket with ADC12

Material	ADC12
Tensile strength (N/mm <sup>2</sup> )	310
Shear Modulus (N/mm <sup>2</sup> )	172000
Elastics Modulus (GPA)	71.0
Yield strength (N/mm <sup>2</sup> )	150

### 5.2.2 Design study of blind bracket

Another, type of bracket which also can be found very commonly in today's aluminium industry is the Blind Bracket. This type of bracket is made of S45C type material, which is a type of stainless steel that consist of 45% Carbon component [72].

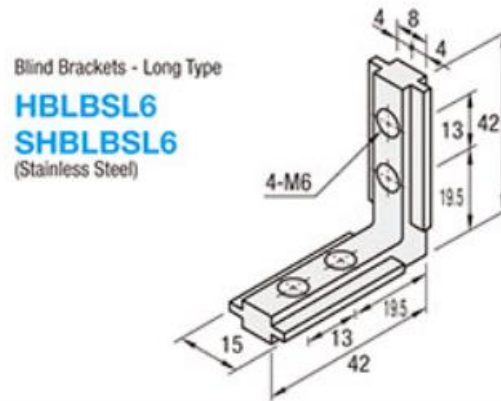


Figure 5-6 Blind Bracket (S45C material)

The current 30×30 aluminum submersible right angle ke is widely used in many different areas of life such as pharmaceuticals, garments, line installation, electronic components assembly line system. The blind bracket has an L-shaped design, slender and long bars usually made of stainless steel, this type is used to thread into the hollow of the profiled aluminum rod, the top of each side has 2 holes available with threads for convenient bolts bolting to the aluminum rod.

1. High durability
2. Sturdy and beautiful glossy surface
3. Easy to assemble products, easy to process
4. Threaded on the ke surface to make catching bolts or screws easier

5. Easily change the design model to become more flexible
6. Cast aluminum material is silver gray, so the surface of the product is always shiny
7. The aesthetics of the product are highly appreciated



The bracket is convenient to use also very easy to adjust and fit the requirements of assembly and disassembly easily, with only bolts and nuts on the bracket. The only thing that needs to be taken into consideration is to determine the amount of load that these two brackets can hold.



Table 5.8. Material of the bracket with Stainless steel (C45)

Material	SC45
Tensile strength (N/mm <sup>2</sup> )	750
Shear Modulus (N/mm <sup>2</sup> )	79000
Elastic Modulus (GPa)	210
Yield strength (N/mm <sup>2</sup> )	580

### 5.2.3 Design study of Stainless Steel bracket

To put into more options for consideration the L-bracket made of stainless steel also plays the same role as the 2 mentioned brackets above, however the assembly method is rather different. The L-corner is made of high-quality stainless steel material, the surface is thoroughly treated, has high corrosion resistance and rust resistance. Therefore, the bracket can be used for the product both indoors and outdoors without worrying about oxidation. The strength of the L-right angle bracket is relatively high, difficult to mutate when encountering strong impacts, withstanding the force. Use in the reinforcement of long-term interior products. The design of the corner

bracket is very compact, when assembling the furniture still ensures aesthetics. Easy to use tools such as screwdrivers to fix parts, the design has bolted holes.

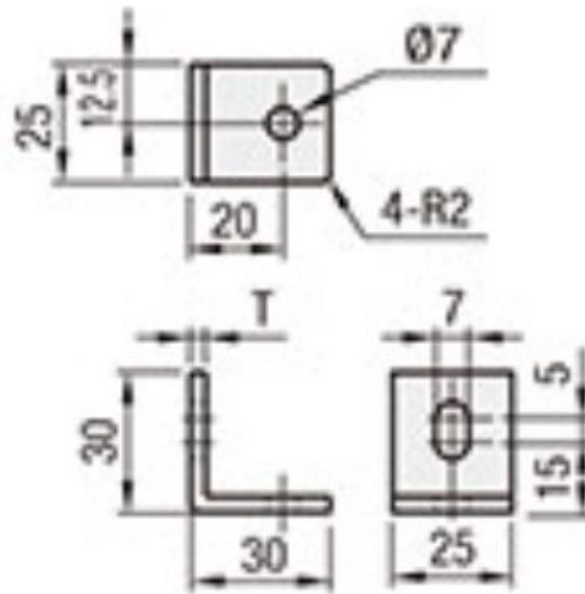


Figure 5-7 Stainless steel bracket

1. The product is made of high-quality stainless steel, with extremely high corrosion and rust resistance
2. Difficult to deform when subjected to strong influences
3. High strength, good bearing capacity
4. The product is designed perpendicular with bolt holes, easy to use screws to try put the details together
5. There are many different sizes, it is easy to choose the right type of angle ke for the purpose of use.

The main thing to keep in mind is the loading capacity of the bracket, however from the manufacture do not calculate this in their catalogue, so the simulation for L-Bracket is being conduct in Solidwork.

## HPTBS6 SHPTBS6



HPTLS6		3.2
--------	--	-----

Figure 5-8 2D dimension specification given by Misumi

The simulation is then divided into 3 phase,

1. Sketch and building the L-Bracket in solidwork based on the given Specification



## 2. Applying material and constrain for the study

The chosen material is suggested to by Misumi to be Chrome Stainless Steel

Table 5.9. Mechanical Properties of Chrome Stainless Steel

Material	Chrome Stainless Steel
Tensile strength (N/mm <sup>2</sup> )	414
Shear Modulus (N/mm <sup>2</sup> )	77000
Elastics Modulus (GPA)	200
Yield strength (N/mm <sup>2</sup> )	172

The constrains is that on top of the bracket will have a Load exerted on the surface with 2 hole being fix.



To determine the maximum load, change the load applied until the Max. von Mises is higher than the Yield strength of the properties. This load magnitude is not sufficient enough, to determine whether the bracket will fail or not, best to determine the safety factor of the bracket as well. The results of the applied affecting the bracket will be illustrated in Table 5.10

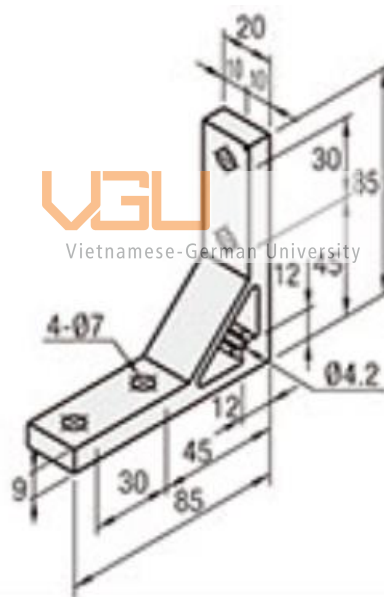
Table 5.10. Properties of the Bracket corresponding to the each load

Applied Load (N)	Max.Stress (MPa)	Safety Factor
1300	170	1.011
1200	157	1.095
1100	144	1.195
1050	138	1.25



Although at 1300N the bracket still hold it's shape, for the safety purpose the bracket should not be expose to load at more than 1050N.

#### 5.2.4 Study design of extruded L-Bracket



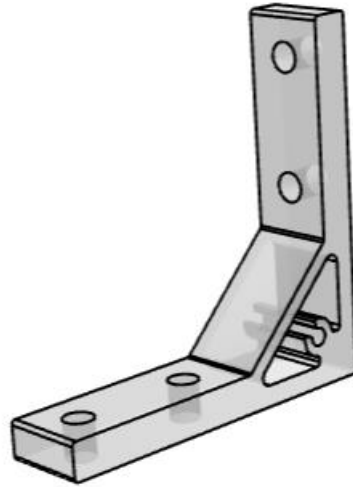


Table 5.11 Material properties of the extruded L-bracket

Material	6063-T5
Tensile strength (N/mm <sup>2</sup> )	245
Shear Modulus (N/mm <sup>2</sup> )	25800
Elastics Modulus (N/mm <sup>2</sup> )	69972
Yield strength (N/mm <sup>2</sup> )	145

### 5.2.5 Comparison between 4 kind of bracket

Let put into consideration the 2 type of joining loading capacity, as suggested by the manufacture [Misumi]. The loading capacity of the joint by Misumi is define by as follow

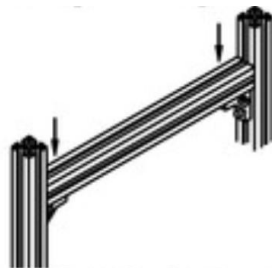


Figure 5-9 Loading condition to determine the allowable load of bracket

Allowable load per one bracket is calculated with one beam extrusion between two vertical extrusions supported by a bracket under each side of the beam as shown in Fig 5.4.5. Allowable load here means the load applied when all mounting holes of the bracket are fixed with bolts nuts or screw without break or sliding.

The 4 type of bracket has different loading capacity due to difference in material and shape design which is illustrated in table 5.8 below according to Misumi for LBSBL and SHBLBLS6 and type HBLTSW6 . Regarding the SHBTSSL6 the loading capacity take from chapter 5.4.4

Table 5.12. Result table for 4 type of bracket

Type	Mass	Bolts used	Nuts used	Loading capacity (N)
LBSBL	15g	M6*12	T-nuts for M6	1548
SHBLBLS6	38g	M6*8	No need for nuts	957
SHBTSSL6	64g	M6*10	T- nuts M6	1050
HBLTSW6	76g	M6*15	T- nuts M6	1764

## 5.2.6 Decision matrix for choosing bracket

Table 5.13. Grading criteria for bracket

No.	Grading criteria	Grade
1	Mass Load	2
2	Easily dissembly and assembly	3
3	Not Brittleness (not easily crack) of material used	5
4	Loading capacity	4
5	Popularity	2

Table 5.14. Result of decision matrix for bracket

Criteria		1	2	3	4	5	Sum
Weighting factor		3	3	5	4	2	17
LBSBL	Core	3	3	2	2	2	12
	Weighted score	9	9	10	8	4	40
SHBLBLS6	Core	3	3	3	1	1	11
	Weighted score	9	9	15	4	2	39
SHPTBS6	Core	3	3	5	2	2	16
	Weighted score	9	9	25	8	4	55

HBLTSW6	Core	2	3	4	4	2	15
	Weighted score	6	9	20	16	4	55

### 5.3 Design of sensor modular mechanism and option

#### 5.3.1 Option 1 : Common linear mechanism

Applying the linear mechanism which include in the section 2.5, the selection is various, however in this phase of the project, the choice is narrow down to just operating manually. Put in the fact that, the adjustable system has to be easy to assemble and disassemble easily. The option now is narrow to just 2 different decide : The roller wheel guide and the linear guides

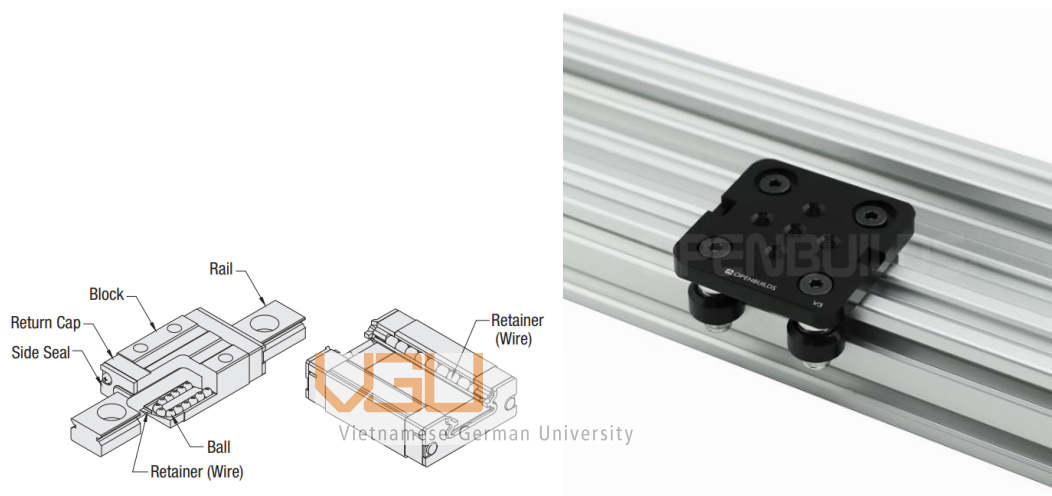


Figure 5-10 Linear guides and roller wheel guide respectively

Both need a custom rail way, however the linear guides rail way is much harder to find (in Vietnam) and need more component to actually make the mechanism works. Whereares, the roller wheel guide rail way is much easier to assemble and could found in viarious store in Vietnam . That is why in this case using roller wheel guide is a better option to suit the job.

#### Features and Functions

1. A single item combines a bearing with a 90° V groove.
2. There is design flexibility for the spacing between tracks when employing single-sided tracks.
3. Only one double-sided track is required for system assembly.
4. Because the circle of the wheels is V-shaped, they produce a wiping action that automatically cleans the track as they rotate. For a longer operating life, grease the track's sliding surface.

## 5. Dimensions in inches.

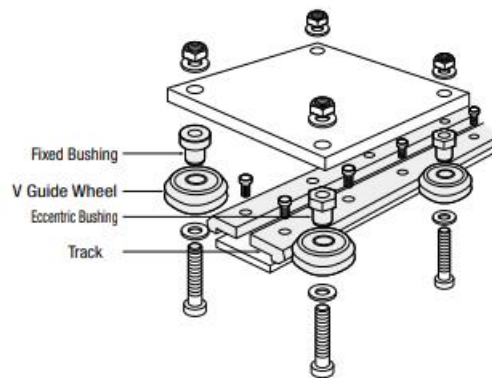
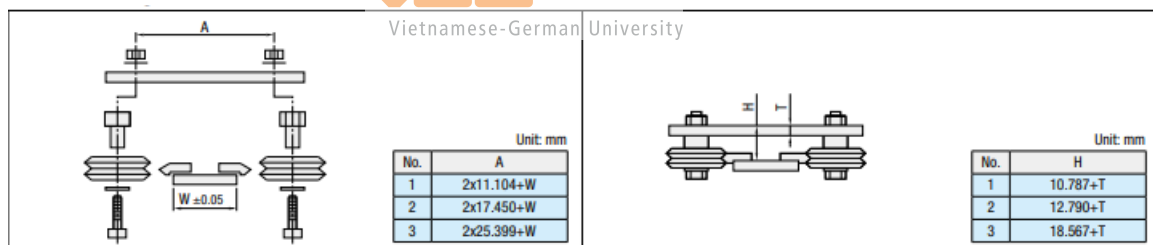


Figure 5-11. Exploded view of the V-Wheel roller mechanism

### Adjusting Method:

1. The straightness and parallelism of the support (back plate) on which the track rails are attached determine how accurate this system is. The rear plate's edges must be chamfered 0.5mm x 0.5mm on all sides before mounting a track rail to them. The rear plate's straightness affects the track rail's straightness 0.05 when installed on a precise back plate.



2. Give the connection sites a small offset when joining parallel railway rails. The wheels can now pass over the joints without any problems.
3. Because the wheel's circumference is formed like a V, it wipes the railway rail as it revolves. As a result, it takes care of cleaning itself.
4. The railway rails' sliding face is covered with grease their time in service.
5. Fixed bushings determine the alignment of the guidance system. On the fixed bushings, the main load must be applied.
6. Rotate the eccentric bushing until the wheel slides over the track rail without resistance, then tighten.

The mechanism is then created and exported into 2d and 3d file. Also the simulation of the mechanism is also conduct in Solidwork to determine whether the mechanism will be able to withstand the weight of the sensor.

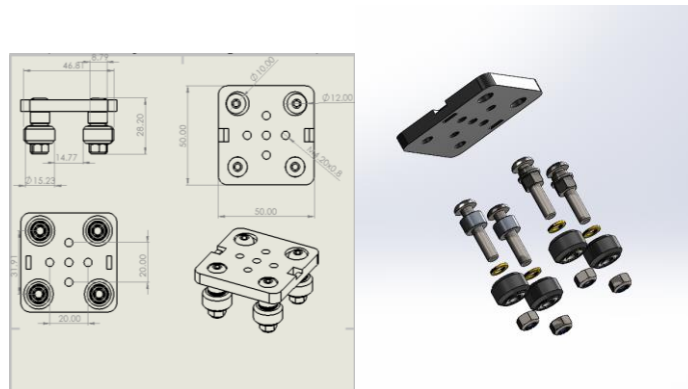


Figure 5-12. Linear mechanism in 2d and 3d

The weight of sensor is around 800g and with the additional bracket of 100g. The total load that the roller wheel mechanism have to withstand is 900g. The constrain of the mechanism is roller fixture with the direction opposite with the gravity and force pull of the mass.

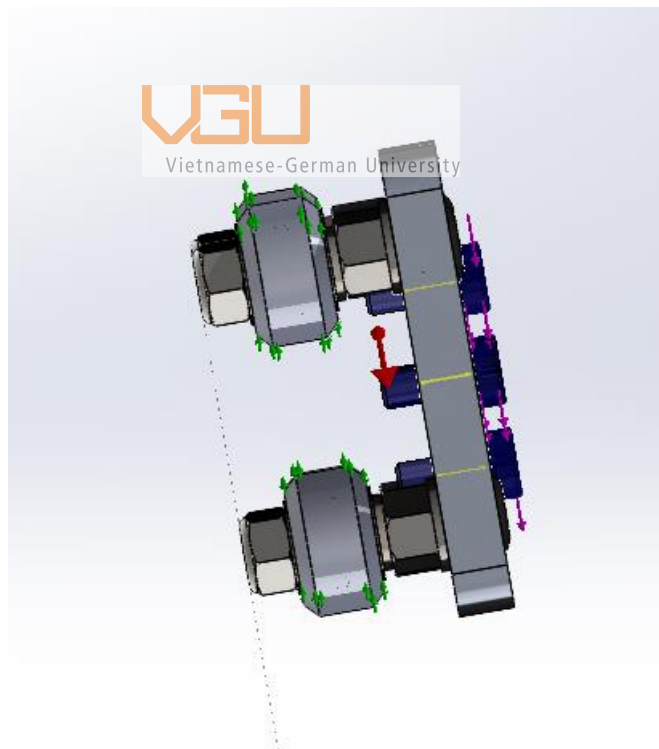


Figure 5-13. Constrain visualization of the simulation

The result will be comprise of Von Mises, Displacemnet and Safety Factor:

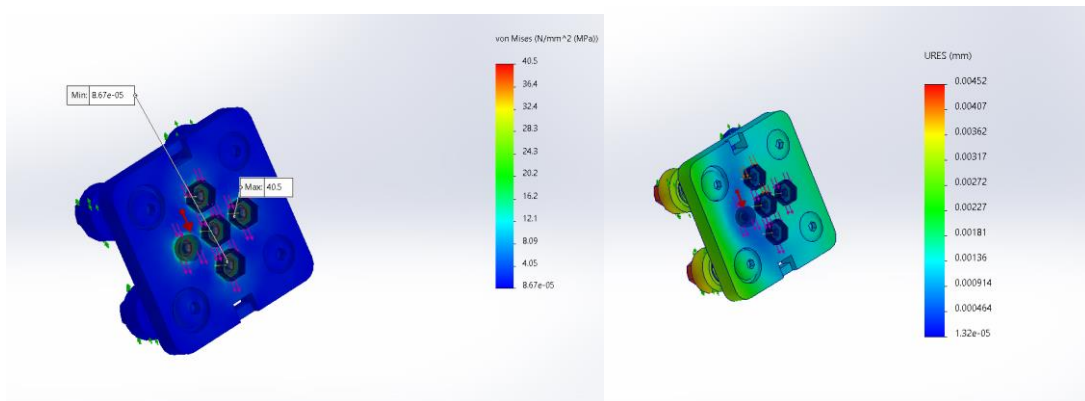


Figure 5-14. Max and Min Von Misses (MPA) and displacement (mm) value

The von mises showed that the mechanism is experienced a stress ranging from 40.5 MPA to 0.0000867 MPA with the load corresponding to the mass of the sensor and the bracket. From the result it is not sufficient enough to conclude that the V-slot mechanism is capable of withstand the load efficiently. So the simulation for calulating the safety factor is also needed.

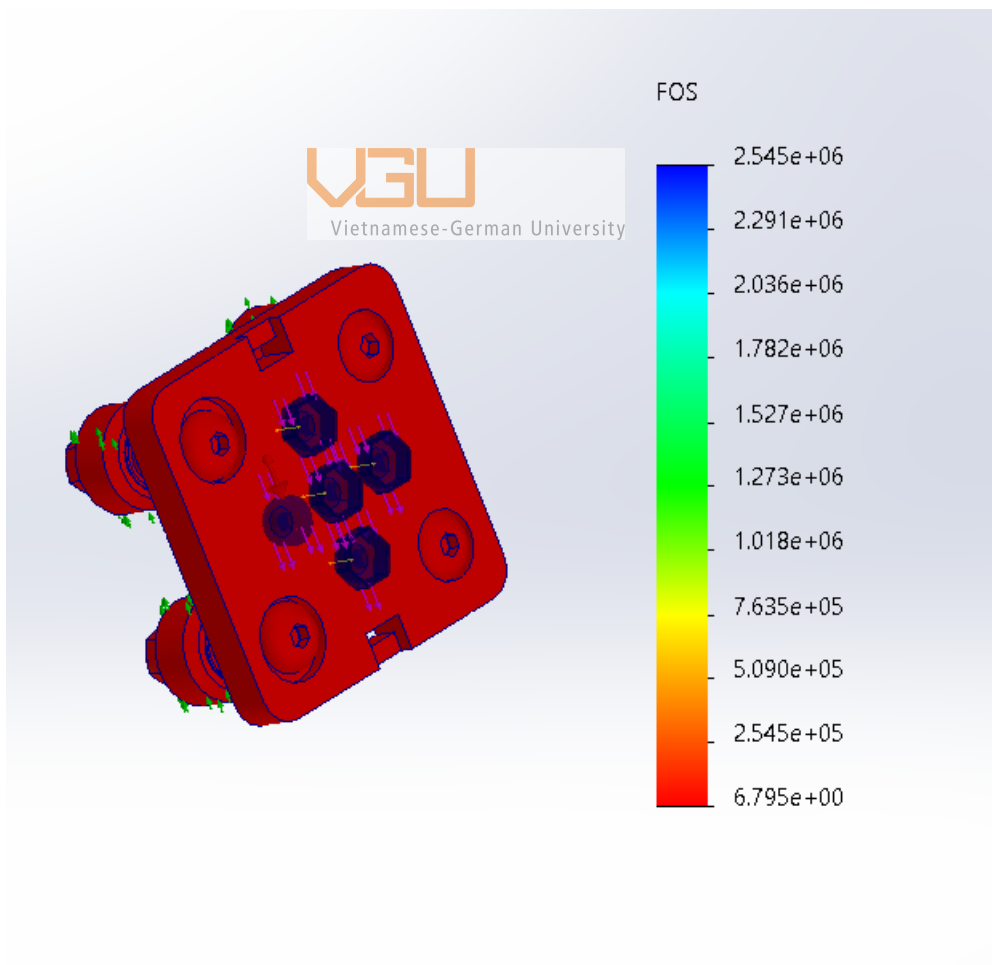


Figure 5-15. Safety factor of the mechanism

From the simulation it is now sufficient to conclude that since the minimum safety factor is around 6.795 the load acting on the mechanism is acceptable and the status of the mechanism will remain unchanged during the course of operation.

### 5.3.1.1 Aluminium sheet design corresponding to option 1

Since using linear V-slot wheel guide mechanism required a large space for the mechanism to move freely and be able to lift the sensor up and down. Placing the mechanism on top of the sheet is not a sufficient way to do due to the limitation of space in order to build the base system to fix the mechanism.

By cutting the square piece and using bracket to fix the rail wheel would save more space for further components and more conveniently to modular the sensor.

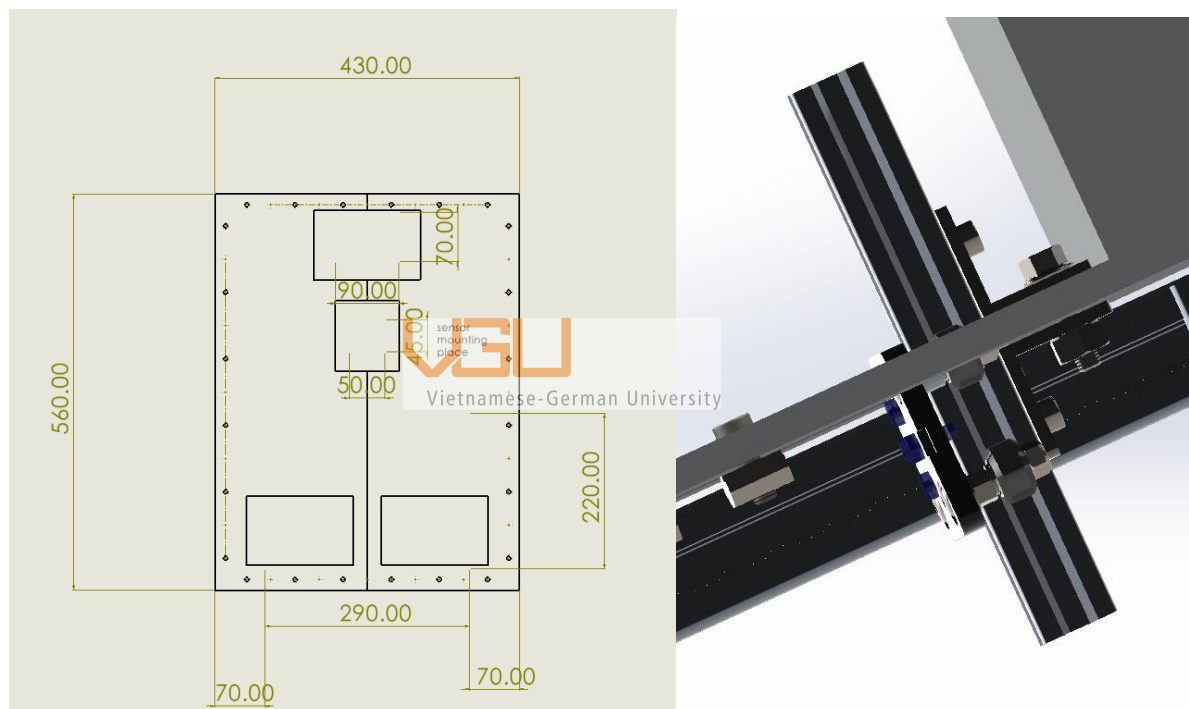


Figure 5-16. Components layout and assembly method for V-Slots wheel guide mechanism

The component layout will affect tremendously to the stability of the centre of gravity of the UGV.



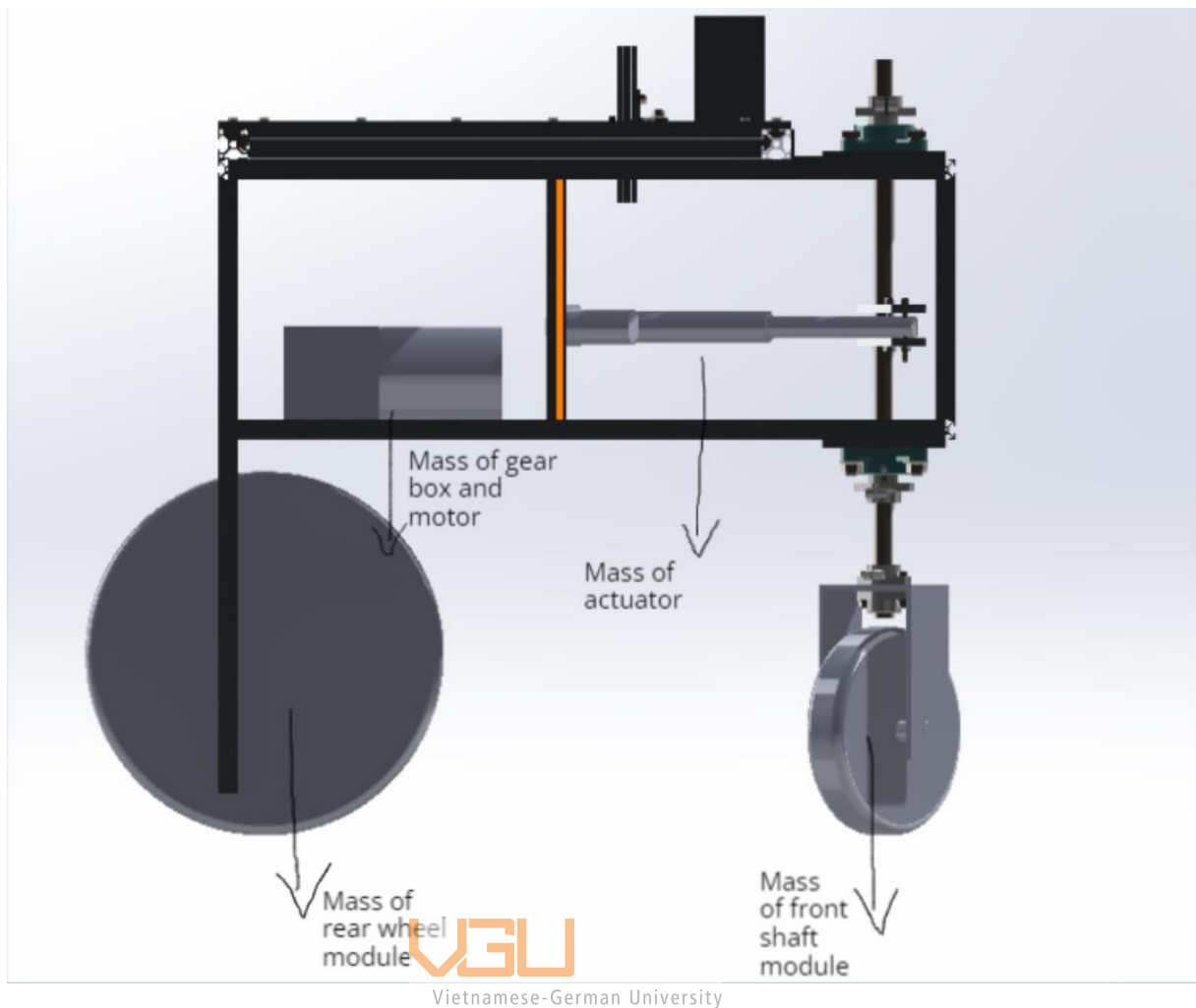


Figure 5-17. Mass distribution of the driving components

The component will be put onto the 8mm thick aluminum sheet will consist of batteries, and a placeholder for the sensor. The goal is to make sure that the weight distributing on the frame is overall balance. To make the UGV stability. The list of component weight affecting the UGV is as follow in table 5.1. The method is to use the batteries as a counter weight against the mass of the driving component.

Table 5.15. Component list of the driving module

Component	Weight (kg)
Steering	6.5
Actuator	0.8
Rear wheel module	1
Motor	3
Total	11.3

The choosing for the battery is rather complex, however due to the specification of the driving component, there are 2 options can be chosen from

- i. 1 12V batteries and 1 24V batteries
- ii. 1 12V batteries or 2 12V batteries that plug in serial with each other.

So there are 2 simulation that needs to be done to determine the safety factor of each senerio and then the result will be evaluated in a decision matrix. The specification of the batteries will be used in 2 simulation is illustrated in table 5.7

Table 5.16. Specification of the batteries

Type	Length	Width	Height	Capacity	Weight (kg)
24V Ritar	328	172	220	50Ah	13.2
12V Vision honda	151	98	95	12Ah	3.56

### 5.3.1.2 Simulation for scenario i

The alumium plate will have a thickness of 8mm and made frome 1060 alloy, and will be drilled 6 hole to insert bolts and connecting with the frame.

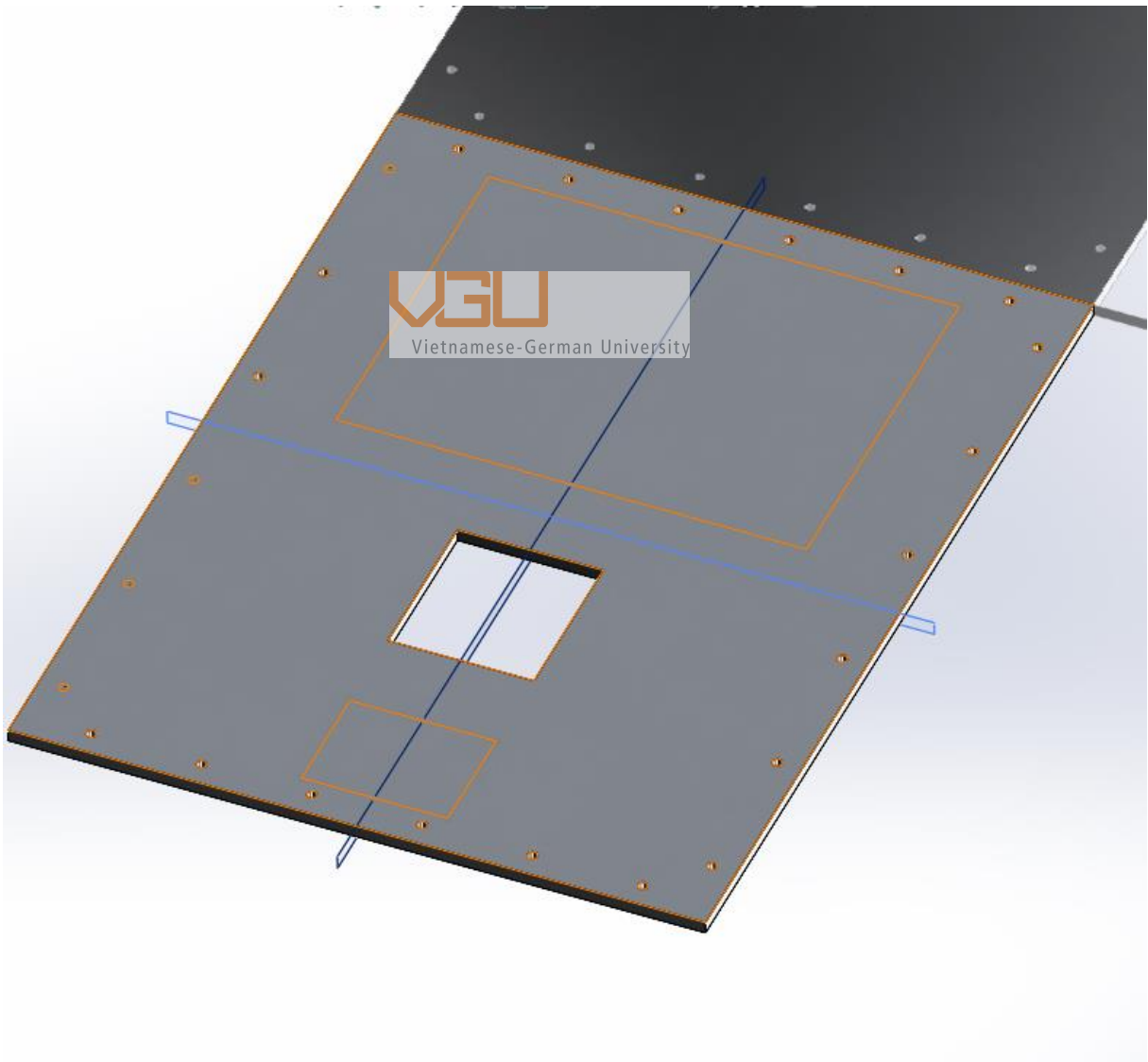


Figure 5-18. 3D modelling for the simulation

Then start to apply geometry load, the load of the 1<sup>st</sup> sensor will be a 24V batteries with the weight of 13.2kg from Ritar company and the 12V with the weight of 5.5kg by Honda. The specification and dimension will be illustrated in table 5.7 below.



Figure 5-19. 24V Ritar batteries



Figure 5-20. 12V Honda Vision batteries

The next step in the simulation phase is to make configuration. Draw the surface area corresponding to the dimension of the batteries size the set each load corresponding to the weight of the batteries. Then fixed all the holes as suggested for bolts connection.

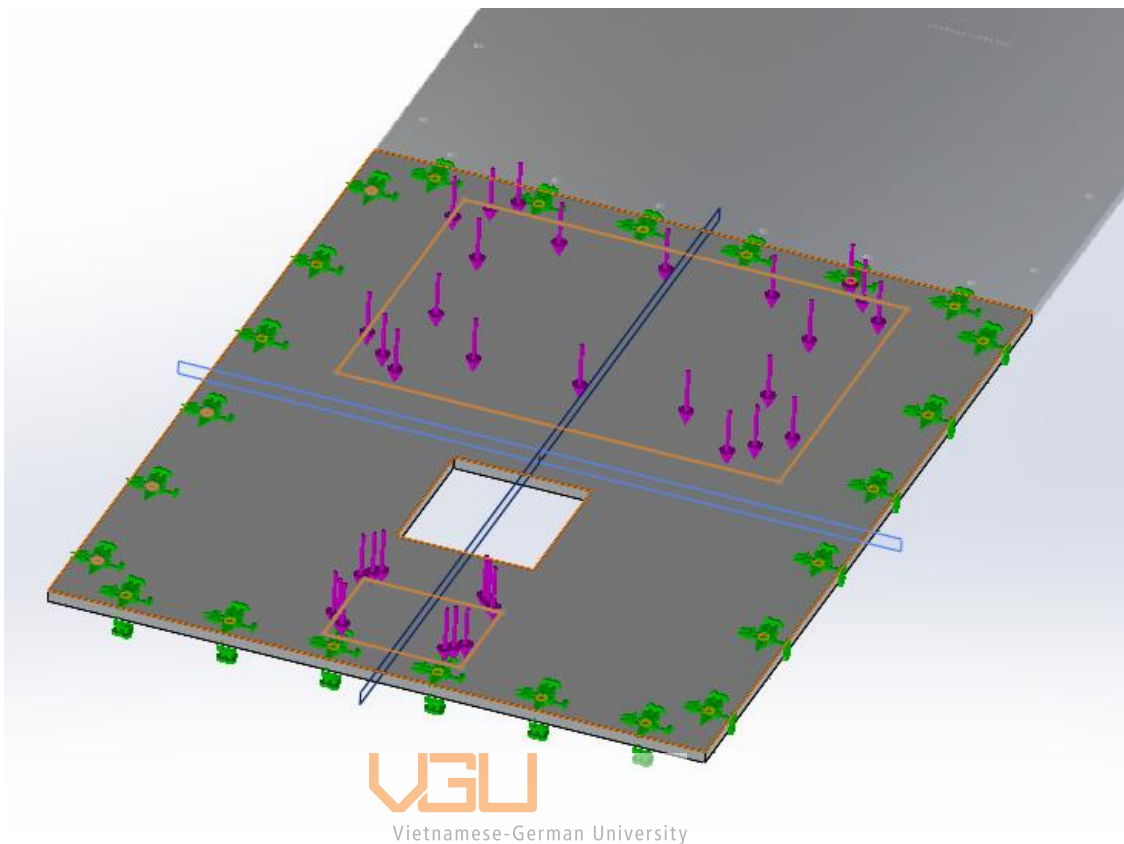


Figure 5-21. Constrain study of senerio I

After constraining the study, then the results will appear, however to determine if the sheet will withstand the load, only the Safety Factor and the Von misses will need to be investigated.

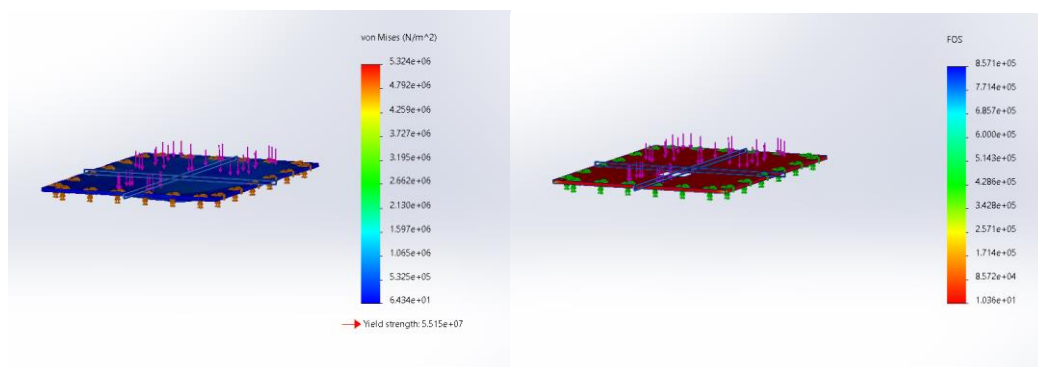


Figure 5-22. Von mises and safety factor results (I)

As illustrated above, the maximum Stress that the sheet will have to face will be 5.53 MPA and the minimum safety factor will be 10.36. So it's fair to say that the aluminum sheet will comfortably withstand the batteries load.

### 5.3.1.3 Simulation for scenario ii

For this senerio, the load will distribute different, since there are 3 batteries currently using, the type of batteries will be the 12V Honda batteries.

Same procedure will be carry out like in scenario i.

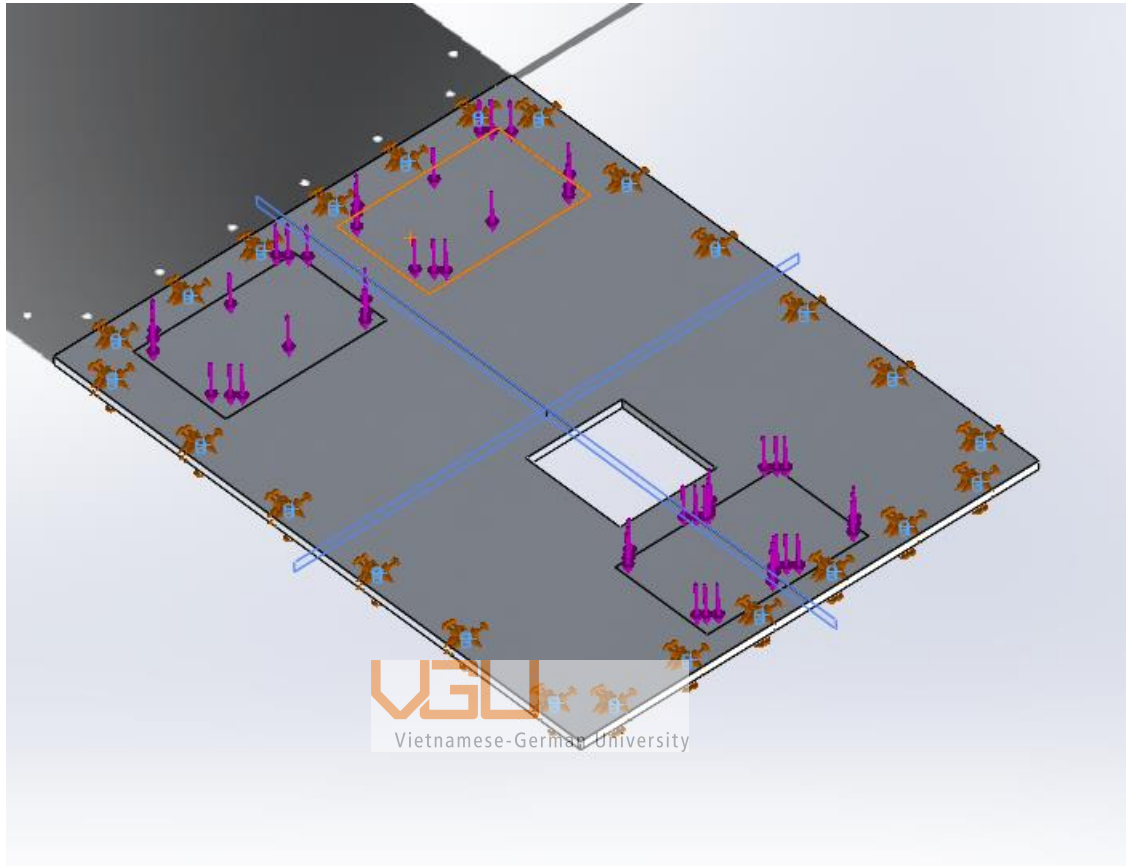


Figure 5-23. Constrain study for senerio II

The constraining phase and procedure is the same but the geometry of the mass will be different and which will lead to different Von Mises (MPa) and safety factor

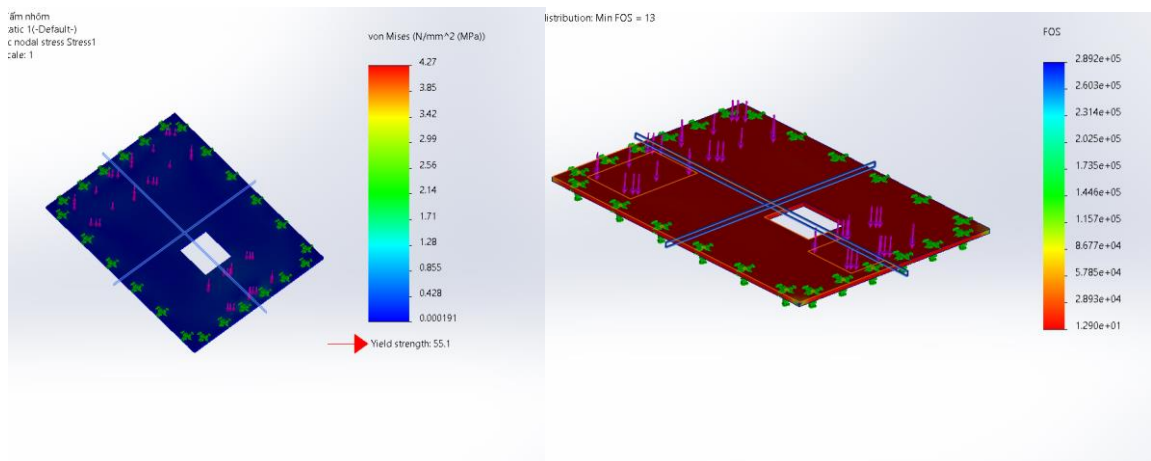


Figure 5-24. Von Mises and safety factor results (II)

However, this option will be varied according to the type of sensor lifting mechanism. Since some linear mechanism required for cutting a place to be able to execute assembly process and some will not. The next option will be illustrated in chapter 5.4.2.

### 5.3.2 Option 2 : Using ball joinning

Option 2 is based around using a ball head for standard camera, the ball head is sufficient because many type of sensor and multispectrum camera nowadays will include a bracket for installing onto the ball head's bracket. The ball head mechanism comes with a quick-release plate is included with the majority of ball heads. The bottom of the camera has a little metal or plastic mount connected to it. Some application which can be done by keep this on constantly so they can utilize it whenever necessary. Additionally, a quick-release plate adds extra security to the camera's base. Speed is the main benefit of employing one. With just one knob, it can be locked and opened. On-the-spot adjustments can be done. The principle of securing the ball onto the housing is by clamping force from screw. For the thesis, the ball using will be the Berno V2 ball head.



Figure 5-25 Ball head illustration

The ball head installation on to the frame is rather complex. The bottom part of the ball head will have a screw joint with size of 9/32 inches. The next step is to design the bracket that will place under the ball head and on top of the alumium sheet which will act as a connection bracket. The bracket will have 3 holes for bolts connection. Using 2 M8 bolts and one

9/32 inches bolt, so in order to easily assembly, the bracket must have 2 hole with diameter of 8.5mm and 1 hole with diameter of 7.5mm.

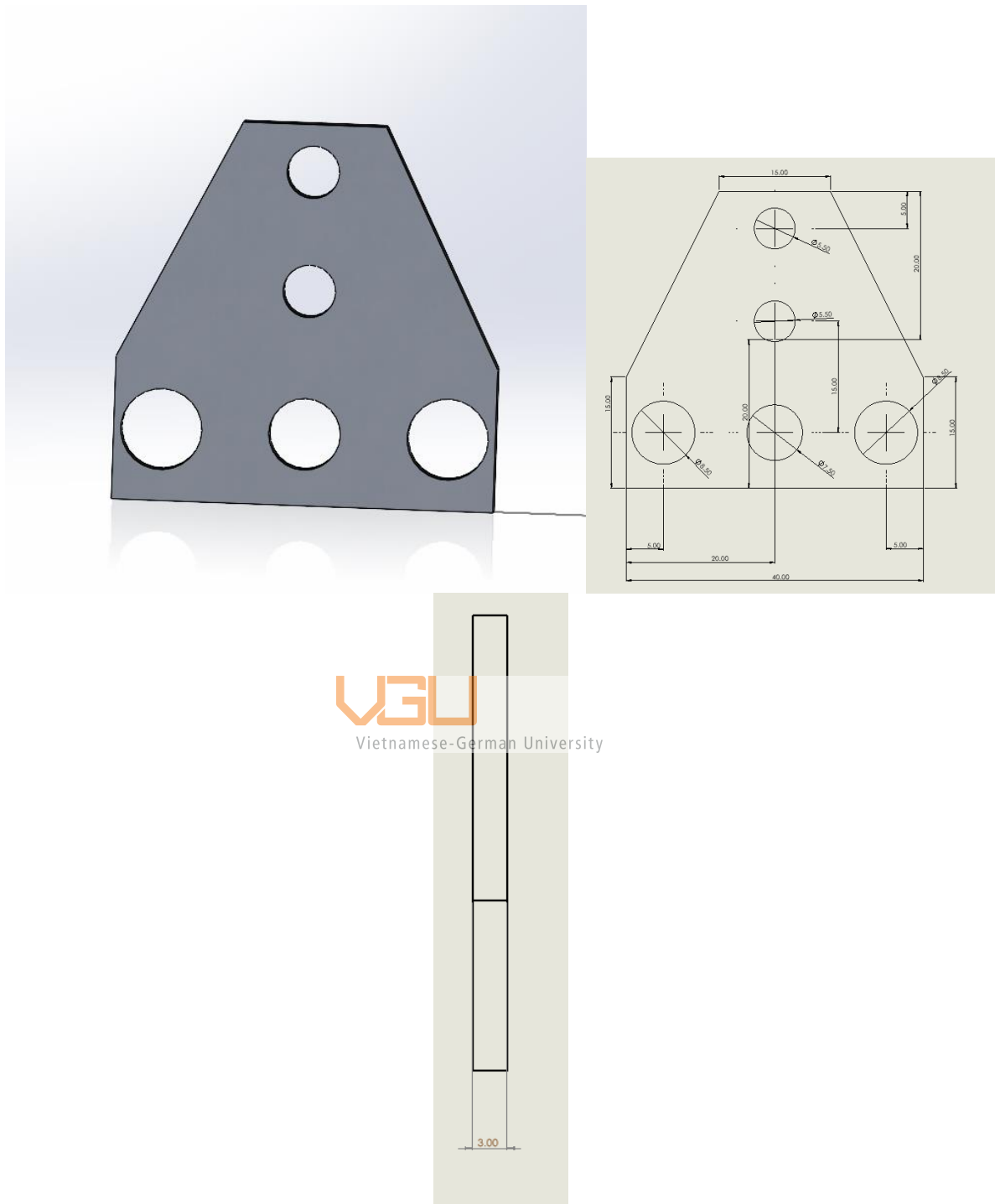


Figure 5-26. Connection bracket design and dimension

The bracket is essential, because it help to stabilize the ball head and acting as a support to fix the gimbal on to the 8mm alumium sheet. Also to futher protect the gimbal from falling apart it is important to have the housing. Pervent the ball head from slipping apart and increase the contact area of the ball head.



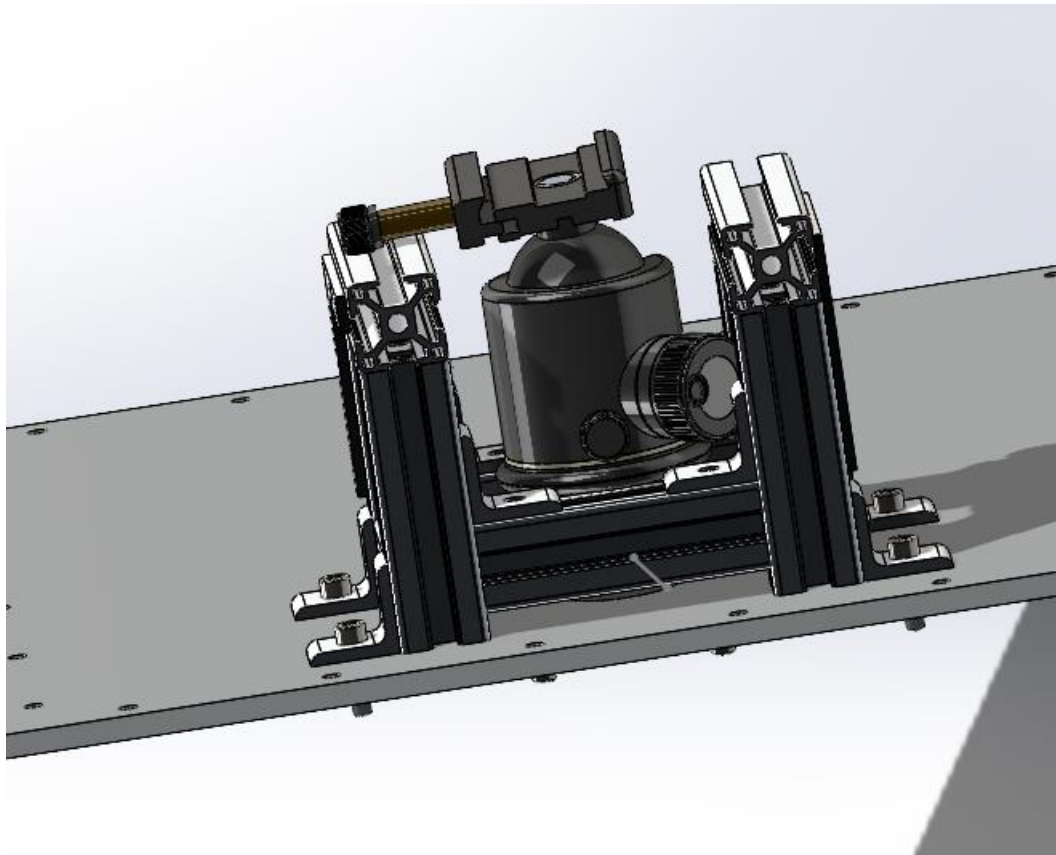


Figure 5-27 Ball head and housing connecting to the aluminum surface

### 5.3.3 Decision matrix for the 2 options

Vietnamese-German University

Table 5.17 Grading criteria for the sensor modular mechanism

No.	Grading criteria	Grade
1	Easily to modular	5
2	Assembly and disassembly easily	3
3	Camera stabilizing	4
4	Popular componets	2
5	Consistency	3
6	Easily to use	2

Table 5.18 Result table for the sensor modular mechanism

Criteria		1	2	3	4	5	6	Sum
Weighting factor		5	3	4	2	3	2	19
Option 1	Core	4	2	3	2	2	2	15
	Weighted score	20	6	12	4	6	4	52



Option 2	Core	4	3	4	1	2	2	16
	Weighted score	20	9	16	2	6	4	57

#### 5.4 Frame joining design calculation of pre load to determine the weakest join of the UGV

Knowing the right type of aluminum required, it is beneficial to choose the right type of bolts and from then the calculation for pre load is conduct to determine the right amount of force needed to glue the component together.

Nomenclature			
$C$	fraction of external load carried by bolt (or 'joint stiffness parameter' as defined by equation	$L$	grip length ( $=t_{m1} + t_{m2}$ ), m
$d$	bore diameter, m	$P$	external separating load, N
$D$	diameter of washer (or bolt head) in contact with clamped member, m	$P_b$	load in bolt (or additional load carried by bolt in external loading stage), N
$A_s$	bolt shank area, m <sup>2</sup>	$P_m$	external load taken by members, N
$E$	Young's modulus, N/m <sup>2</sup>	$t_{m1}$	thickness of member 1 (upper), m
$F_b$	resultant bolt load, N	$t_{m2}$	thickness of member 2 (lower), m
$F_i$	pre-load in the bolt, N	$\nu$	Poisson's ratio
$F_m$	resultant member load, N	$\beta$	ratio of bolt/nut outside diameter to bolt diameter,
$k_b$	bolt stiffness, N/m	$\mu_k$	coefficient of kinetic friction
$k_m$	total member stiffness, N/m	$\mu_s$	coefficient of static friction



Vietnamese-German University

Many engineering textbooks uphold the traditional or classical idea of bolted joints, which is widely recognized e.g. (57, 58, 59). According to conventional theory, the bolt and the sandwiched parts of a certain bolted joint arrangement may both be modeled as parallel linear springs with stiffnesses of  $k_b$  and  $k_m$ , respectively. To further illustrated the problem, 2D schematic sketch is done regarding to the situation of the thesis.

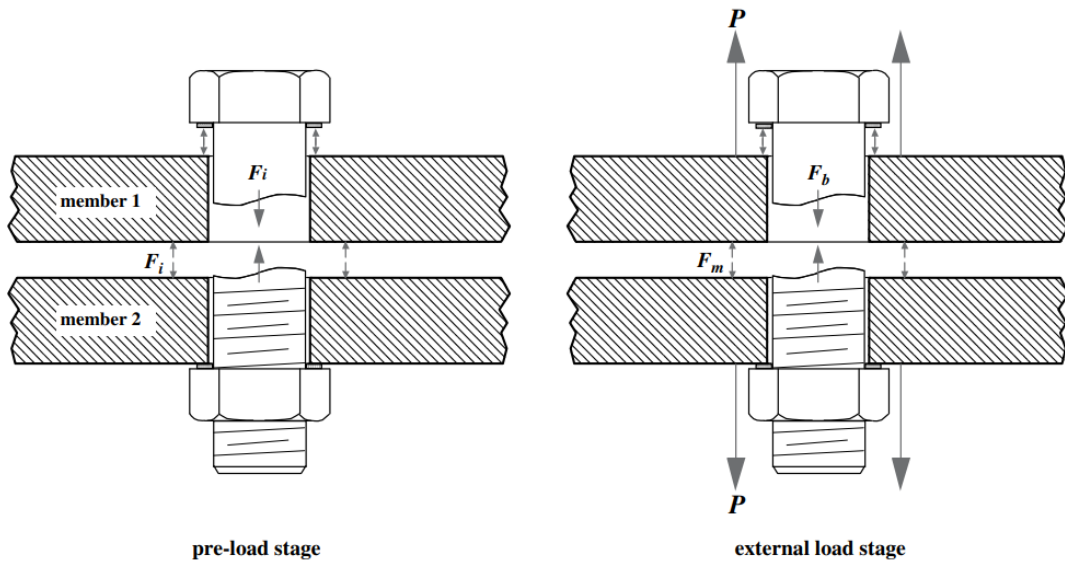


Figure 5-28 Schematic sketch of the joint in the UGV frame

The following relationships for the bolt force,  $F_b$ , and member force,  $F_m$ , illustrated in Fig. 5.2, may be derived from the concept of stiffness at its most basic level and the principles of equilibrium and compatibility:

$$F_b = CP + F_i = P_b + F$$

$$F_m = (1-C)P - F_i = P_m - P_i$$

Vietnamese-German University

Where  $F_i$  is the bolt pre-load,  $P_b$  is the bolt's share of the external force,  $P_m$  is the members' share of the external load, and  $C$  is the joint stiffness parameter, which is defined as:

$$C = \frac{k_b}{k_b + k_m}$$

If member bending or rotational effects are minimal and there is enough initial compression left to prevent the members from separating, the aforementioned equations ought to be true. The typical method for determining the stiffness of a bolt is to imagine the piece of the bolt that is enclosed in the joint as a uniform bar in tension:

$$k_b = \frac{A_s E_b}{L}$$

To create an equivalent length  $L_{eq}$  that recognizes the contribution of stresses in the head/nut to extension of the bolt under load, the length  $L$  should be raised by a percentage of the bolt diameter  $d$ . The bolt head and nut areas are treated as stiff in this formulation. Many authors, notably Bickford [58], have proposed this idea. Due to the nature of the load distribution from the bolt head and nut into the members, calculating the stiffness of the member is significantly

more challenging. Motosh [60] and Burguete [61] examine a wide range of techniques that have been put forth for figuring just how rigid the clamped components are. The "pressure-cone" method, in which the stress distribution in the members is approximated to a truncated cone form with a half-apex angle  $\alpha$ , is the analytical technique that is most frequently employed. The size of the stress field is thought to be insignificant outside of this pressure-cone area. A typical equation for member stiffness is produced as follows [62] by taking into account the deflection of a tiny element of the cone  $dy$  and integrating the effective load bearing area of the members with regard to the vertical position  $y$ . All of which can be illustrated in Figure 5.3

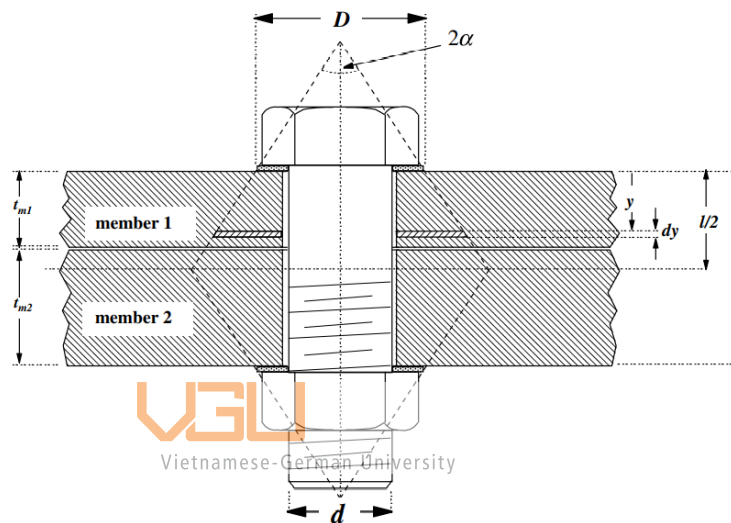


Figure 5-29 Load distribution on the bolts

General expression for member stiffness is obtained as follows:

$$k_m = \frac{\pi E_0 d \tan \alpha}{\ln \left[ \frac{(2t_0 \tan \alpha + D_0 - d)(D_0 + d)}{(2t_0 \tan \alpha + D_0 + d)(D_0 - d)} \right]}$$

For the (alpha value), Various engineering publications [63] frequently use various values for  $\alpha$ . Most are about 30 degrees, thus in order to compare with the conventional method, a pressure cone angle of 30 was used. The procedure of determine the value for the stiffness member and bolts was conduct in Matlab 2018 (A.8). Depending on the bolts type, the length grip, major diameter is illustrated a can be found using the table A.6 in Appendix. Choosing the bolts is depending on the size of the profile aluminum. The bolts using will be M6 with additional washer. The specification and technical data the serve calculation the of the bolts can be found also in A.5 and the coefficient  $k$  is choosing to be 0.2 according to [62,63] study. Let first name the position where the bolts will be use to connect the component.

The used bolts here will be the T-bolts as suggested by the supplier [Mitsumi], the bolts is then created in 3d and has been done via solidwork as illustrated below.

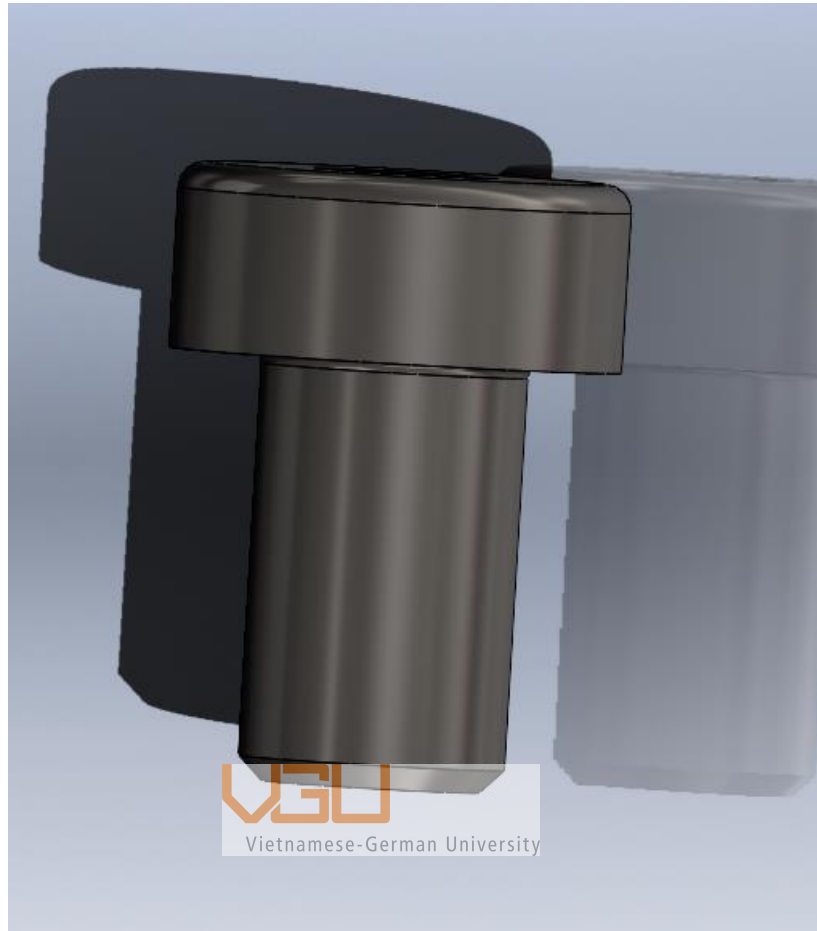


Figure 5-30 Bolts M6 in solidworks

Then from the 3d part the bolts is exported into 2d form for better understanding and getting all the required data for calculation.

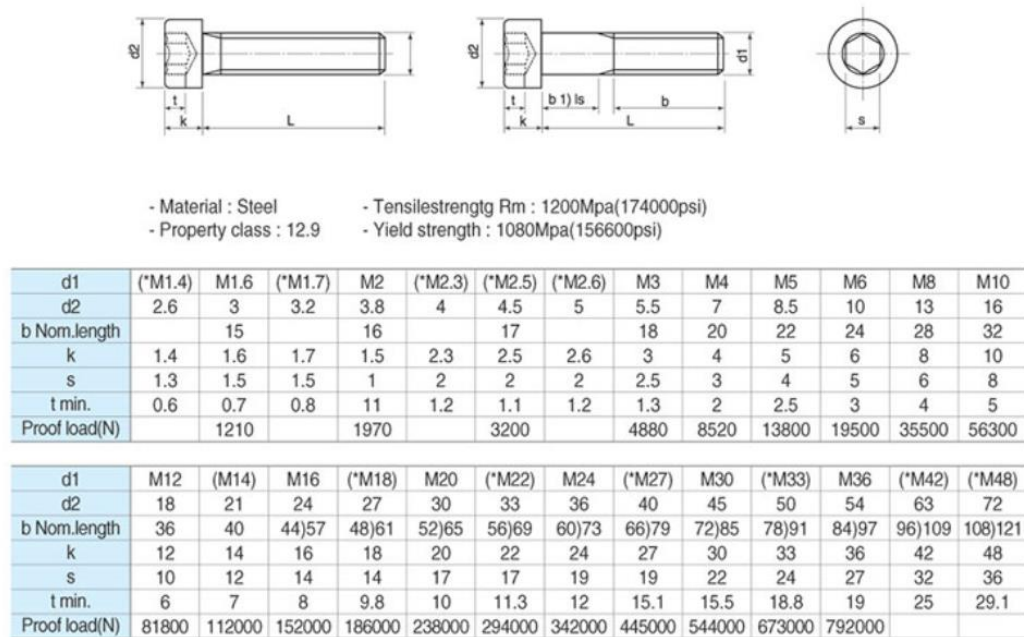


Figure 5-31 Overall specification of the bolts according to misumi

The calculation is divided in 3 part

1. Calculate the stiffness based on the member the bolts attached
2. Calculate the Proof load and Pre Load of the bolts
3. Calculate the shear stress that affected on the bolts and safety factor of the bolts

If the final calculation of the safety factor is greater than 1.25, the joining will be acceptable according to Karl-Grote studies [70]. Another things that need to be considered is that if the Pre Load is greater than the external load then the joint will fail [70,71]. The Pre-Load calculation is divided into 2 separated formula for non permanent joint and permanent joint. As in the case of UGV it need to be non permanent joint to fit the requirement as cited in chapter 3.


$$F_i = 0.75 F_p \text{ (non-permanent joint)}$$

$$F_i = 0.9 F_p \text{ (permanent joint)}$$

Where  $F_i$  is the actual pre-load and  $F_p$  is the proof load.

$$F_p = A_t S_p$$

In order to calculate to full safety factor of the joint, let consider the amount of load that will put pressure onto the joint. As mention in chapter 5.3, the load of the alumium frame, the beam and the bracket that will extert pressure onto the joint. So to tell the maxium capacity of the join is through trail and error by changing the P value. P is the amount of force that insert on the joint.

Bolts type	Image	Position	Code name
M6		Connection of 2 beam 500mm and to 1200mm	XL1

The given data for the case of XL1 is as below:

Table 5.19. Given data for XL1 type joint

Given Data				
Type of bolts	M6	12.9 Grade	Stainless steel	Sp=970MP A
Material of bolts	Stainless steel		E=205GPA	
Unthread portion	0			
Thread portion	16			
Height of the nuts	6			
Tensile stress area At	20.1(mm <sup>2</sup> )		In A.5 table for bolts	
l1 ( Grip length of the aluminum sheet)	8mm			E=71GPA
l2 (Grip length of the beam)	2.2			E=69GPA

Applying the same procedure to find the maximum capacity of the joint, the results table is as follow

Table 5.20. Results table of the joint of location XL1

Total stiffness of the joint	1579 (N/mm)
Fi	14623N

Load	1050N
Stress	776.6 N/mm
Safety factor	1.25

From the table it's possible for joining at position XL1 to withstand the maximum loading up to 776.6 N. The coding format is illustrated in Appendix A8 and A9.

## 5.5 General design

### 5.5.1 Statics frame analysis using finite elements

Like mentioned in chapter 5.2, the beam that would carry the most load is the 1.2m beam of the frame, however after designing the whole structure as in chapter 5.6.1 it is best to calculate the whole frame capacity, by assuming the whole frame is already been fixed and each beam will have 3 DOF due to rotation and translation can be occurred during the loading and the driving process. The process of doing finite element is rather complex and can be summarized in the figure diagram below.

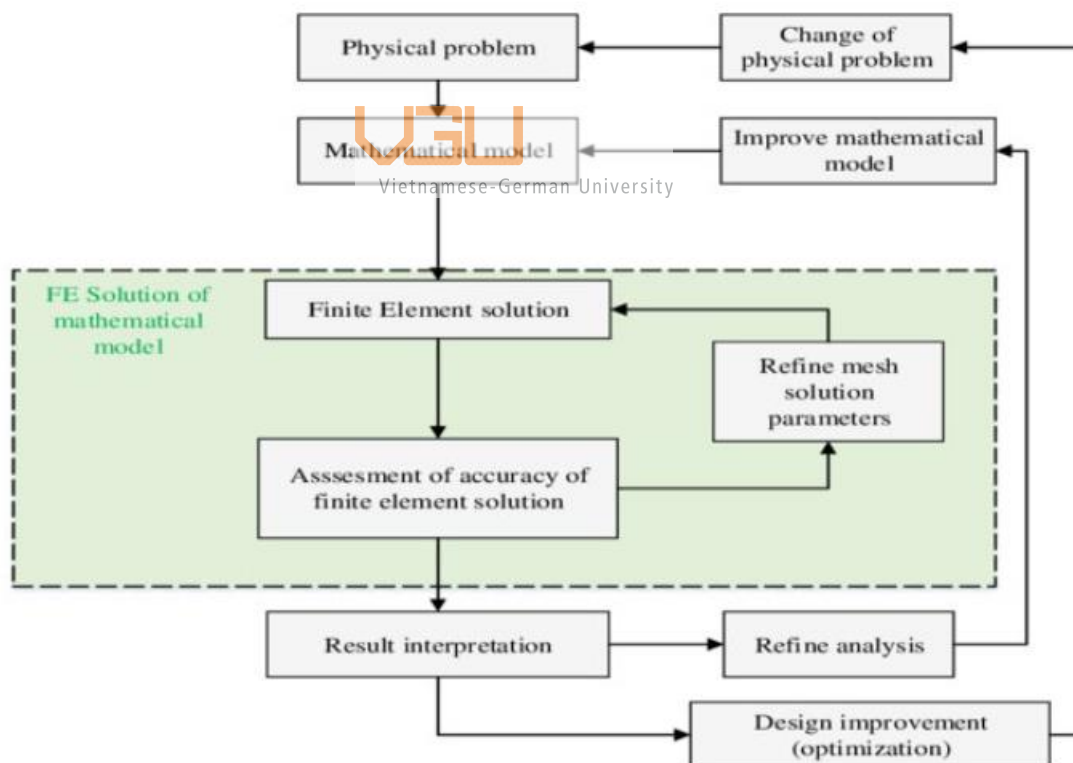
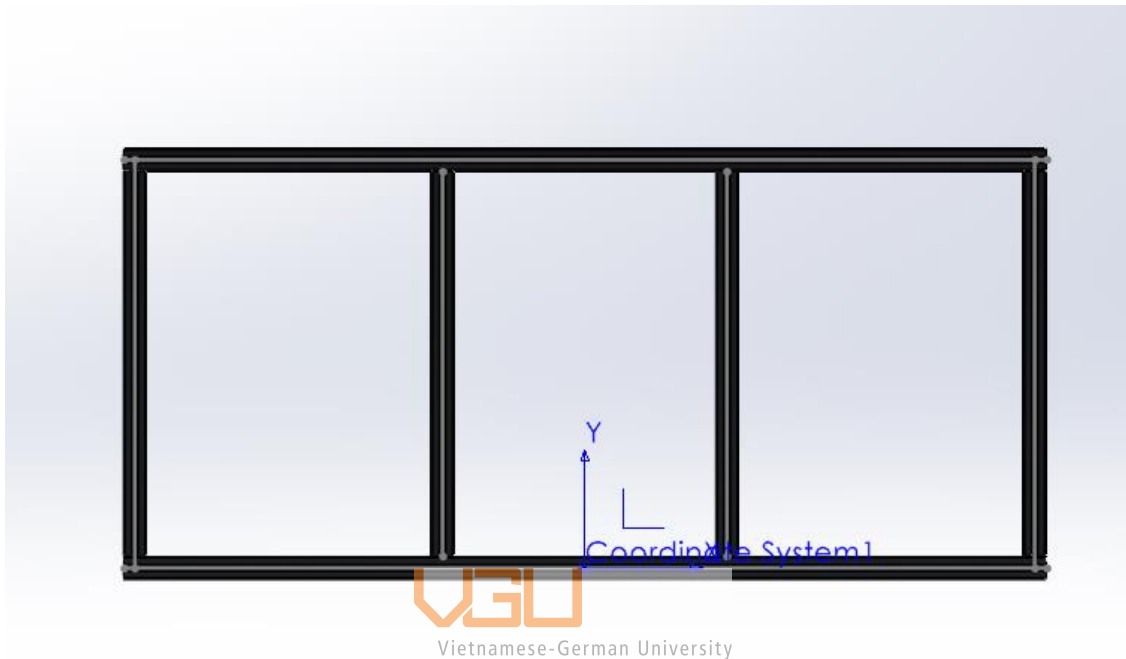


Figure 5-32. Finite element process

Analysis of three-dimensional frames is quite similar to analysis of two-dimensional frames. Now take into account three displacements and three rotations with respect to the three global cartesian axes in each node of the two-node 3D frame finite element. The

problem here is to determine the loading capacity of the upper frame, to determine the maximum amount of load that can be put into the frame and see how much it will affect the whole structure, unlike in chapter 5.3 where only the loading capacity of each link is determined.

Now regarding to the mathematic model, it is best to visualize the structure in 2D problem and import the data as node coordinate and members.



NODAL DATA		
NODE #	X (M)	Y (M)
1	0	0
2	0	0.5
3	0.4	0.5
4	0.4	0
5	0.8	0
6	0.8	0.5
7	1.2	0
8	1.2	0.5

Figure 5-33. Frame structure and nodal coordinates

The nodal is essential in setting up the value of constrain and force for the simulation. The next thing to do is listed out all the material properties of the material using to build the frame which is 6063-T5. Which also been stated in chapter 5.4. After that process to mathematically



illustrated all the load that can will applied onto the frame. The load here will have the total of 20kg as mentions in chapter 5.4

ELEMENT #	NODE-A	NODE-B	MOD. OF EL.	LOAD	AREA	MOMENT OF INERTIA
1	1	2	6.90E+04	0.00E+00	0.03176	2.83
2	2	3	6.90E+04	0.00E+00	0.03176	2.83
3	3	4	6.90E+04	9.26E+01	0.03176	2.83
4	4	1	6.90E+04	0.00E+00	0.03176	2.83
5	4	5	6.90E+04	9.26E+01	0.03176	2.83
6	5	6	6.90E+04	9.26E+01	0.03176	2.83
7	6	3	6.90E+04	9.26E+01	0.03176	2.83
8	6	7	6.90E+04	0.00E+00	0.03176	2.83
9	7	8	6.90E+04	0.00E+00	0.03176	2.83
10	8	5	6.90E+04	0.00E+00	0.03176	2.83

Figure 5-34. Applied constrain and force onto the frame

Finite element method provide a great solution which is through K stiffness matrix. The stiffness matrix is a matrix that represents the system of linear equations that must be solved to determine an approximation to the differential problem in the finite element technique for the numerical solution of elliptic partial differential equations. In the local coordinate system, the stiffness matrix is given by

$$\mathbf{K}^{te} = \begin{bmatrix}
 \frac{EA}{L} & 0 & 0 & 0 & 0 & 0 & -\frac{EA}{L} & 0 & 0 & 0 & 0 & 0 \\
 \frac{12EI_z}{L^3} & 0 & 0 & 0 & \frac{6EI_z}{L^2} & 0 & -\frac{12EI_z}{L^3} & 0 & 0 & 0 & \frac{6EI_z}{L^2} \\
 \frac{12EI_y}{L^3} & 0 & \frac{6EI_y}{L^2} & 0 & 0 & 0 & 0 & -\frac{12EI_y}{L^3} & 0 & -\frac{6EI_y}{L^2} & 0 \\
 \frac{GJ}{L} & 0 & 0 & 0 & 0 & 0 & 0 & 0 & -\frac{GJ}{L} & 0 & 0 \\
 \frac{4EI_y}{L} & 0 & 0 & 0 & \frac{6EI_y}{L^2} & 0 & \frac{2EI_y}{L} & 0 & 0 & 0 & 0 \\
 \frac{4EI_z}{L} & 0 & -\frac{6EI_z}{L^2} & 0 & 0 & 0 & 0 & 0 & \frac{2EI_z}{L} & 0 & 0 \\
 \frac{EA}{L} & 0 & 0 & 0 & 0 & 0 & 0 & 0 & 0 & 0 & 0 \\
 \frac{12EI_z}{L^3} & 0 & 0 & 0 & 0 & 0 & 0 & 0 & 0 & 0 & -\frac{6EI_z}{L^2} \\
 \frac{12EI_y}{L^3} & 0 & \frac{6EI_y}{L^2} & 0 & 0 & 0 & 0 & 0 & 0 & 0 & 0 \\
 \frac{GJ}{L} & 0 & 0 & 0 & 0 & 0 & 0 & 0 & 0 & 0 & 0 \\
 \frac{4EI_y}{L} & 0 & 0 & 0 & \frac{6EI_y}{L^2} & 0 & \frac{2EI_y}{L} & 0 & 0 & 0 & 0 \\
 \frac{4EI_z}{L} & 0 & -\frac{6EI_z}{L^2} & 0 & 0 & 0 & 0 & 0 & 0 & 0 & 0
 \end{bmatrix}$$

Figure 5-35. Stiffness K equation using to solve the problem

Only the calculation conduction was conducted via Matlab because the illustration and plot graphing was rather difficult and complex. So for illustration purpose, the problem is done in solid work for results visualization and the mathematic equation will be done via matlab

(A.10). The results from matlab and solidwork will be put into consideration and listed in table below.

Table 5.21. Results of simulation

	Solidwork	Matlab
Max stress (MPA)	3.43	3.32456
Displacement (mm)	0.02	0.019062

The results are quite similar, which suggested that at 20kg of mass the whole frame will have to affect with the Maximum stresses around 3.35MPa and the maximum displacement occur at around 0.02mm. This suggested that frame is fully capable of withstand the load of all components. It is best to illustrated the place that will have the most displacement and stress.

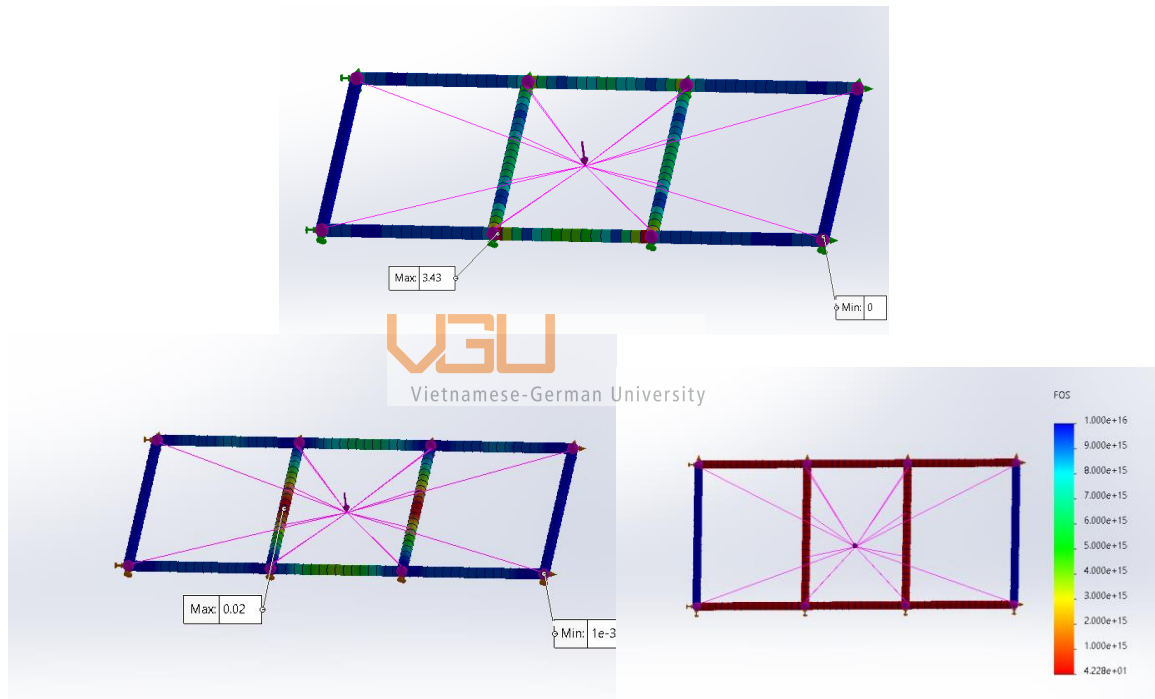
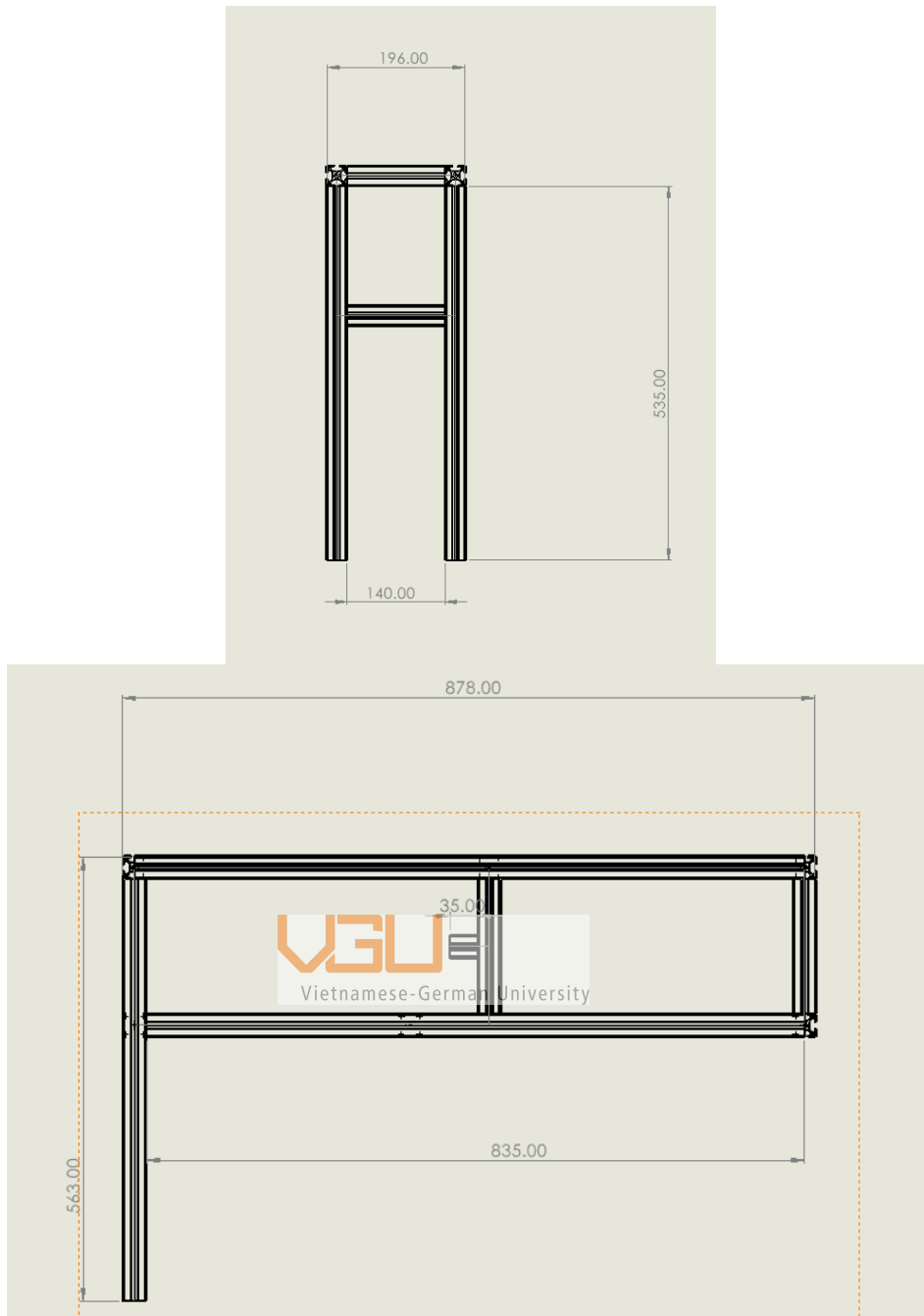


Figure 5-36. Maximum stress, and displacement and safety factor plot of the frame with the correspond applied force of 20kg

## 5.6 Design of the steering and motor frame

The lower frame is design to support the upper frame of the UGV and will need to comprise the front steering module and the motor module, the problem here is to determine the maximum loading capacity of the frame structure and from then choosing the right steering and the motor specification.



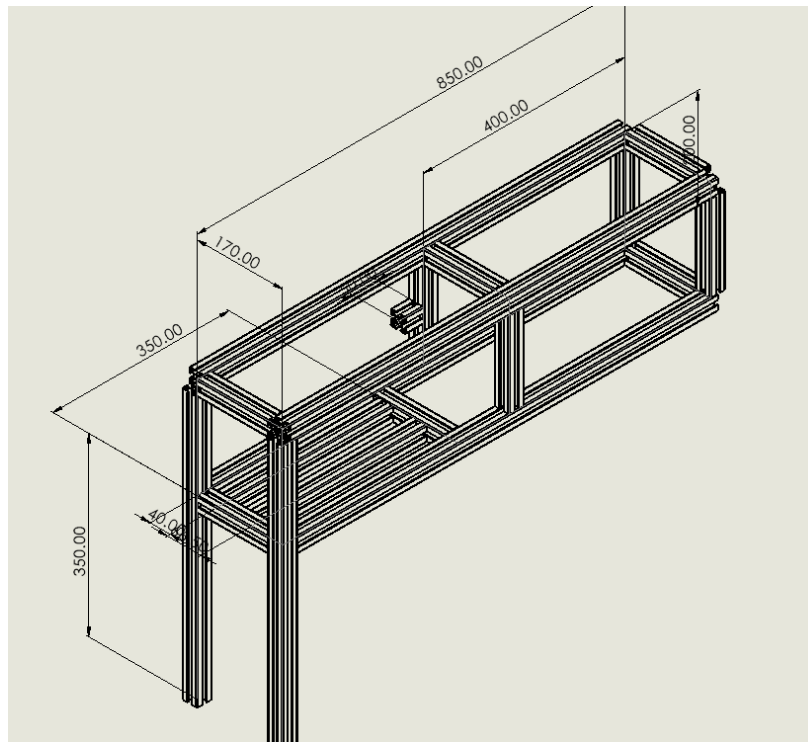


Figure 5-37 Front,side and top view of the steering and motor frame

The studies will be comprise of design simulation statics test to determine the loading capacity of the frame. The study will be conducted via solidwork.

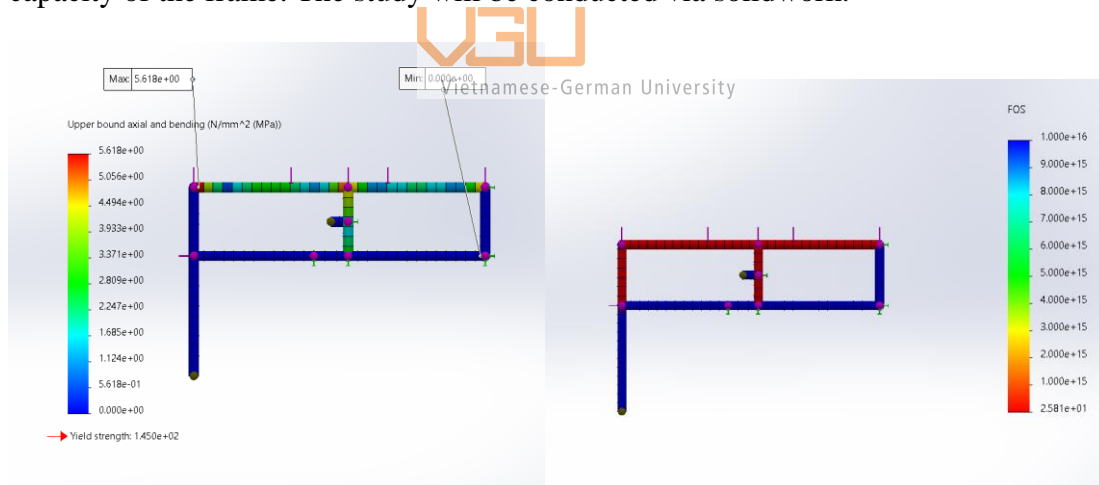


Figure 5-38 Static results of the lower frame as exposed to the loading weight include on the upper frame

As illustrated in fig 5-21, its is enough to conclude that with the loading weight of and the weight of the upper frame the lower frame will be sufficient enough to be able to withstand comfortably without and damage and fatigue. However, the previous only show the stress and strain of the lower frame which only exposed to only the force from the components and weight of the upper frame. There is one more thing that need to be study, which is the beam for placing the actuator.

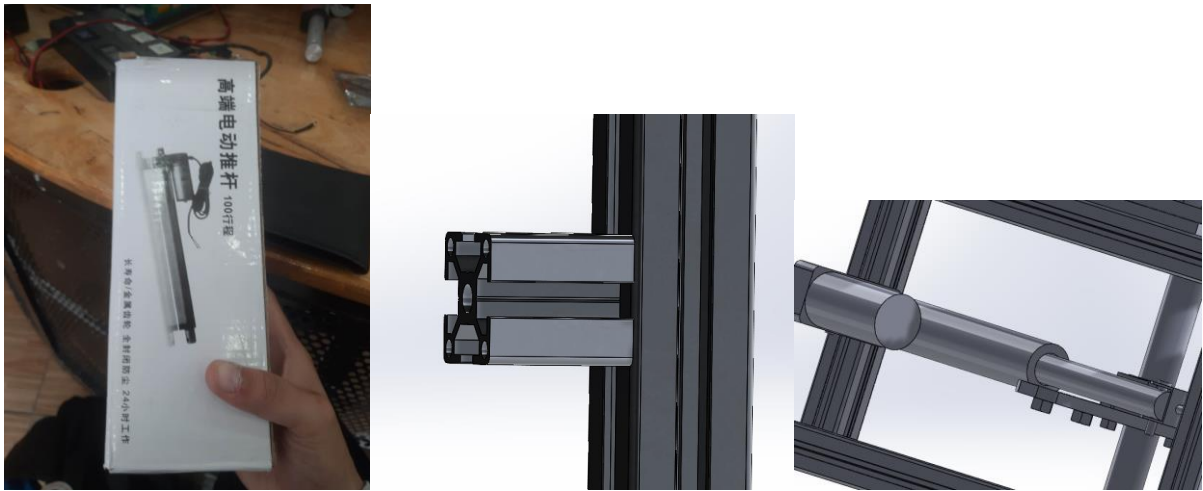


Figure 5-39. The actuator that will be used to steer the UGV and its fixtured beam  
 The steering will produce the force which is equivalent to the steering module weight, in order to steer which is 500N. So the beam must be able to withstand the force which is equivalent to 500N without tearing outs.

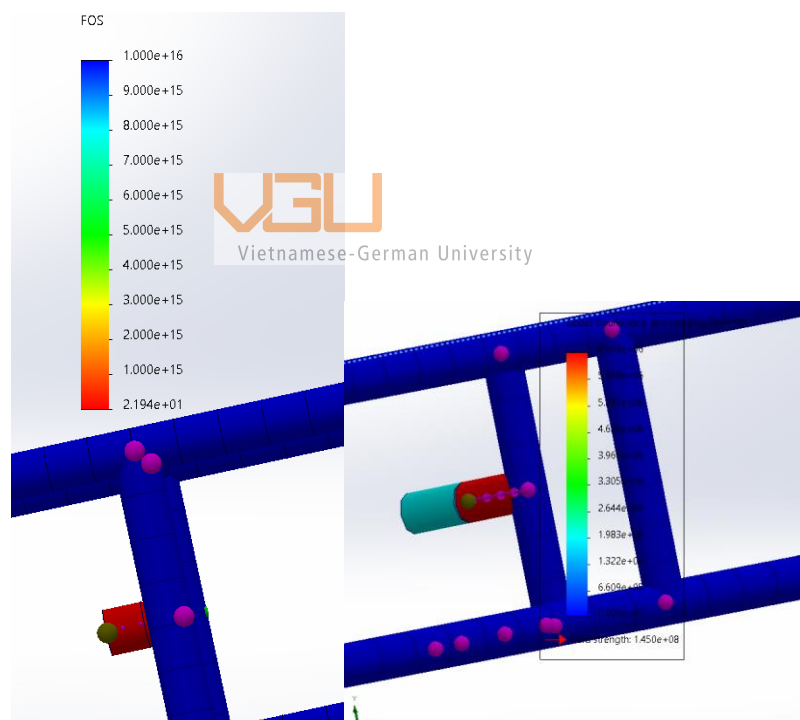


Figure 5-40 Beam stress and safety factor results of the actuator fixture beam

The final product is illustrated in Fig 5-41 below



Figure 5-41 The motor frame and the steering frame after installation

## 5.7 *Width adjustable joining*

As discussed in chapter 2 and 3, it's stated that the UGV need to be able to fit various vegetable plots. As suggested in chapter 2, with the caculation of the desired width vegetable plots the UGV need to be able to fit vegetable plot that have with from 0.8 to 1.2m.

### 5.7.1 **Option I: Width adjustable using ball screw linear guide mechanism**

A ball screw (also known as a ballscrew) is a mechanical linear actuator that smoothly converts rotational motion to linear motion. Ball bearings that function as a precision screw have a helical raceway provided by a threaded shaft. High thrust loads may be applied or absorbed, and they can do so with little internal friction. Due to their near tolerance construction, they may be used in applications requiring a high degree of accuracy. The threaded shaft serves as the screw, while the ball assembly serves as the nut. Ballscrews are often more substantial than traditional leadscrews because they require a device to recirculate the balls. Compared to alternatives, ball screws have a high mechanical efficiency due to their



low friction. A common ball screw could have a 90 percent efficiency [72] , compared to an Acme lead screw of the same size's 20 to 25 percent efficiency. Because there is no sliding friction between the nut and screw, screw assemblies last longer (particularly in no-backlash systems), which reduces the need for lubrication and downtime for maintenance. This might more than make up for the initial expenses of adopting ball screws due to the improvements in overall performance and lower power consumption. In lead screw and nut pairings, blowback is prevalent; ball screws may lessen or even eliminate it. Preloading the balls can prevent "wobble" between the ball screw and ball nut. In applications like machine tools where the screw's load changes fast, this is especially beneficial.

### 5.7.2 Option II: Width adjustable using bracket

Using the same bracket as stated in chapter 5.3, pivoting the intersecting point and fixed using screw, each intersection joint need four 4 brackets to hold the upper frame and the lower frame tightly. When changing the width, loosen the bolts and slide correspondingly to the path of the profile aluminum.



Figure 5-42 Width adjustable using bracket

### 5.7.3 Decision matrix for both options

Table 5.22 Grading criteria for the modular linear mechanism

No.	Grading criteria	Grade
1	Easily to modular	5
2	Assembly and disassembly easily	4
3	Popular componets	2
4	Consistency	3
5	Easily to use	2

The criteria is based on the discussion with supervisor and determine that in this phase of the thesis the out come products are able to modular and easily to used is placed as the main targets.

Table 5.23 Decision matrix result for the modular linear mechanism

Criteria		1	2	3	4	5	Sum
Weighting factor		5	4	2	3	2	16
Option 1	Core	5	2	1	3	2	13
	Weighted score	25	8	2	9	4	48
Option 2	Core	4	4	2	2	2	14
	Weighted score	20	16	4	6	4	50

## 5.8 Overall specification of the design

The frame is divided into 3 main frame the upper frame is placed on top and the motor and steering will act as a too supporting frame for the top one. The top frame is responsible for placing and means of load

After calculation and consideration, the design for the UGV has been initiated, the specification of the vehical and the component quantities is illustrated in table 5.24 and 5.25 respectively.

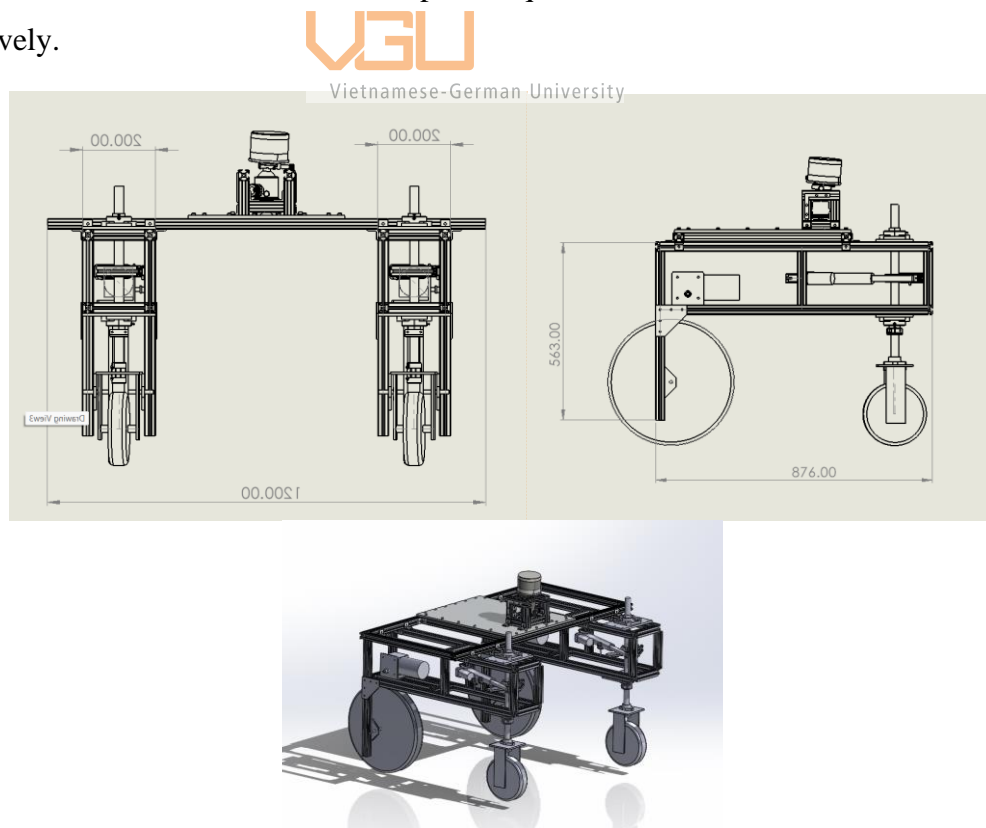


Figure 5-43 Virtual design of a UGV



The virtual design is a guide line to move on to the actual and assembly phase, it provide a detail look and overall shape of the vehical. The specification is used to determine what capacity can the UGV do, also provide information on what purpose the customer can do.

The

Table 5.24 Overall design specification

<b>Overall design specification</b>	
Dimension (mm)	1200*876*563
Gross Weight (kg)	80
Maximum loading capacity when moving (kg)	65kg
Type of surface	Flat, Garden or field surface
Slope Climbing	5°
Type of drive	2 rear wheel drive
Weakest joints capacities at load	1050 N

Table 5.25 Overall component quantities

<b>Overall components specification</b>	
Siemens S7-1500 PLC	1
Electric actuator for steering	2
Front-wheel module	2
Back wheel	2
Driving DC 12V motor	2

Battery 12V	2
Driving time	30 minutes

## 6 Manufacturing

### 6.1 Mechanical Components

After calculating in chapter 5, in this chapter the focus is shift onto the component only also to review and come up with a list of what to comprise in the UGV system regarding the mechanical part for assembling the frame .

Part	Quantities	Value each part	Total	Place
30*30 alumium profile	4.4m	140.000/m	616000	Linhkien283
Alumium bracket 30*30	56	10000	560000	Linhkien283
T- nuts (30*30)	130	1700	221000	Linhkien283
Bolts M6 (12mm)	106	800	84800	Linhkien283
Bolts M6 (16mm)	24	1000	24000	Linhkien283
Bolts M6 (30mm)	4	1500	6000	Linhkien283
Nuts M6 (30mm)	4	400	1600	Linhkien283
Alumium sheet	1	500000	500000	HCM: 1A – Đào Trinh Nhất ( Đường 11) – Linh Tây – Thủ Đức – TPHCM
Roller guide ( V- slots alumium)	0.2m	75000		
Wheel Roller module	1	350000		
12V batteries	3	600000	1800000	389 Nguyễn Công Trứ, P Cầu Ông Lãnh, Q1, TPHCM
Stabalize bracket	1	20000	20000	HCM: 1A – Đào Trinh Nhất ( Đường 11) – Linh Tây – Thủ Đức – TPHCM
Leveling bracket	1	15000	15000	Linhkien283
Alumium profile 30*30	0.93m	140000/m	140000	Linhkien283
M8 bolts *40	2	1250	2500	Linhkien283
Nuts M8 (40mm)	2	500	1000	Linhkien283
			3991900	

Figure 6-1 List of mechanical components

### 6.2 Electrical part



Vietnamese-German University

The electrical is mainly focus on the signal and electrical component which will make the UGV to drive. This chapter will mainly discuss about the PLC S7-1500 and it comprised code in order to make the system works.



Figure 6-2 PLC S7-1500

We are using TIA portal V-16 programme to code for the PLC. The PLC needs a 24V batteries supplies and through a switch to reverse the current. Regarding to the output, the components needed will comprise of 1 contactor, 2 DC motor controller, 8 relays and. All of which will be put inside the electrical box.

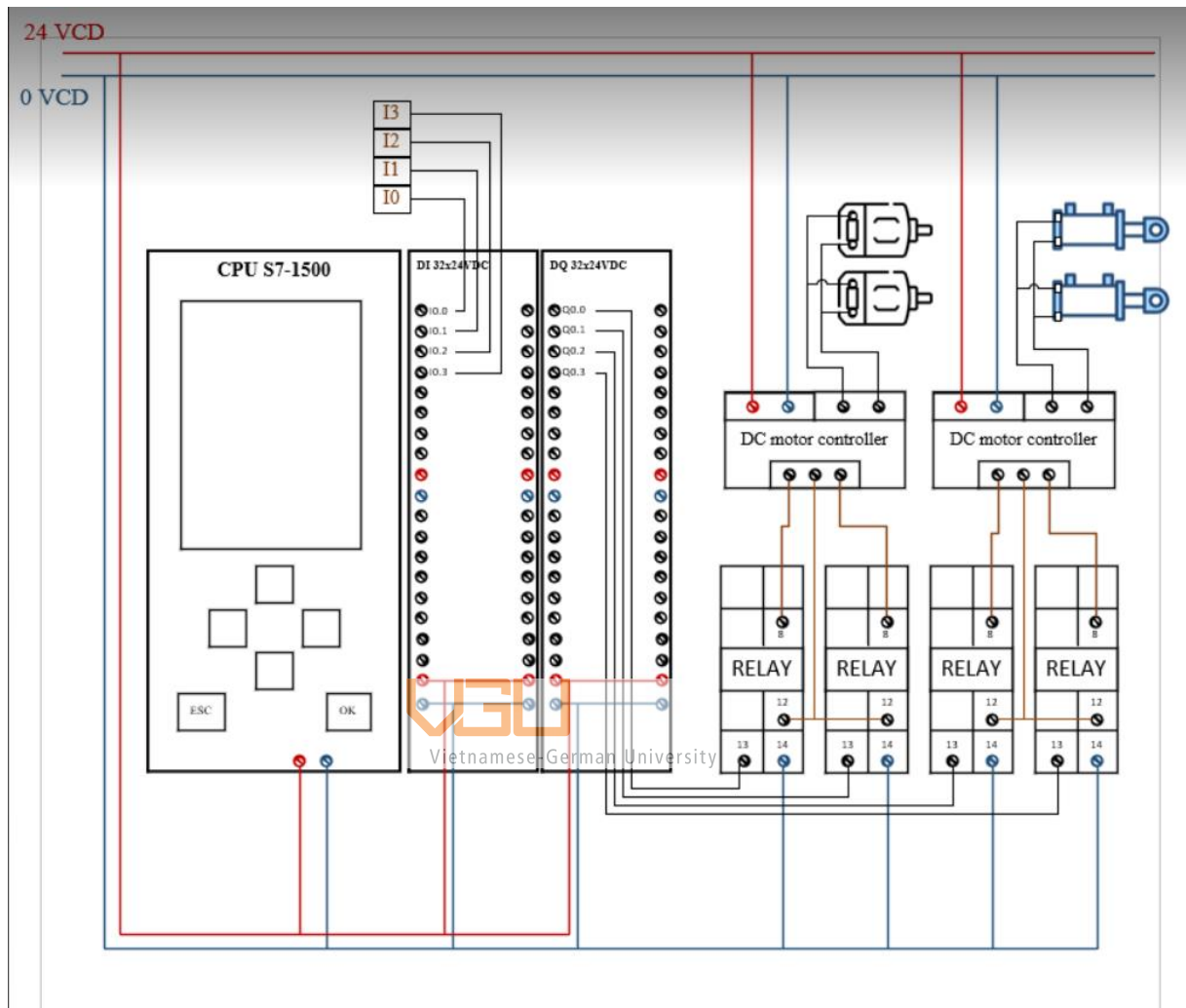


Figure 6-3 Wiring diagram system for the PLC

The final step is to add in the code, which is illustrated in figure 6-4 below.

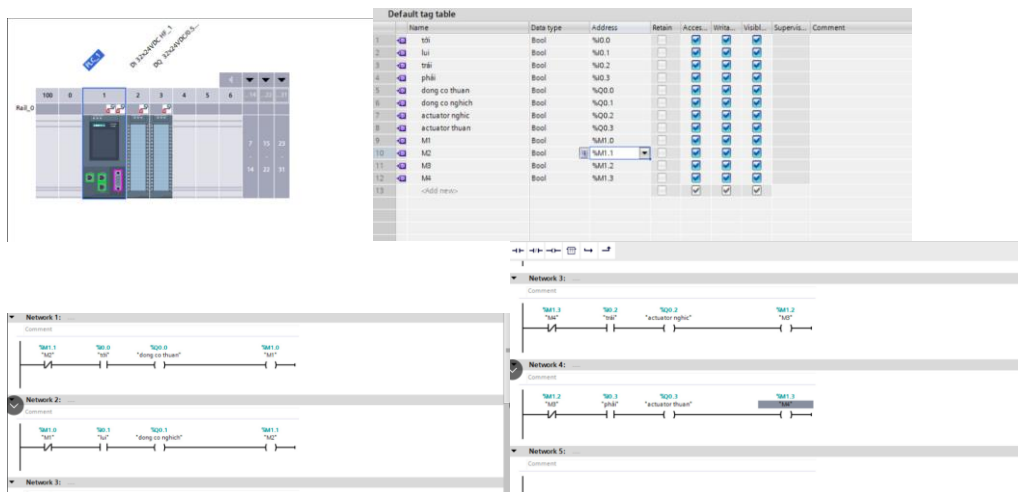


Figure 6-4 PLC programming

The code is divided into 4 different networks, and each will be responsible for 4 separate jobs. The first and second network are responsible for controlling the rotating motion of the motor. The third and fourth network are used to control the rotating motion for the actuator. This will translate to the vehicle motion such as moving forward and backward with turning right and left.

The final product of the PLC and the electric cabinet is illustrated via Fig 6-5

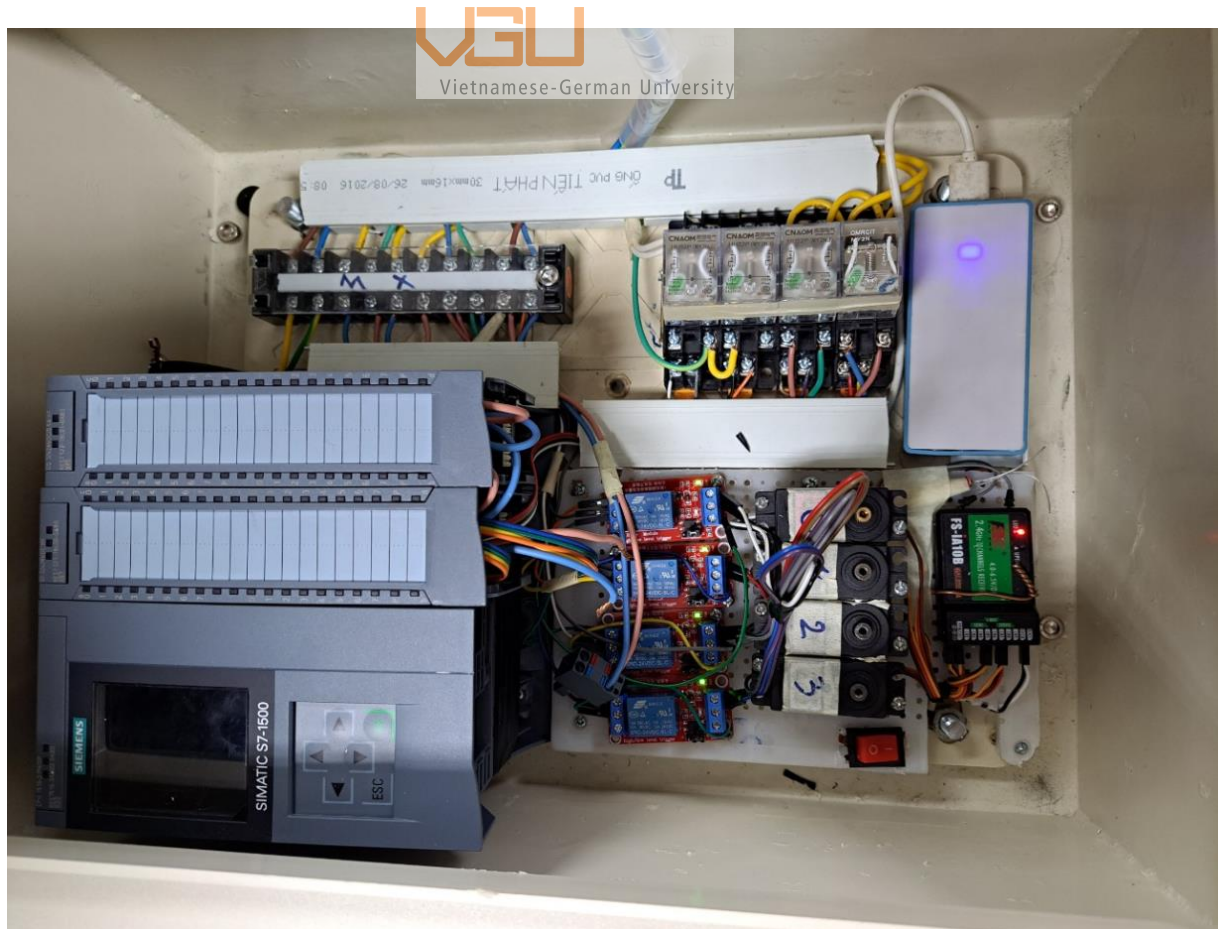


Figure 6-5 Electrical cabinet after installing the PLC and other electrical components

## 6.3 User manual

### 1. Starting

- Check the resistance between the two watersheds of the whole shutdown using a resistance meter to perform a short circuit test.
- Turn on the total power switch, when the 5V relay is on bright green led light

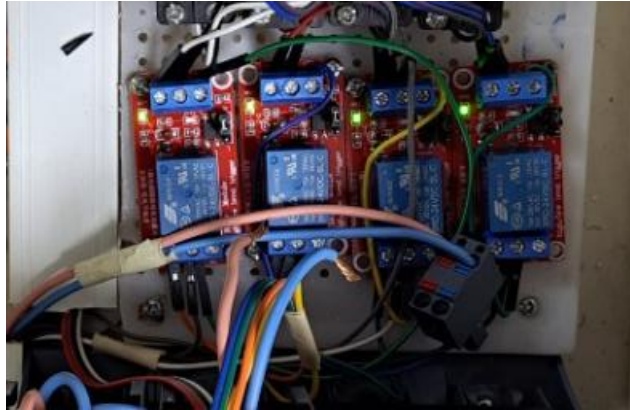


Figure 6-6 5V relay is on  
Vietnamese-German University

- Turn on the receiver power until the receiver led light flashes



Figure 6-7 Receiver Power is on

- Turn on the power of the handle (make sure all switches are turned on to avoid a "switch error")
  - Make that the handle and receiver are linked; if the led receiver flashes (lit constantly), it has been connected.
- ### 2. Power supply for the batteries
- Preparing a 12V charger
  - Attach the first battery to the charger in accordance with the positive negative pole

- Remove the battery charger when the charger says it is full (the charger will also disconnect itself)
  - Do the same for the second batteries
3. Power supply for the receiver
- Remove the power cord from the battery
  - Proceed to charge with 5V battery, micro USB jack
4. Power supply for the PLC
- Connecting the batteries to supply power for the PLC
  - Insert USB card to the PLC to proceed coding
  - Insert the wifi connection jack to the PLC with the computer
  - Proceed to establish internet connection
  - Proceed coding as in Fig 6-4
  - Checking the input and output are fully wired as illustrated in Fig 6-3
  - After applying the code, take off the wifi connection jack and the system is ready to go.
5. Operate
- Move: flick the left joystick up or (the car will move forward or backward)
  - Turn: turn the joystick right or right (the front wheel will turn left or right respectively)



Vietnamese-German University

Note:

When turning, the wheel rotation angle should not exceed 30°

Do not push the joystick up or down to avoid errors and short circuits

#### 6. Speed adjustment

- Turn the control button (small knob) on the electrical cabinet to increase and decrease the engine speed. The voltage supplied to the motor will vary from 0-24V respectively



Figure 6-8 Actuator control module and control knob



- Turn the control button (big knob) on the electrical cabinet to increase or decrease the cylinder velocity. The voltage supplied to the cylinder will vary from 0-24V respectively

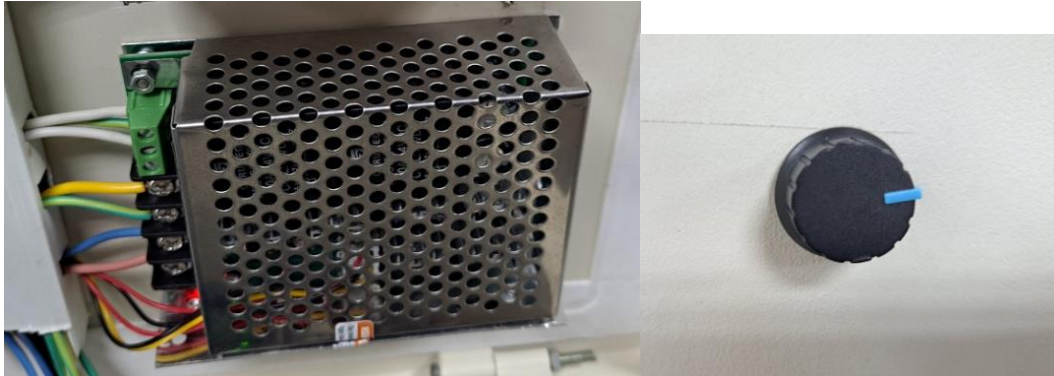


Figure 6-9 Motor control knob and the control module

Note:

The cylinder uses a voltage of 12V, so it is not recommended to adjust the main supply voltage to the cylinder should not be exceeded 14V to avoid cylinder overvoltages



## 7 Results

The frame is divided into 3 main frame the upper frame is placed on top and the motor and steering will act as a too supporting frame for the top one. The top frame is responsible for placing and means of load

After calculation and consideration, the design for the UGV has been initiated, the specification of the vehical and the component quantities is illustrated in table 5.24 and 5.25 respectively.

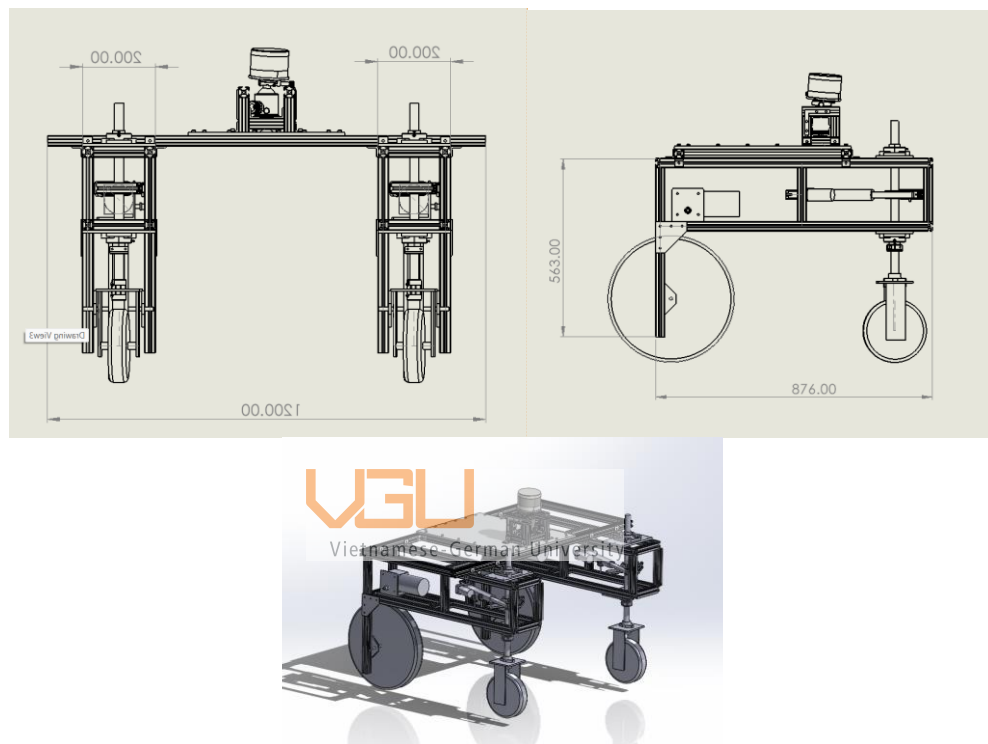


Figure 7-1 Virtual design of a UGV

The virtual design is a guide line to move on to the actual and assembly phase, it provide a detail look and overall shape of the vehical. The specification is used to determine what capacity can the UGV do, also provide information on what purpose the customer can do.

This thesis is mainly focus on the analysis part of the frame and the loading capacities of the vehical when moving and standing still. The loading capacities when standing still has been caculated in chap 5 by determine the weakest joint of the frame which is 1050N. However, the dynamic load is determine via testing. By loading and moving until any kind of problem occurs.



Figure 7-2 Testing loading capacities

The increased of load is increase up to 65kg, at 65kg the frame will experience the fatigue phenomenon. As also illustrated in table 7.1, the data is collected and record via excel.

Load (Kg)	Situation report
20kg	German University
25kg	
30kg	
35kg	
40kg	
45kg	
50kg	
60kg	
65kg	<b>Fatigue in the bolts</b>

Table 7.1 Collected data for loading capacity when the vehical is moving

Table 7.2 Overall design specification

Overall design specification	
Dimension (mm)	1200*876*563
Gross Weight (kg)	80
Maximum loading capacity when moving	65kg

(kg)	
Type of surface	Flat, Garden or field surface
Slope Climbing	5°
Type of drive	2 rear wheel drive
Weakest joints capacities at load	1050 N

Table 7.3 Overall component quantities

<b>Overall components specification</b>	
Siemens S7-1500 PLC	1
Electric actuator for steering	2
Front-wheel module	2
Back wheel	2
Driving DC 12V motor	2
Battery 12V	2
Driving time	30 minutes

The final product has been thoroughly examine and testing to get the result as illustrated in table 7-2 and 7-3. The driving time of the the vehical is tested by letting the vehical to operate in the grass field and after 30 minutes the batteries is ran out.





Figure 7-3 UGV moving on the grass field

The final product is also illustrated in the following figure



Figure 7-4 The UGV final phototype after testing

## 8 Conclusion

The thesis was to create and design a prototype of the UGV ( Unnamed Ground Vehical) that can move on the open field area. The photype has successfully delivered the task. The UGV was able to move, also have a lot of placeholder for further application. The width of the vehical can be change ranging from 0.8 to 1.2m, moreover, it serve the task of moving on the grass and dirt area.

The method was mainly based on Bernoulli Beam Theory , Navier–Stokes and Gralerkin equation to create a FEM simulation for the frame respectively. Regarding the Pre Load and loading capacities the thesis was mainly using the application of Norton RL. Machine design book's.

However, there is a significant limitation of the design. Which is the lack of shelter for the motor and the actuator, as the result the UGV cannot move on areas that have a lot of humidity and cannot withstand long time operation under the hot weather. Another limitation is that the phototype is having a slippery motion when moving at maxium motor capacities.

The UGV should have more cover for all the electrical part . Moreover, increase the load to improve the stability of the UGV to avoid the slippery motion that has been occurring during operation. By building in a suspension system also help to improve the stability of the UGV. Moreover, the steering of the UGV can also be develop to be able to turn in harsh grass environment.

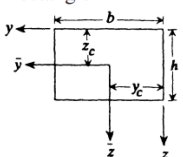
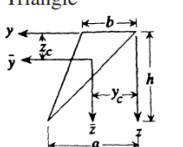
## 9 Appendix

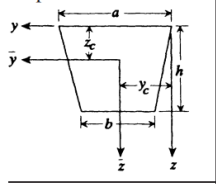
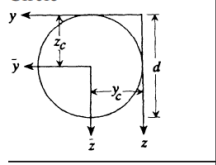
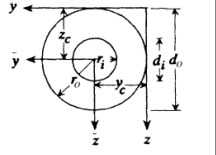
Mechanical properties of commonly investigated aluminium alloys.

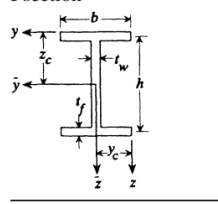
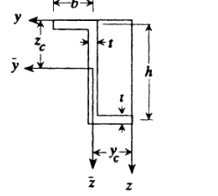
Author(s) (date) [Reference]	Aluminium grade	$f_{0.2}$ [MPa]	$f_u$ [MPa]	$E$ [GPa]	$f_{0.2}/$ $f_u$	$n$
Alsanat et al. (2019) [13]	5052-H36	211.6	257.8	64.2	0.82	–
Su et al. (2014) [14]	6061-T6	234.0	248.0	66.0	0.94	12
Su et al. (2014) [14]	6063-T5	179.0	220.0	69.0	0.81	10
Moen et al. (1999) [15]	6082-T4	120.1	221.0	66.9	0.54	26
Moen et al. (1999) [15]	6082-T6	312.2	324.2	66.7	0.96	74
Moen et al. (1999) [15]	7108-T7	314.0	333.4	66.9	0.94	65

A 1 Mechanical properties of the aluminum alloys

TABLE 2-1 AREAS, CENTROIDS, MOMENTS OF INERTIA, AND RADII OF GYRATION OF COMMON CROSS SECTIONS

Shape of Section	Area, Location of Centroid ( $y_c, z_c$ )	Moments of Inertia and the Polar Moment of Inertia ( $J_x = I_{\bar{y}} + I_{\bar{z}}$ ) with Respect to Centroidal Axial Axis	Transverse Radii of Gyration and the Polar Radius of Gyration $r_p = r_x$
<b>1.</b> Rectangle 	$A = bh$ $y_c = \frac{1}{2}b$ $z_c = \frac{1}{2}h$	$I = I_{\bar{y}} = \frac{1}{12}bh^3$ $I_{\bar{z}} = \frac{1}{12}hb^3$ $I_{\bar{y}\bar{z}} = 0$ $J_x = \frac{1}{12}bh(b^2 + h^2)$	$r_{\bar{y}} = h/\sqrt{12}$ $r_{\bar{z}} = b/\sqrt{12}$ $r_p = \sqrt{\frac{1}{12}(b^2 + h^2)}$
<b>2.</b> Triangle 	$A = \frac{1}{2}bh$ $y_c = \frac{1}{3}(a + b)$ $z_c = \frac{1}{3}h$	$I = I_{\bar{y}} = \frac{1}{36}bh^3$ $I_{\bar{z}} = \frac{1}{36}bh(b^2 - ab + a^2)$ $I_{\bar{y}\bar{z}} = \frac{1}{72}bh^2(2a - b)$ $J_x = \frac{1}{36}bh(h^2 + b^2 - ab + a^2)$	$r_{\bar{y}} = h/\sqrt{18}$ $r_{\bar{z}} = \left[\frac{1}{18}(b^2 - ab + a^2)\right]^{1/2}$ $r_p = \sqrt{\frac{1}{18}(b^2 + h^2 - ab + a^2)}$

<p>3. Trapezoid</p> 	$A = \frac{1}{2}h(a + b)$ $y_c = \frac{1}{2}a$ $z_c = \frac{h}{3} \frac{a + 2b}{a + b}$	$I = I_{\bar{y}} = \frac{h^3}{36} \frac{a^2 + 4ab + b^2}{a + b}$ $I_{\bar{z}} = \frac{1}{48}h(a + b)(a^2 + b^2)$ $I_{\bar{y}\bar{z}} = 0$ $J_x = I_{\bar{y}} + I_{\bar{z}}$	$r_{\bar{y}} = \frac{h(a^2 + 4ab + b^2)^{1/2}}{\sqrt{18}(a + b)}$ $r_{\bar{z}} = \left[ \frac{1}{24}(a^2 + b^2) \right]^{1/2}$ $r_p = \sqrt{J_x/A}$
<p>4. Circle</p> 	$A = \frac{1}{4}\pi d^2$ $y_c = \frac{1}{2}d$ $z_c = \frac{1}{2}d$	$I = I_{\bar{y}} = I_{\bar{z}} = \frac{1}{64}\pi d^4$ $I_{\bar{y}\bar{z}} = 0$ $J_x = \frac{1}{32}\pi d^4$	$r_{\bar{y}} = r_{\bar{z}} = \frac{1}{4}d$ $r_p = d/\sqrt{8}$
<p>5. Annulus</p> 	$A = \frac{1}{4}\pi(d_o^2 - d_i^2)$ $y_c = \frac{1}{2}d_o$ $z_c = \frac{1}{2}d_o$	$I = I_{\bar{y}} = I_{\bar{z}} = \frac{1}{4}\pi(r_o^4 - r_i^4)$ $I_{\bar{y}\bar{z}} = 0$ $J_x = \frac{1}{32}\pi(d_o^4 - d_i^4)$	$r_{\bar{y}} = r_{\bar{z}} = \frac{1}{4}(d_o^2 + d_i^2)^{1/2}$ $r_p = \sqrt{\frac{1}{8}(d_o^2 + d_i^2)}$

<p>12. I section</p> 	$H_1 = h + t_f$ $H_2 = h - t_f$ $A = 2bt_f + H_2t_w$ $y_c = \frac{1}{2}b$ $z_c = \frac{1}{2}H_1$	$I_{\bar{y}} = \frac{1}{12}[bH_1^3 - (b - t_w)H_2^3]$ $I_{\bar{z}} = \frac{1}{12}(H_2t_w^3 + 2t_ft_b^3)$ $I_{\bar{y}\bar{z}} = 0, J_x = I_{\bar{y}} + I_{\bar{z}}$	$r_{\bar{y}} = \sqrt{I_{\bar{y}}/A}$ $r_{\bar{z}} = \sqrt{I_{\bar{z}}/A}$ $r_p = \sqrt{J_x/A}$
<p>13. Z section</p> 	$H_1 = h + t$ $B = b + \frac{1}{2}t$ $C = b - \frac{1}{2}t$ $A = t(h + 2b)$ $y_c = b, z_c = \frac{1}{2}(h + t)$	$I_{\bar{y}} = \frac{1}{12}[BH_1^3 - C(H_1 - 2t)^3]$ $I_{\bar{z}} = \frac{1}{12}[H_1(B + C)^3 - 2hC^3 - 6B^2hC]$ $I_{\bar{y}\bar{z}} = -\frac{1}{2}htb^2$ $J_x = I_{\bar{y}} + I_{\bar{z}}$	$r_{\bar{y}} = \sqrt{I_{\bar{y}}/A}$ $r_{\bar{z}} = \sqrt{I_{\bar{z}}/A}$ $r_p = \sqrt{J_x/A}$

A 2 Moment inertia formula

Bolt Condition	K
Nonplated, black finish	0.30
Zinc-plated	0.20
Lubricated	0.18
Cadmium-plated	0.16
With Bowman Anti-Seize	0.12
With Bowman-Grip nuts	0.09






## A 3 Suggested K value for bolts calculation

Size	s1 (mm)	t1 (mm)	a1 (mm)	h1 (mm)
M4	5	10 - 11	3.5 - 4.5	8 - 10
M5	6	11 - 12.5	5 - 6	11 - 13
M6	8	14.5 - 16	7 - 8	15 - 18
M8	10	16 - 18	7 - 8	17 - 21
M10	12	19 - 21	8 - 9	20 - 25
M12	14	23 - 25	9 - 11	23 - 28
M16	18	30 - 32	12 - 14	30 - 36

Size	s2 (mm)	t2 (mm)	a2 (mm)	h2 (mm)
M4	5	9	2.5	6
M5	6	10	4	8
M6	8	13	6	10
M8	10	15	6	12
M10	12	18	7	16
M12	14	22	8	19
M16	18	28	10	25



Bolt Grade Markings & Strength Chart - Metric Steel Bolts						
Head Marking	Grade/Specification	Material	Proof Load (MPa)	Tensile Strength min (MPa)	Yield Strength Min (MPa)	Hardness Min/Max
	<b>Class 4.6</b>	Low or medium carbon steel	220	400 (58,000 psi)	240	HRB-67 / HRB-95
	<b>Class 5.8</b>	Low or medium carbon steel, quenched and tempered	380	520 (75,000 psi)	420	HRB-82 / HRB-95
	<b>Class 8.8</b>	Medium carbon steel, quenched and tempered	600	830 (120,000 psi)	640	HRC-22 / HRC-34
	<b>Class 10.9</b>	Alloy steel, quenched and tempered	830	1040 (150,000 psi)	940	HRC-32 / HRC-39
	<b>Class 12.9</b>	Alloy steel, quenched and tempered	970	1220 (176,000 psi)	1220	HRC-39 / HRC-44
Usually stamped A-2 or A-4	<b>A2 &amp; A4 Stainless</b>	Steel alloy with chromium and nickel	N/A	500 Min 700 Typical	210 Min 450 Typical	

#### A 4 Bolts specification based on metric standard



Vietnamese-German University

clear; close all; clc;

points = struct;

beams = struct;

%---For each major point in the beam, define x and y coordinates.

points(1).x = 0;

points(1).y = 0;

points(2).x = 210;

points(2).y = 0;

points(3).x = 420;

points(3).y = 0;

%---Determine displacement and rotation angle boundary conditions per

%---point. 0 means fixed, non-zero values means unknown B.C.

points(1).dy = 0;

points(1).ph = 0;

```

points(2).dy = 0;
points(2).ph = 1;
points(3).dy = 0;
points(3).ph = 0;

%---Determine point forces and moments for each point in the beam.
%---If no point load or moment, leave zero.
points(1).fy = 0;
points(1).mz = 0;
points(2).fy = 0;
points(2).mz = 0;
points(3).fy = 0;
points(3).mz = 0;

%---For each segment in the beam, determine end points as an array,
%---Young's Modulus E, area moment of inertia I, distributed load
%---if it is present, and number of divisions for discretization.
beams(1).points = [1 2];
beams(1).dis_for = [9 50];
beams(1).E = 69.973e03;
beams(1).I = 2.03e04;
beams(1).div = 5;
beams(2).points = [2 3];
beams(2).dis_for = [50 9];
beams(2).E = 69.973e03;
beams(2).I = 2.03e04;
beams(2).div = 5;

[f,d,K,n,e] = solve_beam(points,beams);    %---Solves the beam problem.

for cnt=1:length(n)
    fprintf('Node%4i\t\ttx = %7.4e\t\ty = %7.4e\t\t dy = %7.4e' ...
        ,cnt,n(cnt).x,n(cnt).y,n(cnt).dy);
    fprintf('\t\tphi = %7.4e\t\tfy = %12.4e\t\t mz = %7.4e\t\t'n' ...
        ,n(cnt).ph,n(cnt).fy,n(cnt).mz);

```



```

end

t = zeros(size(e));
for cnt=1:length(e)
    nl{cnt}(1) = e(cnt).nodes(1);
    nl{cnt}(2) = e(cnt).nodes(2);
end
df = draw_frame([e.L],t,nl);

x = [df.x];

figure(3)
v = d(1:2:end);
phi = d(2:2:end);
subplot(2,1,1);
plot(x,v);
ylabel('u_y');
subplot(2,1,2);
plot(x,phi);
xlabel('x');
ylabel('\phi_z');

scale = 1e0;
dn = [[df(:).x]' d(1:2:end)*scale+[df(:).y]'];

figure(1);
for cnt=1:length(nl)
    plot([dn(nl{cnt}(1),1) dn(nl{cnt}(2),1)], ...
        [dn(nl{cnt}(1),2) dn(nl{cnt}(2),2)], 'r--o', ...
        'LineWidth',1.5);
    hold on;
end

animate(df,dn,72,24,nl);

```



A 5 Coding script for calculate beam problem using finite elements method

```

% Create random data from a normal distribution
% with mean 1,09 and sd 0.27.
data = (randn(1,21)*0.27 + 1.09)';
% Run bootci (percentile method is chosen since that's how we're
% computing it below in the other method.
nBoot = 100; %number of bootstraps
[bci,bmeans] = bootci(nBoot,{ @mean,data },'alpha',.05,'type','per'); %95 confidence interval
% Compute bootstrap sample mean
bmu = mean(bmeans);
% Now repeat that process with lower-level bootstrapping
% using the same sampling procedure and the same data.
bootMeans = nan(1,nBoot);
for i = 1:nBoot
    bootMeans(i) = mean(data(randi(numel(data),size(data)))));
end
CI = prctile(bootMeans,[5,95]);
mu = mean(bootMeans);
% Plot the bootci() results
figure()
ax1 = subplot(2,1,1);
histogram(bmeans);
hold on
xline(bmu, 'k-', sprintf('mu = %.2f',bmu),'LineWidth',2,'FontSize',12)
xline(bci(1),'k-',sprintf('%.1f',bci(1)),'LineWidth',2,'FontSize',12)
xline(bci(2),'k-',sprintf('%.1f',bci(2)),'LineWidth',2,'FontSize',12)
title('bootci()')

```

A 6 Coding script for bootstrap computation confidence intervals of 95%

```

% length of the grip
l = 16;
% Major diameter of the bolts
d = 6;
% total thread length

```

```

Lt= 2*d+6;
% Height of the nuts
H=6;
% Required bolts length
Lreq= l+H ;
% stress area of threaded portion
At= 20.1;
% Area of unthread area
Ad = pi * (d/2) ^2;
% stiffness of the bolts E of bolts is 205GPA
kd = (Ad * 205000)/( l*d);
kt = ( At * 205000)/( l*d); K= (kd*kt)/( kd+kt);
% diameter of the washer
dw = 1.5*d;
l1= 8;
l2= 9.2 ;
D= dw + 2*(l1-((l2+l1)/2)*0.5774);
% stiffness on frusta 1
k1=(0.5774*pi*370*d)/log(((1.155*((l2+l1)/2)+dw-
d)*(d+dw))/((1.155*((l2+l1)/2)+dw+d)*(dw-d)));
% stiffness on frusta 2
k2=(0.5774*pi*370*d)/log(((1.155*((l2+l1)/2)-l1)+D-d)*(d+D))/((1.155*((l2+l1)/2)-
l1)+D+d)*(D-d)));
% Stiffness on frusta 3
k3= (0.5774*pi*71*d)/log(((1.155*l2+dw-d)*(d+dw))/((1.155*l2+dw+d)*(dw-d)));
% Total Km
Km= 1/(1/k1)+(1/k2)+(1/k3);
    A 7 Stiffness M6 bolts connecting the 30*30 bracket with 30*30 alumium frame
% Calculation of proof load
Sp = 970;
% Proof load
Fp = Sp * At;
% Pre-load
Fi= 0.75* Fp;
% Required torque wench

```

```

Tr = 0.2 * Fi* d;
% Calculating C (joint stiffness parameter)
C = K/(K+Km);
%Calculating Fb with P= 1050
P=1050;
Fb = (P*C)+ Fi;
% Tensile stress on the bolts
Stress = Fb/At;
%yeilding factor of safty of the joint
np= (Sp/Stress);
% Loading factor
nl= ((Sp*At)-Fi)/(P*C);
    A 8 Safty factor and Pre Load M6 bolts connecting the 30*30 bracket with 30*30 alumium
        frame

% L: length of bar
E=69e06; A=0.03176;
Iy=28.3e-5; Iz=28.3e-5; G=25.8e6;
numberElements=8;
E_vec=69e6*ones(1,numberElements);
G_vec=25.8e6*ones(1,numberElements);
A_vec=0.03176*ones(1,numberElements);
Iy_vec=28.3e-5*ones(1,numberElements);
Iz_vec=28.3e-5*ones(1,numberElements);
% generation of coordinates and connectivities
nodeCoordinates=[0 0;
0 0.5;
0.4 0.5;
0.4 0;
0.8 0;
0.8 0.5;
1.2 0;
1.2 0.5;];
xx=nodeCoordinates(:,1);
yy=nodeCoordinates(:,2);
elementNodes=[1 2;2 3; 3 4; 4 1; 4 5; 5 6; 6 4; 6 7; 7 8; 8 6];

```

```

numberNodes=size(nodeCoordinates,1);
numberElements=size(elementNodes,1);
% for structure:
% displacements: displacement vector
% force : force vector
% stiffness: stiffness matrix
% GDof: global number of degrees of freedom
GDof=3*numberNodes;
force=zeros(GDof,1);
stiffness=zeros(GDof);
% calculation of the system stiffness matrix
% and force vector
% stiffness matrix
K_assembly=formStiffness3Dframe(GDof,numberElements,elementNodes,nodeCoordinates,
E_vec,A_vec,Iz_vec,Iy_vec,G_vec,J_vec);
% boundary conditions and solution
prescribedDof=1:4*6;
%force vector
F_col=nan(GDof,1);
F_col(4*6+1:end)=0;
F_col(37)=-15;
% solution
[D_col,F_col]=solution(prescribedDof,K_assembly,D_col,F_col);
% displacements
disp('Displacements')
jj=1:GDof; format long
f=[jj; displacements'];
fprintf('node U\n')
fprintf('%3d %12.8f\n',f)

```



A 9 Calculation for frame under the mass of components

Size - Nominal Diameter (mm)	Pitch <sup>1)</sup> (mm) (in)	Clearance Drill (mm) (in)	Tap Drill (mm) (in)
M 1.6	0.35	1.8	1.25
M 2	0.40	2.4	1.60
M 2.5	0.45	2.90	2.00
M 3	0.50	3.40	2.50
M 3.5	0.60	3.90	2.90
M 4	0.70	4.50	3.30
M 5	0.80	5.50	4.20
M 6	1.00	6.60	5.00
M 8	1.25	9.00	6.80
M 10	1.50	12.00	8.50
M 12	1.75	14.00	10.20
M 14	2.00	16.00	12.00
M 16	2.00	18.00	14.00
M 20	2.50	22.00	17.50
M 22	2.50	25.00	19.50
M 24	3.00	27.00	21.00
M 27	3.00	30.00	24.00
M 30	3.50	33.00	26.50
M 36	4.00	40.00	32.00
M 42	4.50	46.00	37.50
M 48	5.00	53.00	43.00
M 56	5.50	62.00	50.50
M 64	6.00	70.00	58.00
M 68	6.00	74.00	62.00

Vietnamese-German University

### A 10 The most used coarse threads up to size M 68

Nominal Major Diameter $d$ mm	Coarse-Pitch Series			Fine-Pitch Series		
	Pitch $p$ mm	Tensile-Stress Area $A_t$ mm <sup>2</sup>	Minor-Diameter Area $A_r$ mm <sup>2</sup>	Pitch $p$ mm	Tensile-Stress Area $A_t$ mm <sup>2</sup>	Minor-Diameter Area $A_r$ mm <sup>2</sup>
1.6	0.35	1.27	1.07			
2	0.40	2.07	1.79			
2.5	0.45	3.39	2.98			
3	0.5	5.03	4.47			
3.5	0.6	6.78	6.00			
4	0.7	8.78	7.75			
5	0.8	14.2	12.7			
6	1	20.1	17.9			
8	1.25	36.6	32.8	1	39.2	36.0
10	1.5	58.0	52.3	1.25	61.2	56.3
12	1.75	84.3	76.3	1.25	92.1	86.0
14	2	115	104	1.5	125	116
16	2	157	144	1.5	167	157
20	2.5	245	225	1.5	272	259
24	3	353	324	2	384	365
30	3.5	561	519	2	621	596
36	4	817	759	2	915	884
42	4.5	1120	1050	2	1260	1230
48	5	1470	1380	2	1670	1630
56	5.5	2030	1910	2	2300	2250
64	6	2680	2520	2	3030	2980
72	6	3460	3280	2	3860	3800
80	6	4340	4140	1.5	4850	4800
90	6	5590	5360	2	6100	6020
100	6	6990	6740	2	7560	7470
110				2	9180	9080

### A 11 Bolts specification by Norton



## 10 Reference


1. [Oxford English Dictionary](#), 3rd ed. "agricultural, *adj.*" Oxford University Press (Oxford), 2012.
2. [Oxford English Dictionary](#), 3rd ed. "agriculture, *n.*" Oxford University Press (Oxford), 2012.
3. [See also, e.g., Provincial Agricultural Land Commission. "What is Agricultural Land? Archived August 11, 2014, at the Wayback Machine"](#) The Province of British Columbia. Accessed 1 Aug 2014.
4. [FAO. FAOSTAT Glossary Archived May 27, 2013, at the Wayback Machine:](#) "Agricultural area".
5. [OECD. Glossary of Statistical Terms: "Agricultural land". Archived 2016-03-03 at the Wayback Machine](#)

From [https://en.wikipedia.org/wiki/Agricultural\\_land](https://en.wikipedia.org/wiki/Agricultural_land)>

6. [Kỹ thuật trồng rau \(lamdong.gov.vn\)](#)
7. [\[EBOOK\] KỸ THUẬT TRỒNG RAU SẠCH TRỒNG RAU ĂN LÁ, PGS. TS. TA THU CÚC, NXB PHỤ NỮ-tailieunongnghiep.com.pdf - Google Drive](#)
8. 'Antony Hayes 'Probability statistics for engineering, 4th ed (2012) - page 216 '
9. Hooke's law - Wikipedia
10. [1, p. 17]
11. [1, pp. 15-17]
12. [1, pp. 15-17]
13. [1, p. 46]
14. [1, p. 50]
15. [1, p. 51]
16. Marinoudi, V.; Sorensen, C.G.; Pearson, S.; Bochtis, D. Robotics and labour in agriculture. A context consideration. Biosyst. Eng. 2019, 184, 111–121.
17. King, A. Technology: The future of agriculture. Nature 2017, 544, S21.

18. Bechar, A.; Vigneault, C. Agricultural robots for field operations: Concepts and components. *Biosyst. Eng.* 2016, 149, 94–111.
19. Auat Cheein, F.A.; Carelli, R. Agricultural robotics: Unmanned robotic service units in agricultural tasks. *IEEE Ind. Electr. Mag.* 2013, 7, 48–58
20. Shamshiri, R.R.; Weltzien, C.; Hameed, I.A.; Yule, I.J.; Grift, T.E.; Balasundram, S.K.; Pitonakova, L.; Ahmad, D.; Chowdhary, G. Research and development in agricultural robotics: A perspective of digital farming. *Int. J. Agric. and Biol. Eng.* 2018, 11, 1–14.
21. Bawden, O.; Ball, D.; Kulk, J.; Perez, T.; Russell, R. A lightweight, modular robotic vehicle for the sustainable intensification of agriculture. In *Proceedings of the Australian Conference on Robotics and Automation (ACRA 2014)*, Melbourne, Australia, 2–4 December 2014; Australian Robotics & Automation Association ARAA: Broadway, Australia, 2014.
22. Ruckelshausen, A.; Biber, P.; Dorna, M.; Gremnes, H.; Klose, R.; Linz, A.; Rahe, R.; Resch, R.; Thiel, M.; Trautz, D.; et al. BoniRob: An autonomous field robot platform for individual plant phenotyping. *Prec. Agric.* 2009, 9, 841–847.
23. Switch to Smartweeding with Ecorobotix. Available online: [www.ecorobotix.com](http://www.ecorobotix.com) (accessed on 27 February 2020).
24. Chang, C.L.; Lin, K.M. Smart agricultural machine with a computer vision-based weeding and variable-rate irrigation scheme. *Robotics* 2018, 7, 38.
25. Reiser, D.; Sehsah, E.-S.; Bumann, O.; Morhard, J.; Griepentrog, H.W. Development of an Autonomous Electric Robot Implement for Intra-Row Weeding in Vineyards. *Agriculture* 2019, 9, 18.
26. Roure, F.; Moreno, G.; Soler, M.; Faconti, D.; Serrano, D.; Astolfi, P.; Bardaro, G.; Gabrielli, A.; Bascetta, L.; Matteucci, M. GRAPE: Ground Robot for vineyard Monitoring and Protection. In *Robot 2017: Third Iberian Robotics Conference, Proceedings of the Third Iberian Robotic Conference, Sevilla, Spain, 22–24 November 2017*; Ollero, A., Sanfeliu, A., Montano, L., Lau, N., Cardeira, C., Eds.; Springer: Cham, Switzerland, 2017; pp. 249–260
27. Strisciuglio, N.; Tylecek, R.; Blach, M.; Petkov, N.; Biber, P.; Hemming, J.; Van Henten, E.; Sattler, T.; Pollefeys, M.; Gevers, T.; et al. Trimbot2020: An outdoor robot for automatic gardening. In *Proceedings of the 50th Symposium on Robotics (ISR)*, Munich, Germany, 19–22 June 2018; VDE VERLAG GmbH: Berlin, Germany, 2018; pp. 495–500.
28. Underwood, J.P.; Calleija, M.; Taylor, Z.; Hung, C.; Nieto, J.; Fitch, R.; Sukkarieh, S. Real-time target detection and steerable spray for vegetable crops. In *Proceedings of*

- the International Conference on Robotics and Automation: Robotics in Agriculture Workshop, Seattle, WA, USA, 25–30 May 2015.
29. Yan, X.T.; Post, M.A.; Bianco, A.; Niu, C.; Palazzetti, R.; Melville, Y.L.C.; Kisdi, A.; Tubby, W. The AgriRover: A Reinvented Mechatronic Platform from Space Robotics for Precision Farming. In *Reinventing Mechatronics*; Yan, X.T., Bradley, D., Russell, D., Moore, P., Eds.; Springer: Cham, Switzerland, 2020.
  30. Xiong, Y.; Ge, Y.; Grimstad, L.; From, P.J. An autonomous strawberry-harvesting robot: Design development integration and field evaluation. *J. Field Robot.* 2019, 36, 1–23.
  31. Klein, F.B.; Wilmot, A.; De Tejada, V.F.; Rodriguez, B.L.; Requena, I.; Busch, S.; Rondepierre, A.; Auzeeri, T.; Sauerwald, T.; Andrews, W.F.P.; et al. Proof-of-concept modular robot platform for cauliflower harvesting. In *Precision Agriculture '19, Proceedings of the 12th European Conference on Precision Agriculture, Montpellier SupAgro, France, 8–11 July 2019*; John, V., Ed.; Wageningen Academic Publishers: Wageningen, The Netherlands, 2019; pp. 783–789.
  32. Feng, Q.; Wang, X.; Wang, G.; Li, Z. Design and Test of Tomatoes Harvesting Robot. In *Proceedings of the IEEE International Conference on Information and Automation, Lijiang, Yunnan, China, 8–10 August 2015*; pp. 949–952.
  33. [1, p. 52]
  34. [2]
  35. Altintas, Y., Verl, A., Brecher, C., Uriarte, L. & Pritschow, G. Machine tool feed drives. *CIRP Ann Manuf Technol* 60, 779–796 (2011).
  36. GOLZ H U, W. H. Vorspannungsregelung im Kugelgewindetrieb – ein neuer Ansatz fu'r den Werkzeugmaschinenbau? *WT. Zeitschrift fuer Industrielle Fertigung (Werkstattstechnik)* 80, 366–368 (1990).
  37. Spath, D., Rosum, J., Haberkern, A. & Weule, H. Kinematics, Frictional Characteristics and Wear Reduction by PVD Coating on Ball Screw Drives. *CIRP Ann Manuf Technol* 44, (1995).
  38. [1, p. 59]
  39. [1, p. 99]
  40. [1, p. 100]
  41. [3, pp. 185-186]
  42. B. Oostra, *Phys. Teach.* 44, 283 (2006).
  43. S.C. Hong and S.I. Hong, *Phys. Teach.* 51, 139 (2013).

44. Zhang Z, Zhang J, Shang Y, Zhang T. Study on the Optimal Cross-Sectional Shapes of the PEMFC Endplates by Using a Moment of Inertia and 3D FEM Models. *Sustainability*. 2022; 14(19)
45. E.A. Witmer (1991-1992). "Elementary Bernoulli-Euler Beam Theory". MIT Unified Engineering Course Notes. pp. 5– 115 to 5–165.
46. Euler-Bernoulli Beam Equation, [http://en.wikipedia.org/wiki/Euler-Bernoulli\\_beam\\_equation](http://en.wikipedia.org/wiki/Euler-Bernoulli_beam_equation)
47. E.P Popov., *Mechanics of Materials*, Prentice-Hall, 1978.
48. F. Bassi, S. Rebay, Junning Qin, Hongzhi Zhong, A Galerkin Time quadrature element formulation for linear structural dynamics, *Applied Mathematics and Computation*, Volume 413, 2022,
49. A High-Order Accurate Discontinuous Finite Element Method for the Numerical Solution of the Compressible Navier–Stokes Equations, *Journal of Computational Physics*, Volume 131, Issue 2, 1997, Pages 267-279
50. Tornabene, F., Fantuzzi, N. and Bacciocchi, M. (2014) “The strong formulation finite element method: stability and accuracy”, *Frattura ed Integrità Strutturale*, 8(29), pp. pages 251–265.
51. G.R. Bhashyam, G. Prathap, Galerkin finite element method for non-linear beam vibrations, *Journal of Sound and Vibration*, Volume 72, Issue 2, 1980, Pages 191-203,
52. [4] 
53. Saad, Y., and M.H. Schultz, GMRES: A generalized minimal residual algorithm for solving nonsymmetric linear systems, *SIAM J. Sci. Statist. Compute*, 7 (1986), pp. 856–869.
54. Ana Catalina Torres, Autar Kaw: Comparing Methods of First Derivative Approximation Forward, Backward and Central Divided Difference, University of South Florida
55. S Rao. Gunakala, D.M.G. Comissiong, K.Jordan, Alana Sankar: A Finite Element Solution of the Beam Equation via MATLAB , Vol. 2 No. 8; October 2012
56. Hakan T. Türker (2020): A modified beam theory for bending of eccentrically supported beams, *Mechanics Based Design of Structures and Machines*
57. Shigley JE. *Mechanical engineering design*. 1st metric ed. McGraw Hill; 1986.
58. Bickford JH. *The handbook of bolts and bolted joints*. Hardback edition. Dekker; 1998.
59. Norton RL. *Machine design: an integrated approach*. 2nd ed. Prentice Hall; 2000.
60. Motosh N. Determination of joint stiffness in bolted connections. *ASME Journal of Industrial Design* 1976;98(3):858–61

61. Burguete RL. Methods to calculate joint stiffness. A review and classification of joint types. ASME Materials Engineering 1992:347–54
62. Engineering Sciences Data Unit. Analysis of pre-tensioned bolted joints subject to tensile (separating) forces. Data item 85021. London: ESDU; 1985 [amended 1995].
63. Budynas–Nisbett: Shigley’s Mechanical Engineering Design, Eighth Edition. Screws, Fasteners, and the Design of Nonpermanent Joints, p.398-456
64. Aluminium in construction [Internet]. All about aluminium; 2019 [accessed 1 June 2020]. Available from: <https://aluminiumleader.com/application/construction/>.
65. Kaufman JG. Introduction to aluminium alloys and tempers. Materials Park (OH): ASM International; 2000.
66. Evangelia Georgantzia, Michaela Gkantou, George S. Kamaris: Aluminium alloys as structural material: A review of research, Engineering Structures, Volume 227, 2021,
67. Ashutosh Bijalwan, Anadi Misra "Design and Structural Analysis of Flexible Wearable Chair Using Finite Element Method", Open Journal of Applied Sciences, Vol.6 No.7, 2016
68. Ammour, Saliha Khalafalla, Mohamed And Malyuta, Daniel : FINITE ELEMENT ANALYSIS OF ASCE STEEL BEAM – A BEAM APPROACH, November, 2013
69. Karl-Grote: Engineering design: Bolts calculation
70. Engineering ToolBox, (2005). Threaded Bolts - Stress Area. [online] Available at: [https://www.engineeringtoolbox.com/bolt-threads-stress-d\\_856.html](https://www.engineeringtoolbox.com/bolt-threads-stress-d_856.html) [Accessed Day 13 Mo 11. Year 2022].

